Universidade do Minho
Escola de Engenharia

Débora Carina Gonçalves de Abreu Ferreira

Design of new strategies for breast cancer diagnosis

Outubro de 2013

Design of new strategies for breast cancer diagnosis
Débora Carina Gonçalves de Abreu Ferreira
Uminho | 2013

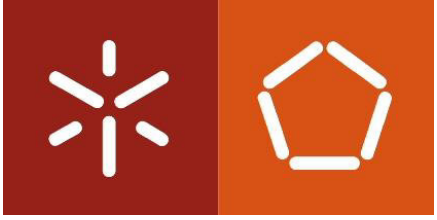

Universidade do Minho

Escola de Engenharia

Débora Carina Gonçalves de Abreu Ferreira

Design of new strategies for breast cancer diagnosis

Dissertação de Mestrado

Mestrado em Bioengenharia

Trabalho efetuado sob a orientação da

Professora Doutora Lígia Raquel Marona Rodrigues

e co-orientação do

Doutor Leonardus Dorothea Kluskens

Outubro 2013

Universidade do Minho, ____/____/_____

Assinatura:_____

ACKNOWLEDGEMENTS

Para o desenvolvimento e concretização deste trabalho contribuíram várias pessoas a quem quero expressar o meu sincero agradecimento.

Aos meus orientadores, Professora Lígia Rodrigues e Doutor Leon Kluskens, pelo apoio, disponibilidade, orientação, compreensão e confiança que depositaram em mim ao longo destes vários meses. Agradeço também ao Joaquim Barbosa, por todo o interesse que demonstrou durante a execução do trabalho, pelos ensinamentos e pelos conhecimentos que me transmitiu.

Aos meus colegas da Plataforma de Biologia Molecular e Sintética pelo bom ambiente, boa disposição e por todo o apoio que me deram durante o trabalho laboratorial, predispondo-se sempre a ajudar. Um muito obrigado à Carla Magalhães, Franklin Nóbrega, Tânia Mendes, Rita Costa, Sofia Meirinho e Joana Cunha.

To Yunlei Zhang I would like to thank for the great help regarding the final part of the work developed.

Um especial agradecimento aos meus amigos de mestrado pela motivação, amizade e alegria que me dedicaram durante todo este processo. Diana, Elisabete, Elísia, Vanessa, Mário, Pedro e Alexandra obrigado pelas hilariantes horas que partilhamos.

Ao Rui Nunes pela presença, carinho, força e paciência ao longo deste ano. Não há palavras para descrever o meu agradecimento por todos os bons momentos a teu lado.

E claro que não me podia esquecer das pessoas mais importantes na minha vida. Aos meus pais e ao meu irmão obrigada pelo infindável apoio, incentivo, pela ajuda, pelos conselhos pelos meios que me proporcionaram, pelo carinho e inesgotável paciência durante este percurso. Não podia deixar de agradecer também à minha avó Gracinda, a minha segunda mãe, por todo o imenso amor e carinho.

Agradeço ainda a todas as pessoas que, de alguma forma, me ajudaram na realização deste projecto.

ABSTRACT

Cancer represents a public health problem worldwide due to the high incidence, prevalence and mortality in the human population, mainly in developed countries. Adoption of a cancer-associated lifestyle and population aging are considered as the main reasons for the increase in the burden of cancer. Early diagnosis is important since treatment is most effective. The difficulty of diagnosing cancer patients at an early stage of the disease may lead to lower rates of successful treatment, so new diagnostic tools are required. Currently, diagnoses of many types of cancers include only non-invasive examinations and biopsies.

Cancer diagnosis can be very sensitive if based on molecular features, but the lack of molecular tools makes the cancer understanding at this level a difficult task. Elucidating the molecular features of specific tumors can increase our knowledge about the mechanisms underlying disease development and progression.

In this work, cell-based systematic evolution of ligands by exponential enrichment (Cell-SELEX) was used as an approach to evolve aptamers capable of specifically discriminate between human breast carcinoma MDA-MB-435 cells and mouse embryonic fibroblast 3T3 cells, used as non-target cells.

The selected aptamers were characterized taking into account their primary sequences and homologies between them; the conserved domains of secondary structures were also analyzed. Two different sequences, selected against a different breast cancer cell lines, and presenting near 100% homology were used as a comparison when the sequences that target MDA-MB-435 were used.

Then, the carbodiimide methodology was utilized for the conjugation of amine labeled aptamer with silica particles. For the characterization of this ligation, the colorimetric method was used.

Binding assays were performed using FAM (Fluorescein Amidite) aptamer and aptamer-functionalized silica particles. For the aptamer 1A selected for breast cancer cell line MDA-MB-435 results were promising. Hybridization seems to occur with the breast cancer cells visible under microscope or flow cytometry. For the negative control cell line no fluorescence was detected. Unlike, the aptamer 2A did not exhibit fluorescence when incubated with target cells.

This could indicate that aptamer 1A have a good affinity and selectivity to discriminate markers in the cell surface meaning a successful Cell-SELEX for the cell lines in study.

SUMÁRIO

O cancro representa um problema de saúde pública em todo o Mundo devido à sua alta incidência, prevalência e mortalidade na população, principalmente em países desenvolvidos.

A adoção de um estilo de vida de risco e o envelhecimento são consideradas as principais razões para o aumento da incidência do cancro. Um diagnóstico precoce é muito importante para um tratamento mais eficaz. A dificuldade de diagnóstico de um paciente com cancro numa fase inicial da doença pode levar a menores taxas de sucesso do tratamento, por isso novas ferramentas de diagnóstico são necessários. Atualmente, o diagnóstico dos vários tipos de cancro incluem exames não invasivos e biópsias.

O diagnóstico do cancro pode ser muito sensível se baseado em características moleculares, mas a falta de ferramentas moleculares faz com que a compreensão do cancro a este nível seja uma tarefa difícil. A elucidação das características moleculares de tumores específicos pode aumentar o nosso conhecimento acerca de mecanismos subjacentes ao desenvolvimento e progressão da doença.

Neste trabalho foi utilizado o Cell-SELEX para selecionar *aptamers* capazes de especificamente discriminar entre células do carcinoma da mama humano MDA-MB-435 e fibroblastos embrionários de rato 3T3 como células não alvo.

Os *aptamers* selecionados foram caracterizados tendo em conta as suas sequências primárias e as homologias entre elas; também as regiões conservadas das estruturas secundárias foram analisadas. Duas sequências diferentes, selecionadas para uma linha de cancro de mama diferente e apresentando uma homologia de quase 100% foram usadas como comparação onde as sequências com o alvo MDA-MB-435 forem usadas.

Depois, a metodologia de *carbodiimide* foi utilizada para a conjugação do aptamer marcado com partículas de sílica. Para a caracterização desta ligação, um método colorimétrico foi utilizado.

Os ensaios de ligação foram feitos utilizando o aptamer marcado com FAM e as partículas de sílica funcionalizadas com o aptamer. Para o aptamer 1A selecionado para a linha celular MDA-MB-435 os resultados foram promissores. Parece ocorrer hibridização com as células de cancro da mama visíveis quer por microscopia quer por citometria. Para a linha celular de controlo nenhuma fluorescência foi detetada. Ao contrário, o aptamer 2A não apresentou nenhuma fluorescência quando incubado com as células alvo.

Isto pode indicar que o aptamer 1A tem uma boa afinidade e seletividade para descriminar marcadores na superfície das células o que significa um Cell-SELEX bem-sucedido para as linhas celulares em estudo.

TABLE OF CONTENTS

TABLE OF CONTENTS (CONT.)

LIST OF FIGURES

CHAPTER 1: INTRODUCTION

CHAPTER 2: MATERIALS AND METHODS

LIST OF FIGURES (CONT.)

CHAPTER 3: RESULTS AND DISCUSSION

LIST OF FIGURES (CONT.)

LIST OF TABLES

CHAPTER 1: INTRODUCTION

CHAPTER 2: MATERIALS AND METHODS

CHAPTER 3: RESULTS AND DISCUSSION

CHAPTER 6: APPENDIXES

LIST OF ABBREVIATIONS

BB: Binding Buffer

Cell-SELEX: Cell Systematic Evolution of Ligands by Exponential Enrichment

DLS: Dynamic Light Scattering

DMEM: Dulbecco's Modified Eagle Medium

DNA: Deoxyribonucleic acid

dNTPs: Deoxyribonucleotide triphosphate

dsDNA: double strand Deoxyribonucleic acid

EDC: 1-ethyl-3-(3-dimethylaminopropyl)-carbodiimide hydrochloride

EDTA: Ethylenediaminetetraacetic acid

FAM: Fluorescein Amidite

FBS: Fetal Bovine Serum

HPLC: High-Performance Liquid Chromatography

IDT: Integrated DNA Technologies

Kd: Dissociation Constant

LB: Luria-Bertani

MES: 2-(N-morpholino)ethanesulfonic acid

MRI: Resonance imaging

NP: Nanoparticle

OD: Optical Density

PBS: Phosphate Buffered Saline

PCR: Polymerase Chain Reaction

LIST OF ABBREVIATIONS (CONT.)

PEG: Polyethylene Glycol

PI: Propidium Iodide

PLA: Polylactic Acid

PSMA: Prostate Specific Membrane Antigen

QD: Quantum Dot

RNA: Ribonucleic acid

SELEX: Systematic Evolution of Ligands by Exponential Enrichment

SEM: Scanning Electron Microscope

ssDNA: single strand Deoxyribonucleic acid

Sulfo-NHS: N-hydroxysulfosuccinimide sodium salt

TAE: Tris-acetate-EDTA

TEM: Transmission Electron Microscope

WB: Washing Buffer

SCLC: Small Cell Lung Cancer

MOTIVATION AND AIM OF THE PROJECT

Breast cancer is a major public health issue worldwide. It is the second leading cause of cancer death in women, surpassed only by lung cancer. Prognosis and survival rates for this type of cancer differ significantly depending on the cancer stage, type, treatment and geographical location of the patient.

The overall cost for the treatment of patients with breast cancer increases with the more advanced stages of the disease. Therefore, diagnosis of breast cancer at earlier stages is beneficial to the patient and reduces the financial burden associated with treatment. Currently, the diagnosis of breast cancer combines non-invasive examinations, such as mammography, ultrasound or magnetic resonance imaging (MRI) and biopsy tests.

Significant progress has been made in both the detection and treatment of this type of cancer during the last decades; nevertheless it still remains one of the leading causes of death. Early diagnosis and timely treatment have been considered to be the most effective forms to improve survival rate. However, despite the diagnostic improvements, the detection of breast cancer in early stages is still a great challenge. The main drawback is the lack of current molecular contrast agents, which can disclose the presence of early stage malignancies, tracking cell migration, monitoring surgical and pharmacological response.

The aptamers discovery, particularly those selected for binding tumor markers or cancer cells, may offer an excellent solution for cancer early diagnosis and therapy. Aptamer-based diagnostic exhibits a desired selectivity, affinity and specificity, but also shows some distinguished advantages, such as the ability of passing through some barriers and the ease of molecular modification and design.

For these reasons, the aim of the work presented in this thesis consists in using an iterative selection–amplification process known Cell-SELEX methodology to select and identify a panel of new aptamers that, when tested *in vitro*, are capable of recognizing specifically breast cancer cells. The selection experiment will be targeted against the MDA-MB-435 breast carcinoma cell line. Furthermore, the generated aptamers will be equipped and optimized with fluorescent properties, in order to enable their use for diagnosis purposes.

CHAPTER 1

INTRODUCTION

In the last decade, major efforts towards a fast development of anti-cancer therapies have been conducted (Forbes, 2010; Shankar and Pillai, 2011), however many challenges remain and there is still no clear and defined solution to diagnose and treat cancer (Rodrigues and Kluskens, 2011). Most cancers are diagnosed in a late stage thus with reduced treatment effectiveness. This clinical outcome could be greatly improved with an early diagnosis (Shangguan *et al.*, 2008). This is particularly important in breast cancer that is the most common cancer in women worldwide. It is estimated that more than 1.6 million new cases of breast cancer occurred among women worldwide in 2010. It is also the main cause of death for women globally (Forouzanfar *et al.*, 2011).

Cancer cells lead to alterations in the expression of key proteins that result not only in different behaviors of the diseased cells, but also in alterations of the cells at the molecular and morphological levels. Traditionally, cancers are diagnosed mainly based on the morphology and anatomy of tumor cells or tissues using techniques such as MRI, computed tomography and positron emission tomography (Kang *et al.*, 2009). However, these morphological characteristics are difficult to be used if an early diagnosis is envisaged, or if one aims to assess the complex molecular modifications that lead to cancer proliferation. Cancer diagnosis can be extremely specific and highly sensitive if based on molecular features (Shangguan *et al.*, 2006). In this sense, aptamers could serve as an attractive new diagnostic tool.

1.1. Aptamers

Aptamers are oligonucleotides, such as ribonucleic acid (RNA) and single-strand deoxyribonucleic acid (ssDNA), or peptide molecules that can specifically recognize and tightly bind with high affinity a broad variety of targets that range from small ions, single molecules to proteins, and even whole cells (Bunka and Stockley, 2006; Stoltenburg *et al.*, 2007). The oligonucleotide aptamers are 20–80 base pair long which are folded into distinct three-dimensional conformations due to several intramolecular interactions (Kanwar *et al.*, 2011). Based on their three-dimensional structures, the aptamer-target binding occurs due to their specific and complex shape characterized by loops, hairpins, stems, bulges, pseudoknots, triplexes, or quadruplexes (Figure 1.1) (Stoltenburg *et al.*, 2007). This connection results from structure compatibility, stacking of aromatic rings, van der Waals and electrostatic interactions, and hydrogen bonding, or from a combination of these effects (Strehlitz *et al.*, 2012).

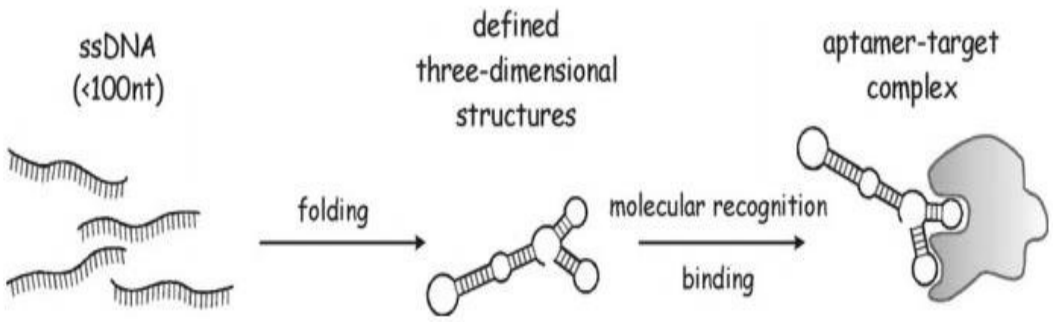

Figure 1.1 - Schematic representation of the functionality of aptamers (Adapted from (Stoltenburg *et al.*, 2007))..

The use of antibodies as the most popular and conventional class of molecules for molecular recognition in a broad range of applications has been around for a long time. Aptamers have become attractive molecules in diagnostics and therapeutics rivaling and, in some cases, surpassing antibodies, because these molecules can overcome some of the weaknesses of antibodies (Han *et al.*, 2010).

The high stability of aptamers is one of its best characteristics. Aptamers are more robust at elevated temperatures and the thermal denaturation of aptamers is a reversible process. Indeed, they maintain their structures over repeated cycles of denaturation/renaturation (Song *et al.*, 2012). Aptamers have the ability of easily recovering their native conformation and can bind to targets after re-annealing, whilst antibodies easily undergo irreversible denaturation (Mascini, 2008). Additionally, they are stable to long-term storage and can be transported at ambient temperature.

Once selected, aptamers can be synthesized in great amounts with great accuracy and reproducibility via a chemical reaction, which is more cost-effective than the production of antibodies. Furthermore, compared to antibodies, aptamers can be more easily modified using chemical methods in order to increase their stability and nuclease resistance, for instance through the incorporation of electrochemical probes, fluorophores or quenchers (Song *et al.*, 2012). At precise locations, several reporter molecules such as fluorescein and biotin can be attached to aptamers.

Another interesting feature is the aptamer's low immunogenicity. Aptamers appear to be moderately immunogenic and toxic, because nucleic acids are typically recognized by the human immune system as non-foreign agents (Song *et al.*, 2012). Moreover, their small size enables the reduction of steric hindrance and increase of the surface coverage during immobilization, and present better tissue penetration as compared to antibodies (Ferreira *et al.*, 2007).

Aptamers can thus be considered as a valid alternative to antibodies and can be regarded as promising substitutes to antibodies in bioassay-related fields. Furthermore, aptamers have been

applied in the study of the mechanisms of interaction with proteins, to find highly efficient and specific inhibitors of proteins, to generate new drugs or targeted delivery systems, or to identify different target molecules for diagnostic purposes (Kulbachinskiy, 2007). Also, by directly blocking protein functions or inhibiting protein-protein interactions, such as receptor-ligand interactions, and thus functioning as antagonists, various aptamers have been pointed as promising therapeutic agents for several diseases, including cancer (Zhou and Rossi, 2009). Extraordinary progress has been achieved by linking cell-internalizing aptamers that recognize cell-specific receptors of a target cell with other molecules of interest (anti-cancer drugs, toxins, siRNA), hence promoting specific cellular uptake via receptor-mediated endocytosis (Hu *et al.*, 2012).

Since aptamers can be selected against almost any target, the possible diagnostic and therapeutic applications range far and wide. The versatility of aptamers is reflected in the fact that there are very few life science research areas to which aptamers cannot be applied (Dua *et al.*, 2011; Famulok and Mayer, 2011; Song *et al.*, 2012; Stoltenburg *et al.*, 2007).

1.1.1. Aptamer Selection

The identification of rare nucleic acid sequences with unique properties from very large random sequence oligonucleotide libraries was first described in 1990 (Ellington and Szostak, 1990; Tuerk and Gold, 1990). These aptamers can be selected by combinatorial chemistry techniques called SELEX (Systematic Evolution of Ligands by Exponential Enrichment) or Cell-SELEX.

Aptamer selection by SELEX

The SELEX technology is widely applied as an *in vitro* selection method to evolve aptamers with new functionalities. This technology is a combinatorial chemistry technique for producing either ssDNA or RNA oligonucleotides that specifically bind to a target ligand or ligands (Tuerk and Gold, 1990).

Many aptamers have been generated against a diversity of targets, including small compounds to large multi-domain proteins (Stoltenburg *et al.*, 2007). Although SELEX is normally carried out using highly purified target molecules, complex heterogeneous targets can also be used for the generation of specific aptamers (Ohuchi, 2012).

Aptamer selection by Cell-SELEX

Aptamers that specifically target proteins on the cell surface or specific cancer cell types, even when the biomarker is not known, can also be generated using a slightly different methodology. Selection can be pursued through Cell-SELEX, which is a molecular tool for cell studies, including cancer. Cell-SELEX is becoming an emerging methodology in which live cells are used to select aptamers for target recognition, without the requirement of prior knowledge of the target (Jiang *et al.*, 2003). In this methodology, oligonucleotides can potentially link to any molecule exposed in the cell surface (Zhang *et al.*, 2010b).

The experimental procedure of the Cell-SELEX methodology is schematized in Figure 1.2.

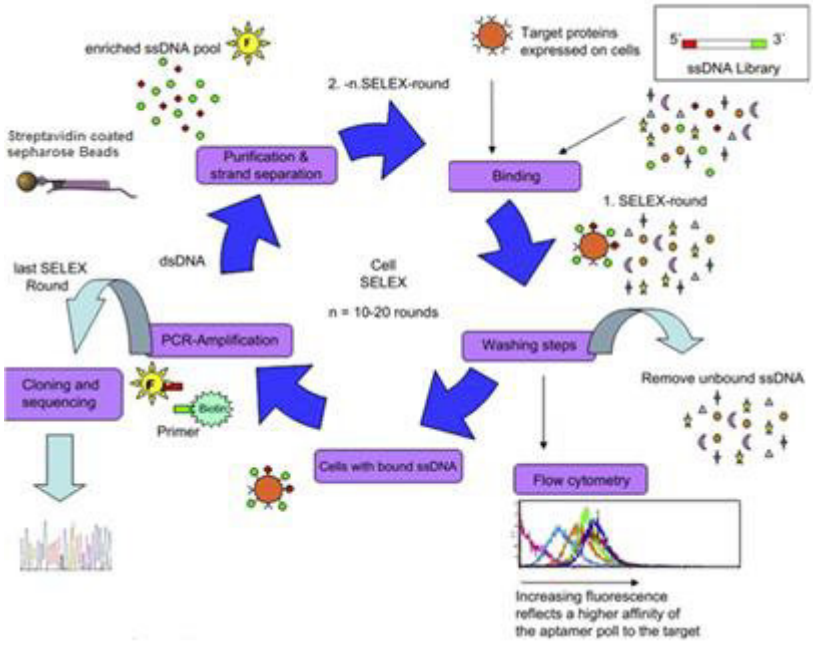

Figure 1.2 - Schematic drawing of the Cell-SELEX methodology. Aptamers are selected through selection cycles comprising three steps: selection, counter selection and amplification (Adapted from (Avci-Adali *et al.*, 2008)).

To generate aptamers that specifically target cancer cells, a library of ssDNA is required (Shangguan *et al.*, 2006). This library consists of millions different sequences of ssDNA.

First, the ssDNA pool is incubated with the target cells. After washing, the DNA strands bound to the target cell surface are collected and afterwards are incubated with the negative control cells. These negative control cells are usually normal cells (non-cancer cells). The DNA sequences able to bind the negative control cells are discarded. This step is very important because several proteins on cancer cell surfaces are also expressed by normal cells and therefore, any aptamer

binding to them will not be specific for the cancer cells. The remaining sequences are then kept and amplified for the following round of selection. When the selected pool is sufficiently enriched, the Polymerase Chain Reaction (PCR) product of the evolved pool is cloned and sequenced for aptamer identification (Zhang *et al.*, 2010).Typically, approximately 10 to 20 rounds of Cell-SELEX are needed to isolate aptamers with the highest affinity and selectivity to the target cells (Fang and Tan, 2010; Kunii *et al.*, 2011; Ye *et al.*, 2012).

A large number of aptamer probes have been successfully chosen from Cell-SELEX for different types of cancer cells. Sefah and collaborators (Sefah *et al.*, 2009) found one aptamer that showed important selectivity to the target acute myeloid leukemia cell line and that could identify the target cells within a complex mixture of normal bone marrow aspirates. In addition, a series of aptamers that bind to two types of ovarian cancer cells, namely against ovarian clear cell adenocarcinomas and ovarian serous adenocarcinomas, has been selected (Van Simaeys *et al.*, 2010).

Recently, a DNA aptamer that recognizes SBC3, an adherent small cell lung cancer (SCLC) cell line, was selected using Cell-SELEX. The aptamer can be a potential and useful SBC3-specific marker since this cell line does not express the common biomarker pro-GRP that is commonly used to diagnose SCLC (Kunii *et al.*, 2011).

The Cell-SELEX methodology has been successfully used to raise aptamers against many other types of cancer (Jiménez *et al.*, 2012; Sefah *et al.*, 2010a; Zhang *et al.*, 2012a).

1.1.2. Aptamers modification

Although aptamers are exceptional agents, there are some issues that have to be solved to enable their use in practical applications. One problem is that aptamers are susceptible to nuclease degradation. This issue is more relevant for RNA aptamers, because these molecules are less stable to hydrolysis whenever in contact with biological fluids (Lee *et al.*, 2010). To overcome this hurdle, some chemical modifications can be done to increase the biostability of the chosen aptamers. Also, changes can be introduced to optimize binding parameters to the target or relevant molecules. The two essential regions with increased susceptibility are the phosphodiester backbone and the 5′ and 3′-termini.

Some altered oligonucleotides can be incorporated within the aptamer, either during or after selection, for improved stability. Several chemical modifications introduced in the selection step

include 2'-fluoro pyrimidines and 2'-amino pyrimidines. Certain modified nucleotide triphosphates, especially 2'-O-modified pyrimidines, can also be competently incorporated into the aptamer by T7 RNA polymerases. It is very important to incorporate these modified nucleotides during the selection process, since they can ultimately affect aptamer binding affinity and folding.

After selection, further modifications as the chemical incorporation of 2'-O-methyl ribose purines and pyrimidines can be performed. However, it is important to notice that post-selection modifications can negatively affect the aptamer activity, so additional alterations must be first tested (Lee *et al.*, 2010; Ni and Castanares, 2011).

Other important modifications, such as the use of Locked-Nucleic Acids (LNAs) modified RNA nucleotides, hold an important promise to stabilize aptamers, because of their increased thermostability and brilliant mismatch discrimination when hybridized with DNA or RNA. Moreover, they are resistant to degradation by nucleases (Stoltenburg *et al.*, 2007).

Furthermore, some nanomaterials can protect the oligonucleotides from nuclease digestion and competently deliver them into cells, further improving the possibility of aptamers for intracellular imaging (Aravind *et al.*, 2012a, 2012b; Bagalkot *et al.*, 2007; Lee *et al.*, 2010; Li *et al.*, 2012).

In addition to modifications towards the improvement of nuclease stability, other chemical alterations can be used, such as polyethylene glycol (PEG) for reduced systemic clearance rates and prolonged circulation half-life *in vivo* (Aravind *et al.* 2012a; Stoltenburg *et al.* 2007).

Figure 1.3 presents an overview on the modifications that can be incorporated during the selection step of the Cell-SELEX methodology.

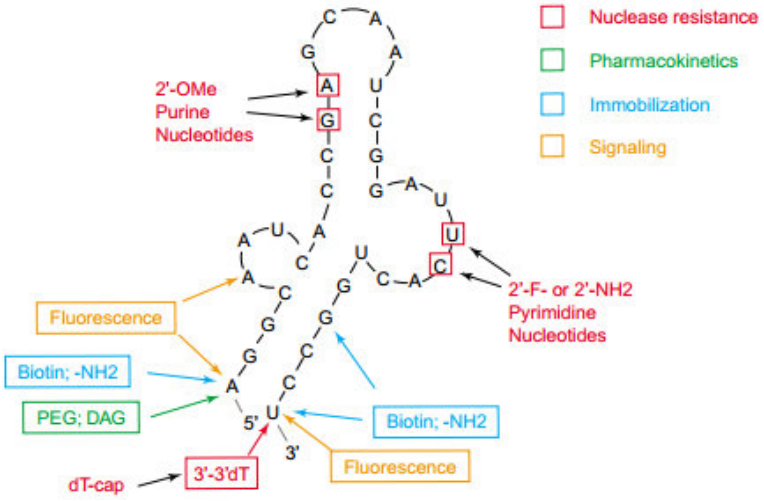

Figure 1.3 – Different types of chemical modifications (Taken from (Blank and Blind, 2005)).

1.1.3. Aptamers applications

Aptamers have attracted the attention of many scientists, because they not only possess all the advantages of the antibodies, but they also have unique merits. With these considerations, it is easy to understand the use of aptamers in almost every aspect of molecular biology and biosensing, particularly wherever antibodies have been traditionally used. Furthermore, aptamers can be used for both basic research and clinical purposes as macromolecular drugs.

Aptamers as therapeutic agents

Therapeutic agents are typically small organic molecules that fit into slits on the surface of their target macromolecule, forming an intricate network of stabilizing interactions (Tu *et al.*, 2005; Varghese *et al.*, 1995). Aptamers can fill the roles of many therapeutic agents. These molecules can also fit into crevices on macromolecules and can fold to form slits into which prominent parts of the target protein can link. This enhances the number of contacts made with the target, permitting aptamers to form more specific interactions than other smaller molecules (Bunka and Stockley, 2006). These aspects can greatly increase the potential therapeutic usage of aptamers.

Since aptamers can be virtually selected against any target, their mode of action is strongly dependent on their target. In most cases, the aptamer-target binding inhibits its biological activity, due to the interference with the enzymatic catalytic site, or to the ligand-receptor recognition sites, or possibly to the induction of allosteric effects with subsequent loss of function (Missailidis and Hardy, 2009; Ulrich and Wrenger, 2009). Due to this ability to promote the target loss of function, aptamers have found a niche in virtually every area of pathology, including virology (Proske *et al.*, 2005), vaccine production (Becker and Becker, 2006; Lee *et al.*, 2006), oncology (Pestourie *et al.*, 2005) and parasitology (Adler *et al.*, 2008; Missailidis and Perkins, 2007).

Up to now, aptamer commercialization is limited to only one aptamer-based drug receiving Food and Drug Administration (FDA) approval (Ng *et al.*, 2006), however their uniqueness constitutes a great promise to the medical field. Table 1.1 highlights the current development of aptamers used for therapeutic purposes and their clinical study status.

Table 1.1 - Current aptamers in various stages of clinical development.

Aptamer (Company)	Aptamer type	Target	Phase	Clinical Application	References
Pegaptanib (Pfizer/Eyetech)	RNA	VEGF	Phase II	Macular degeneration	(Chakravarthy *et al.*, 2006; Gragoudas *et al.*, 2004; Ng *et al.*, 2006)
AS1411 (Antisoma)	DNA	Nucleotin	Phase II	Acute Myeloid Leukemia	(Bates *et al.*, 2009; Mongelard and Bouvet, 2010; Teng *et al.*, 2007)
REG1 (Regado Biosciences)	RNA	Coagulation Factor IX	Phase II	Coronary Artery Disease	(Becker and Chan, 2009; Chan *et al.*, 2008)
ARC1779 (Archemix)	DNA	vWF	Phase II	Purpura, Thrombotic Thrombocytopenic	(Diener *et al.*, 2009; Gilbert *et al.*, 2007)
NU172 (ARCA biopharma)	DNA	Thrombin	Phase II	Heart Disease	(Waters *et al.*,2009)
NOX-A12 (NOXXON Pharma)	RNA	CXCL12	Phase I	Hematopoietic Stem Cell Transplantation	(Sayyed *et al.*, 2009)
NOX-E36 (NOXXON Pharma	RNA	CCL2	Phase I	Type 2 Diabetes Mellitus	(Kulkarni *et al.*, 2009; Maasch *et al.*, 2008)
ARC1905 (Ophthotech)	RNA	C5	Phase I	Age-Related Macular Degeneration	(Goebl *et al.*, 2007)
E10030 (Ophthotech)	DNA	PDGF	Phase II	Age-Related Macular Degeneration	http://clinicaltrials.gov/show/NCT01089517

Aptamers can be developed to adjust to specific pathological or physiological conditions such as pH or specific factors to the target, such as cells, during the *in vitro* selection process, thus making them stable for *in vivo* usage.

Delivery of therapeutic aptamers

Therapeutic targets can be divided into two main classes; extracellular targets, such as invading viruses and intracellular targets, such as transcription factors.

Aptamers to extracellular targets can be administered subcutaneously or intravenously. Pharmacokinetic studies in humans corroborate that RNAs delivered by these routes are promptly spread throughout the body and taken up by cells in an easy way (Sandberg *et al.*, 2000). The aptamers can be made in their stable functional state and injected directly into the patient. Nevertheless, RNA clearance and degradation is unavoidable, and repeated administration is necessary until treatment is complete. Delivery of aptamers to intracellular targets has been achieved mainly by its expression from viral-based vector systems or by its incorporation into liposome vesicles (Bunka and Stockley, 2006).

Liposomes are the most well-reported and successful drug-delivery systems (Cao *et al.*, 2009; Kang *et al.*, 2010; Mann and Bhavane, 2011). They have been shown to increase the residence time of aptamers in the bloodstream (Willis *et al.*, 1998). Previous efforts on liposomal drug delivery have focused on developing long-circulating liposomes that target tumor tissues (Maeda *et al.*, 2000).

Although aptamers have been very effective *in vitro*, most of them cannot be taken up by cells without external assistance. Naturally, internalization ability is central for the application of aptamers *in vivo*, particularly in targeted drug delivery.

Targeted drug delivery is principally significant in cancer treatment as many anti-cancer drugs are non-specific and highly toxic to both normal and cancer cells (Tan *et al.*, 2011), thus yielding global systemic toxicity with only a modest improvement in patient survival.

One example of the relevance of the aptamers in the delivery of drug molecules to treat cancer was described by Chu and co-workers (Chu *et al.* 2006). The aptamer anti-PSMA conjugated with the recombinant plant toxin gelonin can be used to deliver the toxin to specific prostate cancer cells that overexpress the biomarker PSMA. Aptamer-toxin conjugates show potency of at least 600 fold higher than cells that do not express PSMA. As suggested by the results, the aptamers can be very useful for target specific treatment in cancer.

Figure 1.4 gives a schematic overview of an aptamer conjugated with nanoparticle for delivery of drugs in cancer treatment.

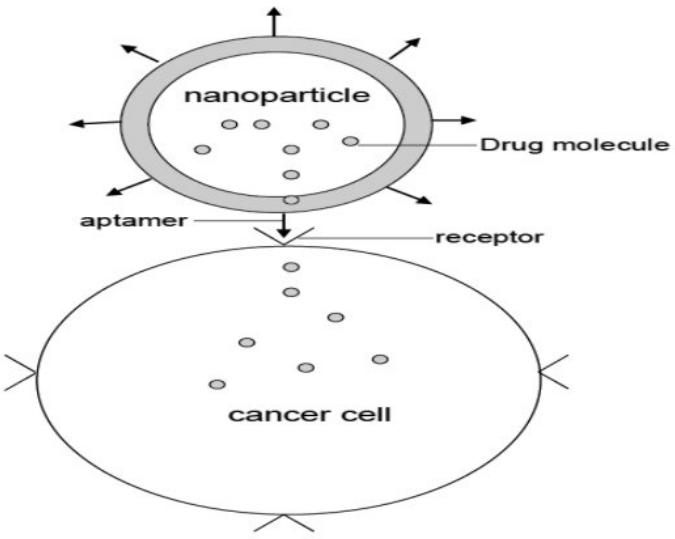

Figure 1.4 - Aptamer conjugated nanoparticle for delivery of drugs to treat cancer (Taken from (Stalin and Dineshkumar, 2012)).

Aptamers for Diagnostic Assays

Another biomedical application of aptamers is in the diagnosis of diseases given their high affinity and specific nature against their target molecules as previously mentioned.

For diagnostic purposes, the aptamer should recognize and bind to a specific target, while for therapeutic uses the aptamer should be in addition a function-blocking compound and be capable to directly interrupt the disease process (Cerchia *et al.*, 2002).

Aptamers have the ability to differentiate tumor from normal cells by identifying molecular level differences, and they can even distinguish cancer cells by stage of development, by type or by patient profile. These differences have a great importance in aiding the understanding of the biological processes and mechanisms of disease development (Guo *et al.*, 2008; Medley *et al.*, 2011; Shangguan *et al.*, 2006)

Shangguan and co-workers (Shangguan *et al.*, 2006) reported a methodology for the identification of molecular signatures, also called biomarkers (biological molecules that are indicators of physiologic state and also of alteration during a disease process) on the surface of targeted cells using the differences at the molecular level among two different types of cells. Several aptamers have been generated for the particular recognition of leukemia cells. The chosen aptamers can specifically identify target leukemia cells mixed with human bone marrow, and can also recognize cancer cells strictly related to the target cell line in real clinical specimens.

As previously mentioned, based on molecular differences of unknown membrane proteins present on diseased cells compared with normal cells, aptamers can be used to selectively identify different types of cells. Thus, it is expected that new biomarkers can be found as long as the aptamers target protein can be identified (Ye *et al.*, 2012). The new biomarkers discovery not only leads to a better understanding of the disease processes and mechanisms involved, but also is of great clinical value for early detection and fast treatment.

Other applications

The aptamers may also be used for a variety of applications which have not yet been described. Protein purification is one of them. Purification of natural forms of proteins can be reached with aptamers using fewer steps and with high affinity for the protein comparing with the conventional protein purification methods that involve the modification of targeting protein with tags.

The subsequent tag-cleavage steps can frequently affect the folding, structure, capability and so on (Kanoatov *et al.*, 2011).

The recognition of proteins with great affinity and selectivity by aptamers allows the detection of proteins immobilized on a membrane. Gold and co-workers (Bock *et al.*, 2004) have established an aptamer-based microarray permitting immobilized aptamers to be cross-linked with target protein. The microarray system recognizes a broad range of proteins at several concentrations.

Combating infectious agents is another application in which aptamers are widely used. This type of molecules can be used as target-specific anti-infectious agents. They can selectively disrupt membrane functions or inhibit a crucial protein (Dey *et al.*, 2005; Misono and Kumar, 2005).

1.2. Nanoparticles

Bionanotechnology is defined by its ability to work at the molecular level, combining rules of physics and biological materials, chemistry and genetics to create synthetic structures. The result is the generation of a highly functional world of biosensors, microchips, molecular 'switches', and others, all developed in ways that permit these structures to self-assemble. On the other hand, disease diagnosis and treatment progresses are dependent on the understanding of biochemical processes. As previously mentioned, diseases can be recognized based on anomalies at the molecular level and the treatments are designed based on activities in quite low dimensions. Therefore, the use of research tools with dimensions near to the molecular level would be ideal to better understand the mechanisms involved in the processes (Tan *et al.*, 2004).These tools can be nanoparticles (NPs), nanoprobes, or other nanomaterials in small dimensions.

NPs hold great potential because of their high surface-to-volume ratio, unique optical qualities and other size-dependent properties. NPs show also exceptional physical features as particle aggregation, electrical and heat conductivities; and chemical qualities. When combined with surface modifications these properties provide probes for highly selective bioassays (Liu, 2006).

NPs are able to enhance binding affinity and increase the signal strength, multivalent binding, instead of single-aptamer binding, thereby NPs will greatly help detection (Lee *et al.*, 2010; Zhang *et al.*, 2010a). Signal transduction elements are accountable for converting molecular recognition events into detectable signals such as color, fluorescence, electrochemical signals and magnetic resonance image changes (Chiu and Huang, 2009).

The incorporation into NPs of functional aptamers has become a new field that aims at providing novel hybrid sensing systems (sensors) for molecular recognition. This new combination has produced several types of sensors for sensitive and selective detection. Sensors are devices that respond to chemical or physical stimuli and generate a measurable signal. A sensor requires at least two steps to work properly: target recognition and signal transduction. The target recognition element can be any biological or chemical entity like proteins, peptides or aptamers (Lee *et al.*, 2010). The development of general methods to convert the highly specific molecular recognition between aptamers and their targets into detectable signals is highly desirable. Conjugation of aptamers with nanomaterials can be the ideal solution.

In the latest years, with the development of the nanotechnology field, some NPs have been designed and currently play central roles in many fields. Some NPs, such as fluorescent silica nanoparticles, quantum dots, polymeric nanoparticles, magnetic nanoparticles, metallic nanoparticles among others, can be functionalized with desired biomolecules to form probes for sensitive bioassays and also constitute signal transduction elements commonly used (Figure 1.5) (Chan, 1998; Chiu and Huang, 2009; Herr *et al.*, 2006; Jayasena, 1999; Tan *et al.*, 2004; Tombelli *et al.*, 2005; Zhang *et al.*. 2010a).

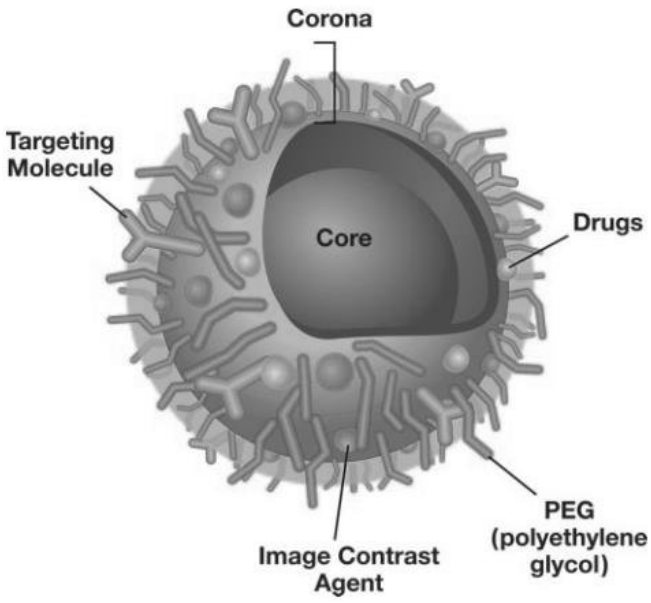

Figure 1.5 – Multifunctional nanoparticle. The nanoparticle 'corona' can be functionalized with hydrophilic polymers, targeting molecules, therapeutic drugs and image contrast agents (Taken from (McNeil, 2005)).

1.2.1. Quantum dots

Quantum dots (QDs) are representative fluorescent nanoparticle probes with increasing research interest and are one type of fluorescent NPs-based sensors with several unique optical properties (Alivisatos, 1996). QDs are ultra-small (usually 1–10 nm in diameter), bright (20 times brighter than most organic fluorophores) and highly photostable (Zrazhevskiy *et al.*, 2010). Their high resistance to photobleaching and their brightness make them appealing for cellular and tissue imaging (Medintz *et al.*, 2005).

However, these NPs present some drawbacks. QDs are difficult to fabricate and the chemistry involved in their surface modification is still under investigation (Medintz *et al.*, 2005; Zrazhevskiy *et al.*, 2010). Despite recent progress, much work still needs to be done to achieve reproducible and robust surface functionalization and also to develop flexible bioconjugation techniques, yet the superiority of QDs over other fluorescent labels for certain biological applications still makes them one of the most interesting fluorescent probes.

By combining the excellent fluorescence properties of QDs with the high affinity and specificity of aptamers, Cui and co-workers (Cui *et al.*, 2011) constructed a QD–aptamer probe that specifically recognizes and labels the influenza A virus. This QD labeling technique provides a new strategy for labeling virus particles for virus detection and imaging. QDs conjugated to PSMA aptamer A9 was shown to selectively label PSMA-positive cells, while showing minimum binding to the PSMA-negative cell line in culture (Chu *et al.*, 2006b).

1.2.2. Gold nanoparticles

Regarding gold NPs, it is well known that this material has uncommon optical and electronic properties, biological compatibility, high stability, controllable morphology and size dispersion, as well as an easy surface functionalization (Sperling *et al.*, 2008; Yang *et al.*, 2011). There are many reports in the literature that refer the use of aptamer-gold hybrids. For example, Huang and collaborators (Huang *et al.*, 2005) developed a specific system for platelet-derived growth factors (PDGFs) and platelet-derived growth factor receptors (PDGFR) that uses gold NPs altered with an aptamer that is specific to PDGFs and used them to detect PDGFs. The same authors (Huang *et al.*, 2009) further showed the potential use of aptamers conjugated with gold NPs for breast cancer cell detection. Their results suggest that the aptamer bioconjugated NPs may be suitable for use in breast cancer therapy.

1.2.3. Magnetic nanoparticles

The majority of magnetic nanoparticle systems use inorganic nanocrystals as their magnetic cores. These NPs exhibit two important features, namely specificity and magnetism. As such, they can interact with an external magnetic field and are ideal media for the manipulation of biological materials, the targeted delivery of therapeutic compounds (Dobson, 2006) and for hyperthermia treatment (Hergt *et al.*, 2006).

Aptamer-functionalized magnetic NPs have been used for small molecule and protein detection. Yigit and co-workers (Yigit *et al.*, 2007) assembled superparamagnetic iron oxide NPs and aptamers for the detection of human R-thrombin protein.

1.2.4. Polymers

A wide variety of polymer carriers have been designed for use as drug transporters. The polymer can be of synthetic or natural source and self-assembled or synthetically cross-linked. Chemical structures like polylactic acid (PLA), PEG, poly(lactate-glycolate) (PLGA) and poly (hydroxyethyl starch) (HES) constitute the most common polymer types used in the design of therapeutic bioconjugates (Hermanson, 2008). Some of them have been used to carry only a chemotherapeutic agent without a targeting molecule while others have incorporated affinity binding agents to gain specificity for the particular cell or tissue type being targeted.

The purpose of polymer coupling is to modify the properties of the attached drug or biomolecule *in vivo* in order to make it more soluble or to protect it from renal filtration, thus promoting their persistence in circulation (Fishburn, 2008). In other cases, the objective is to link multiple copies of the drug to one bioconjugated and thus gain additional therapeutic efficacy at the targeted tumor or tissue.

Conjugation to synthetic polymers such as PEG or PLA is frequently used in order to improve the performance of aptamers as therapeutic agents (Farokhzad *et al.*, 2004).

1.2.5. Silica particles

In bioanalysis, silica has a widespread use in biosensors and biochips. Silica can be synthesized to prepare NPs and is governed by the chemical properties of the surface, which are based on the silanols and siloxane (Spange, 2000).

Silica NPs are considered to be non-toxic delivery carriers for controlled release of numerous therapeutic and imaging agents in biological applications. These particles are often an exceptional choice for drug delivery among the inorganic nanoparticles mainly due to their high stability, rigidity, uniform and tunable pore sizes, biocompatibility, chemical versatility, optical transparency, high surface areas, large pore volumes, controllable surface functionalization and resistance to microbial attacks (Yang, 2011). Additionally, these particles are amenable to surface modification with a diversity of organic functionalities, such as amines, thiols, carboxylic acids, alkoxy groups, and aromatic groups resulting in highly useful organic–inorganic hybrid materials (Descalzo *et al.*, 2006; Klajn *et al.*, 2010) which are considered to be promising nanocarriers for targeted drug delivery.

The flexibility and versatility of silica in synthesis procedures, as well as in surface modifications offers a great advantage to the use of this material in bioanalysis.

Cai and co-workers (Cai *et al.*, 2012) develop three effective probes of aptamer-conjugated silica NPs for human breast carcinoma MCF-7 cells successful labeling.

Synthesis and Characterization

Silica based NPs can be prepared through a wide variety of techniques. There are two general ways. The first is the Stöber method (Figure 1.6-A) (Stöber *et al.*, 1968). Basically, this method consists in silica alkoxide precursor hydrolysis in a mixture of ethanol and aqueous ammonium hydroxide. During hydrolysis, silica particles with nanometer sizes are produced (Shibata *et al.*, 1997).

The second method that can be used is the reverse or water–in-oil microemulsion (Figure 1.6-B) (Santra *et al.*, 2001; Zhao *et al.*, 2003). This method is a robust and efficient way to prepare NPs. Furthermore, it is based on the formation of a stable dispersion of two immiscible fluids (water and oil). The system is stabilized by an added surfactant. These three main components make up the main reaction mixture: water, surfactant, and oil (Tan *et al.*, 2004).

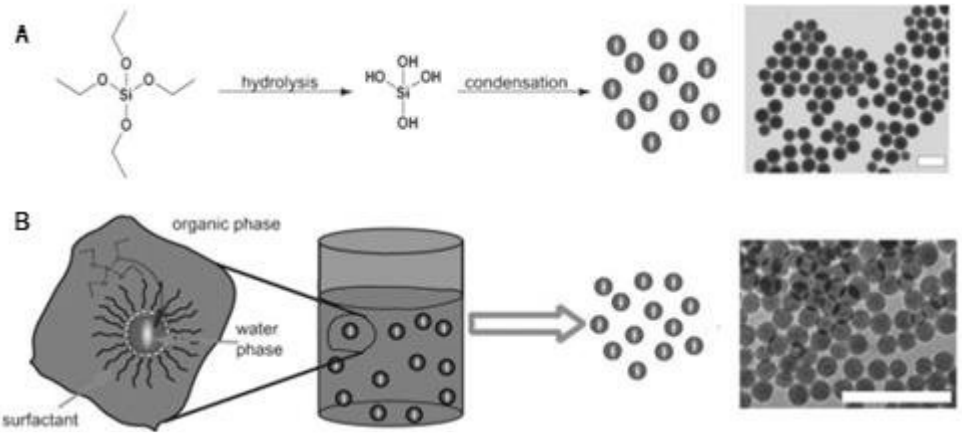

Figure 1.6 - Methods for synthesizing silica nanoparticles. (A) The Stöber method. TEM micrograph shows 125 nm silica nanoparticles. (B) The reverse phase microemulsion. TEM micrograph shows 37 nm silica nanoparticles. The scale bars represents 200 nm (Taken from (Taylor-Pashow *et al.*, 2010)).

The characterization of NPs is important to elucidate the mechanism of nanoparticle formation and also to validate the synthesis protocols. Normally, particle characterization includes the measurement of particle size, surface charge, surface functionality, and optical and spectral features. NPs can be evaluated by their size using transmission electron microscopy (TEM) or scanning electron microscopy (SEM).

Dye-Doped Silica NPs

Silica-based NPs are currently used in many areas because they enable unique applications in bioanalysis and bioseparation. A large number of dye molecules can be incorporated inside a single silica particle producing a highly amplified optical signal compared with a single dye molecule (Tan *et al.*, 2004).

If used correctly, dye-doped silica NPs can provide a great improvement in analytical sensitivity. These nanoparticles contain a large amount of dye molecules trapped inside a silica matrix, and they exhibit an extraordinary signaling strength signal. More than 10000 dye molecules are assumed to be doped inside a 60 nm nanoparticle (Wang *et al.*, 2006).

Moreover, the silica matrix serves as an effective barrier limiting the effect of the outside environment on the fluorescent dye contained in the NPs, thus both photobleaching and photodegradation phenomena that often affect conventional dyes can be minimized (Cai *et al.*,

2012). The great photostability makes these NPs suitable for uses where high intensity or prolonged excitations are needed. ′

The silica chemistry flexibility providing versatile routes for surface modification, as well as the aforementioned brightness and fluorescence photostability over time makes the dye-doped silica a great promise for various biological applications.

1.3. Bioconjugation methodologies

Every conjugation process involves the reaction of one functional group with another. The creation of bioconjugated reagents with selectively or spontaneously reactive functional groups creates the basis for crosslinking of target molecules (Hermanson, 2008). Covalent bioconjugation strategies are more employed than physical adsorption methodology's in order to avoid non-specific adsorption and desorption of the NPs on the biomolecule surface towards a more effective control of the biological moieties (Bae *et al.*, 2012).

Regarding the silica NPs and taking into consideration the versatility of Si chemistry, various reactive functional groups such as amines, thiols and carboxyls, are often introduced by attachment to additional silica coating layers for use as linker molecules, which can provide reaction sites for bioconjugation. The use of additional silica coating that contains suitable functional groups is known as post-coating. These surface modifications enable silica NPs to be conjugated with a large variety of biological molecules such as proteins, enzymes, aptamers, antibodies, among others, through standard conjugation protocols. (Tan *et al.*, 2004).The chemical methods for immobilization of aptamers are all based on methodologies already developed for immobilization of DNA and other biomolecules (Balamurugan *et al.*, 2008).

1.3.1. Carbodiimide Chemistry

A rapid and easy conjugation methodology of biomolecules to NPs surfaces is based on the 1-ethyl-3-(3-dimethylaminopropyl)-carbodiimide hydrochloride (EDC) / N-hydroxysuccinimide (NHS) activation of the carboxylic acid groups on particle surfaces followed by reaction with amino groups of the biomolecule (Figure 1.7 and Figure1.8-A).

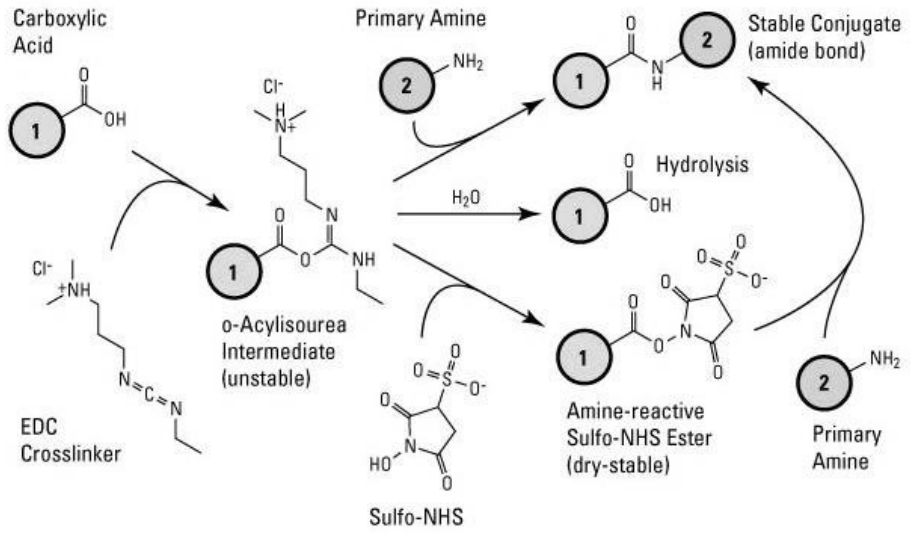

Figure 1.7 - Sulfo-NHS plus EDC crosslinking reaction scheme. Carboxyl to amine crosslinking using the EDC and sulfo-NHS. Addition of Sulfo-NHS to EDC reactions (bottom-most pathway) increases efficiency and enables NP (1) to be activated (Taken from (http://www.piercenet.com/product/nhs-sulfo-nhs)).

EDC and other carbodiimides are zero-length crosslinkers; and can cause direct crosslink of carboxylates (–COOH) to primary amines (–NH_2) without becoming part of the final crosslink between target molecules. EDC reacts with the -COOH group and activates it to form an active O-acylisourea intermediate, allowing it to be coupled to the amino group in the reaction mixture. An EDC by-product is released as a soluble urea derivative after displacement by the nucleophile.

The O-acylisourea intermediate is unstable in aqueous solutions and the failure to react with an amine results in hydrolysis of the intermediate, regeneration of the carboxyls and the release of an N-unsubstituted urea.

NHS or its analog Sulfo-NHS is often included in EDC-coupling protocols to improve efficiency. EDC couples NHS to carboxyls, resulting in an NHS-activated site on a molecule (Nakajima and Ikada, 1995; Staros *et al.*, 1986).

1.3.2. Disulfide-coupling chemistry

In chemistry, a disulfide bond is a covalent bond normally derived by the coupling of two thiol groups (Figure 1.8-B). The disulfide-coupling chemistry has been used for the immobilization of oligonucleotides onto silica NPs (Hilliard *et al.*, 2002), whereby these particles are silanized with 3-mercaptopropyltrimethoxysilane. The reaction permits the conjugation of the thiol-

modified silica NPs to the disulfide-modified oligonucleotides. These disulfide-modified oligonucleotides are then directly linked to the silane-activated silica surface (Bae *et al.*, 2012).

1.3.3. Maleimide–thiol coupling

An effective methodology for the coupling of proteins, antibodies, aptamers or other biomolecules to particle surfaces is based on the reaction of maleimide functionalized particles with thiolated biomolecules (Figure 1.8-C) (DeNardo *et al.*, 2005; Natarajan *et al.*, 2008). This method leads to an ideal orientation of the immobilized biomolecules and conserves their biological functionality in a high level (Grüttner *et al.*, 2007).

1.3.4. Click Reactions

The concept of click-chemistry consists of 'spring-load'-like chemical reactions that occur in a spontaneous way and with high selectivity and yield between stable functional groups (Figure 1.8-D) (Kolb *et al.*, 2001). Perhaps, the most normal example of such reactions is the one occurring between alkyne and azide moieties (Rostovtsev *et al.*, 2002).

The selective reaction of terminal alkyne groups on silica NPs surface with azide groups of biomolecules leads to a covalent conjugation by triazole formation in aqueous solution (Bae *et al.*, 2012).

1.3.5. Non-covalent chemistry

Apart from covalent conjugation chemistry, affinity-based systems found in nature have attracted increasing attention during the last years. Probably the most well-known and well-reported example of receptor-ligand for the binding of DNA to nanoparticles is the avidin–biotin system (Figure 1.8-E) (Green, 1975; Wilchek and Bayer, 1988).

The strong bond and specificity of the avidin-biotin system has allowed it usage for a vast number of applications (Sperling and Parak, 2010).

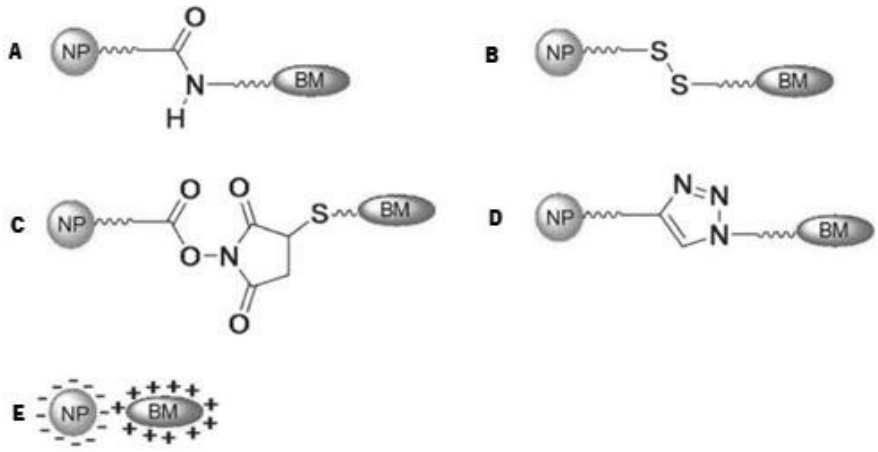

Figure 1.8 – Bioconjugation strategies for attachment of biomolecules to the surface of NPs (Taken from (Bae *et al.*, 2012)).

Common to all chemical surface modification schemes involving functional groups that are present on the NP surface is that they predominantly depend on the ligand or surface coating, and not on the actual inorganic core material. Therefore, provided that the NPs are stable under the reaction condition, identical chemical routes for functionalization are apply for gold nanoparticles, quantum dots or magnetic particles, as well as for silica NPs.

Accurate and sensitive diagnosis is very important in the early stages of tumor in order to ease the choice of effective therapeutic pathways and improve clinical outcomes. However, the detection of malignant cells needs probes able of differentiating the exclusive features of target cells at the molecular level. Aptamers have appeared as a powerful class of ligands for specific biomolecular targeting. In parallel, the development of NPs as aptamer bioconjugates has enhanced the interest of using aptamer-nanoparticle conjugates as potential diagnostic vehicle. By joining such NPs with cancer-related aptamers, a novel class of bioconjugates is emerging.

CHAPTER 2

MATERIALS AND METHODS

2.1. Cell-SELEX

2.1.1. Cell Lines and Buffers

The cell lines used for aptamer selection and counter-selection were MDA-MB-435S (human breast carcinoma) (Figure 2.1-A1, 2.1-A2) and 3T3 (mouse embryonic fibroblast) (Figure 2.1-B1, 2.1-B2) respectively. Both cell lines were kindly supplied by IPATIMUP, Portugal.

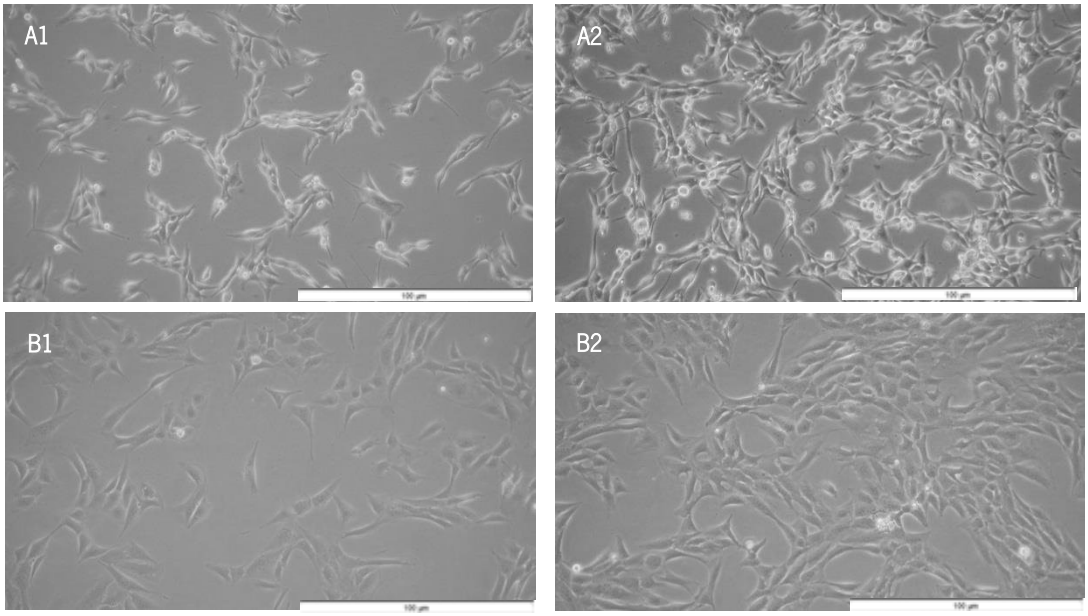

Figure 2.1 – Cell lines used to perform Cell-SELEX. (A1) and (A2) represent low and high density respectively of MDA-MB-435S cells. (B1) and (B2) represent 3T3 cell line with respectively low and high confluence. The imaging of cells was performed with an inverted microscope Leica DMIL (Scale bar 100 µm).

Culture reagents were all supplied by Biochrom, except where mentioned otherwise. Both cell lines were cultured in Dulbecco's Modified Eagle Medium (DMEM) supplemented with 10% (v/v) Fetal Bovine Serum (FBS) and 1% (v/v) of penicillin-streptomycin on tissue culture treated flasks.

Cells were incubated at 37°C and 5% CO_2 humid atmosphere (Hera Cell incubator). Sub-culturing was done when cell confluence reached approximately 80% and was typically sub-cultured at a 1:2 or 1:3 flask ratio. Phosphate Buffered Saline (PBS 1x: 137 mM Sodium Choride [Panreac], 10 mM Sodium Phospate Dibasic [Scharlau], 2.7 mM Potassium Chloride (AppliChem) and Potassium Phosphate Monobaisic [Riedel de Haën]) at pH=7.4 was used to wash cells and trypsin-Ethylenediaminetetraacetic acid (EDTA) was added to detach adherent cells before sub-culturing.

During the selection (section 2.1.5), cells were washed before and after incubation with wash buffer (WB), that were composed by DMEM supplemented with 10% (v/v) of FBS and 1% (v/v) of antibiotic. Binding buffer (BB) used for selection was the same of WB in first cycle of Cell-SELEX. In

second cycle to fifth the WB was complemented with more 10% (v/v) of FBS. From the fifth cycle, to the mixture was added 20% (v/v) of FBS. The increased amount of FBS was to eliminate nonspecific binding.

2.1.2. Cell-SELEX library and primers

Table 2.1 presents the details on the DNA library and primers that were used for Cell-SELEX. These were all purchased from Integrated DNA Technologies (IDT), except for the first three (#1, #2, #3) that were supplied by Invitrogen. All synthesized oligonucleotides were provided as purified by high-performance liquid chromatography (HPLC), except for the DNA library that was desalted. The DNA oligonucleotide library contains a 25 nt (nucleotide) central random region flanked by primer binding regions.

Table 2.1 – DNA library and primers information summary.

ID	Name	Sequence (5´- end start)	Temperature Melting (Tm)°C		
#1	Library	TGGGCACTATTTATATCAAC (N25) AATGTCGTTGGTGGCCC	MIN 61.4°C	MEAN 70.2°C	MAX 78°C
#2	Primer Forward 39mer	CCCGACACCCGCGGATCCATGGGCACTAT TTATATCAAC		70°C	
#3	Primer Reverse 44mer	CGCGGATCCTAATACGACTCACTATAGGGG CCACCAACGACATT		68.5°C	
#4	Primer Forward 20mer	TGGGCACTATTTATATCAAC		47.2°C	
#5	Primer Reverse 17mer	GGGCCACCAACGACATT		55.9°C	
#6	FAM-Primer Forward 20mer	FAM-TGGGCACTATTTATATCAAC		47.2°C	
#7	NH_2-Primer Forward 20mer	NH_2-(C6)-TGGGCACTATTTATATCAAC		47.2°C	
#8	Primer Reverse–biotin 17mer	GGGCCACCAACGACATT-biotin		55.9°C	
#9	M13 Forward 16mer	GTAAAACGACGGCCAG		50.7°C	

ID	Name	Sequence (5´- end start)	Temperature Melting (Tm)ºC
#10	M13 Reverse 17mer	CAGGAAACAGCTATGAC	47°C

2.1.3. Gel electrophoresis experiments

DNA electrophoresis was carried out to check the DNA yield and purity after PCR amplification, as well as to confirm the integrity and handling of the samples under study. The agarose gels (Nzytech), typically 3%, were prepared in 1X Tris-acetate-EDTA (TAE) buffer (TAE 50X: 2 M Tris-Hcl [Fisher Scientific], 1 M Acetic Acid [Fisher Scientific] and 0.05 M EDTA [Fisher Scientific] pH=8.5). The electrophoresis was typically carried out at 80 V for 60 min. Samples were loaded with 50% glycerol (Fisher Scientific). The gels were observed using ChemiDoc XRS (Bio-Rad).

2.1.4. Cell Viability

The dye exclusion test is used to determine the number of viable cells present in a cell suspension. It is based on the principle that live cells possess intact cell membranes that exclude certain dyes, such as trypan blue (Strober, 2001).

The trypsinization/trypsin neutralization protocol was followed. A 1:1 dilution of the cell suspension was prepared in trypan blue (Gibco). About 10 µL of 0.4% Trypan blue solution was added and combined with 10 µL of cell suspension (Figure 2.2). To ensure a uniform cell suspension, it was pipetted up and down several times and then allowed to stand for 10 min.

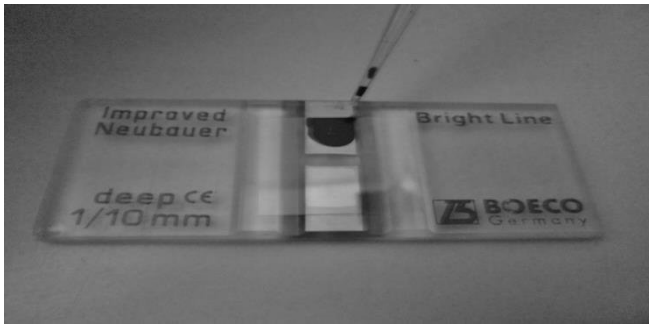

Figure 2.2 – Load a chamber with a mixture of cell suspension and trypan blue.

A small amount of trypan blue cell suspension was transferred to the Neubauer chamber (Boeco) by carefully touching the cover slip at its edge with the pipette tip and allowing each chamber to fill by capillary action.

The number of cells (viable and total) was determined. When there were too many or too few cells to count, the procedure was repeated either diluting or concentrating the original suspension as appropriate.

Each square of the Neubauer chamber (with coverslip in place) represents a total volume of 0.1 mm^3. Since 1 cm^3 is equivalent to 1 mL, the subsequent cell concentration per mL (and the total number of cells) was determined using the following formulas:

- $\%\text{Cell Viability} = \frac{\text{Total Viable Cells (Unstained)}}{\text{Total Cells (Viable+Dead)}} \times 100$
- Viable Cells/mL = Average viable cell count per square x Dilution Factor x 10^4
- $\text{Average viable cell count per square} = \frac{\text{Total number of viable cells in x squares}}{\text{x squares}}$
- $\text{Dilution Factor} = \frac{\text{Total Volume (Volume of sample + Volume of diluting liquid)}}{\text{Volume of sample}}$
- $\text{Total viable cells/Sample} = \text{Viable}\frac{\text{Cells}}{\text{mL}} \times \text{The original volume of the cell sample}$

2.1.5. *In Vitro* Cell-SELEX Procedure

In this study, MDA-MB-435 cells were used as the target cell line and 3T3 cells for the counter-selection steps.

When cells reached approximately 80% confluence, they were detached using trypsin-EDTA. After detachment, cells were transferred to a centrifuge tube and were centrifuged at 200 x g. The pellet was collected and resuspended in DMEM.

A Neubauer chamber was used to determine the concentration and volume of cells to use in each round of Cell-SELEX, as explained in section 2.1.4. In the initial round of selection, $1x10^6$ cells/mL of MDA-MB-435 and $5x10^6$ cells/mL of 3T3 were used. In the following rounds, the number was reduced to $1x10^5$ cells/mL of MDA-MB-435 and $5x10^5$ cells/mL of 3T3.

About 10 nmol of the DNA library was added to BB in a total of 500 µL, mixed and heated at 95°C for 5 min for denaturation and snap-cooled on ice for 10 min. Then, 500 µL was added to the cell suspension. The mixture was incubated at 4°C for 1 h. After incubation, the cells were centrifuged (Eppendorf Centrifuge 5418) at 220 x g for 5 min at 4°C. The supernatant, containing

unbound sequences, was removed and the cell pellet was resuspended in 500 µL of WB. The washing procedure was repeated three times at the same conditions. Next, the cell pellet was suspended in 300 µL of BB, heated at 95°C for 10 min, centrifuged at 11000 x g for 5 min and the supernatant containing eluted DNA was collected.

The total volume of elution was incubated with negative cells for 1h at 4°C. After incubation, the suspension was centrifuged. The supernatant containing eluted DNA was collected.

The recovered sequences were amplified by PCR using the primers previously described in Table 2.1 (#2 e #3). The PCR was performed on a Bio Rad MyCycler Termal Cycler and all reagents were purchased from Kapa Biosystems.

The amplification was performed under the conditions described in Table 2.2. Amplifications were carried out using an initial denaturation step at 95°C for 5 min, proceeded by 30 cycles with 95°C for 30 s, 65°C (the annealing temperature is 5°C lower than the melting temperature (Tm) of the primer set) for 30 s and 72°C for 30 s, followed by a final extension for 5 min at 72°C. After the PCR finished, the size (LIBRARY + PRIMER forward + PRIMER reverse = 108 base pair (bp)) was confirmed by an agarose gel as described in section 2.1.3.

Table 2.2 – Parameters used for amplification of sequences of Cell-SELEX.

Components	50 µl Reaction	Final Concentration
Template DNA	10.0	
KAPA Taq DNA Polymerase	0.2	1 U
10X Buffer B	5.0	1 X
10 mM dNTP	1.0	200 µM
20 µM Forward Primer	0.2	0.08 µM
20 µM Reverse Primer	0.2	0.08 µM
PCR-grade water (Up to 50 µL)	33.4	N/A

On the following rounds, the DNA obtained from PCR was resuspended in lower volumes of BB (2^{nd}-5^{th} rounds=400 µL, 6^{th}-10^{th} rounds =200 µL) and the number of washes was increased (2^{nd}-5^{th} rounds =3 washes, 6^{th}-10^{th} rounds=5 washes). The rest of the experimental protocol remained the same.

Using these conditions, the Cell-SELEX was stopped after the tenth round.

2.1.6. Aptamer Cloning

The PCR product from 10th Cell-SELEX round was purified by ethanol precipitation. First, 50 µL of 3 M sodium acetate (Fischer Scientific) and 150 µL of cold absolute ethanol (Fischer Scientific) were added. DNA was recovered by centrifugation at 11000 x g for 5 min. Supernatant was removed with care and DNA was washed with 500 µL of 70% (v/v) ethanol to eliminate the excess of salt from the pellet. The pellet was dried overnight and resuspended in 50 µL of sterile water.

The purified, recovered DNA was then amplified. The cycling parameters used were similar to those used previously. A 7 min extension step at 72°C after the last cycle was included to ensure that all PCR products are at full length and that the 3' is adenylated. Taq polymerase has a non-template-dependent terminal transferase activity that adds a single deoxyadenosine (A) to the 3´ ends of PCR products.

The linearized vector (Figure 2.3) supplied in this kit has single, overhanging 3´ deoxythymidine (T) residues. This allows PCR inserts to ligate efficiently with the vector. At this point, the PCR product was ready for TOPO Cloning (Invitrogen) and transformation into the competent *Escherichia coli*.

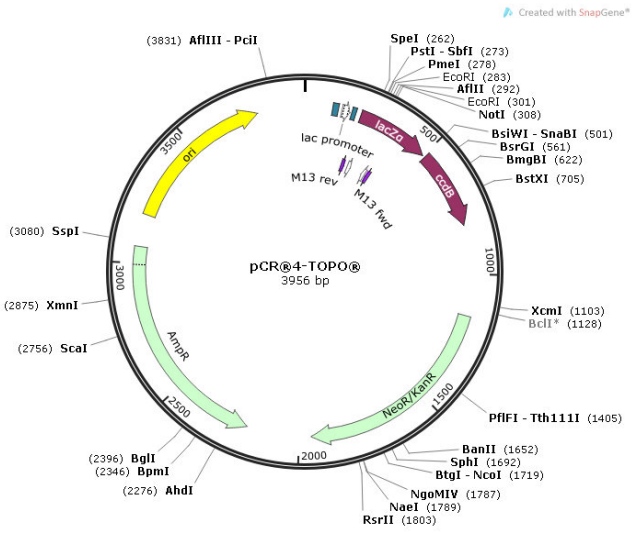

Figure 2.3 – Map of the features of PCR™ 4-TOPO.

About 4 µL of fresh PCR product was mixed with 1 µL of salt solution (provided with kit) and 1 µL of TOPO vector to a final volume of 6 µL. The reaction was gently incubated for 20 min at room temperature (25°C) and then cooled on ice. After this, 4 µL of the TOPO Cloning reaction was added into a vial of competent cells and mixed gently. Next, the reaction was incubated on ice for 15 min and placed at 42°C for 30 s without shaking (heat shock). The tubes were immediately

transferred to ice and 250 µL of room temperature SOC medium (supplied with kit) was added, followed by incubation at 200 rpm at 37°C for 1 h.

After incubation, 50 µL was plated onto Luria Broth (LB) (Liofilchem) plates with kanamycin (Applichem) with a final concentration of 50 µg/mL. The cells incubation was carried out overnight at 37°C.

A colony PCR was done to verify if the insert was present. This technique can be used for rapid confirmation of the insertion of the desired DNA in the plasmid. The primers used generate a PCR product of known size and the colonies that show amplification of the expected size are likely to contain the correct DNA sequence.

The colonies were picked from the culture plate and were placed into PCR tubes with 50 µL of LB medium supplemented with 50 µg/mL of kanamycin. Subsequently, the tubes were incubated at 37°C for 1 h. The cells solution was slightly dense. About 1 µL of this sample was added to the PCR mixture. The amplification parameters were similar to those previously described (Table 2.2).

Finally, the insert presence with the proper length was confirmed by analyzing the PCR product on an agarose gel, as described in section 2.1.3.

2.1.7. Plasmid DNA extraction

A small number of colonies were picked and inoculated into LB media supplemented with 50 µg/mL kanamycin and incubated overnight at 37°C at 200 rpm. Cultures were purified according to manufacturer protocol (GRS Plasmid Purification Kit). It provides an efficient and fast method for the purification of high quality plasmid DNA from cultured bacterial cells.

A 6 mL LB culture was centrifuged at 11000 x g for 1 min. The supernatant was discarded. The pellet was lysed and plasmid DNA was liberated from the *E. coli* host cells by the addition of 200 µL SDS/alkaline solution. This mixture was incubated at room temperature until lysis had completed.

The resulting lysate was neutralized by the addition of 300 µL of neutralization solution. This solution creates the appropriate conditions for binding of plasmid DNA to the glass fiber matrix. Precipitated protein, genomic DNA and cell debris were then pelleted by a centrifugation step of 11000 x g for 5 min. The supernatant was loaded onto the glass fiber matrix and the flow-through was discarded.

Contaminations like salts, metabolites and soluble macromolecular cellular components were removed by simple washing with an ethanol solution. Pure plasmid DNA was finally eluted with 50 µL under low ionic strength conditions with slightly alkaline buffer Tris-EDTA (TE) (5 mM Tris/HCl, pH 8.5).

After these extraction steps, a DNA gel electrophoresis was performed as described in section 2.1.3. The plasmid concentrations were determined using Nanodrop 1000 (Thermo Scientific).

2.1.8. Aptamer Sequencing

Two primers, M13 forward and M13 reverse described in Table 2.1 (#9 and #10) were used to sequence the insert. The higher concentrations of purified plasmid samples were sent for small scale sequencing (Macrogen). The pre-mixed DNA and primer sample (10 µL total volume) were prepared using 5 µL of template DNA with a concentration of 50 ng/µL and 5 µL of primer with 5 pmole/µL.

2.1.9. DNA folding Predictions

The secondary structures of the single-stranded DNA aptamers were predicted using mfold software (http://mfold.rna.albany.edu). The abbreviated name, 'mfold web server', describes a number of closely related software applications available online for the prediction of the secondary structure of single stranded nucleic acids. The objective of this web server is to provide easy access to DNA folding and hybridization software.

After the sequence(s) insertion on the online version of this software, mfold provides the calculated energy matrices that determine all optimal and suboptimal secondary structures for the folded nucleic acid molecule.

The salt conditions used by default in the *in silico* analysis of the sequences were 155.306 mM [Na^{+}] and 0.813 mM [Mg^{2+}]. These values correspond to the salt concentrations present in the medium DMEM supplemented with 10% (v/v) of FBS and 1% (v/v) of antibiotic that was used in the selection steps. The percentage range from the minimum free energy was set to 5.

2.2. Bioconjugation Methodology

2.2.1. Chemicals and Buffers

Fluorescent silica particles (Micromod) with -COOH groups on the surface were used for the aptamer coupling. The fluorescent silica particles are mono-disperse and non-porous with a size of 70 nm and a density of 2.0 g/cm^3. The particles emit green fluorescence upon an excitation of 485 nm and an emission of 510 nm.

The reagents EDC (Sigma Aldrich) and sulfo-NHS (Sigma Aldrich) in the buffer 2-(N-morpholino) ethanesulfonic acid (MES) (Fisher Scientific) were used to the coupling reaction. Glycine (AppliChem) in PBS (pH=7.4) was used to block free carboxylates.

2.2.2. DNA labeling and strands separation

For the functionalization of silica with -COOH groups in the surface with aptamer it is necessary to link a primary amine to DNA. So for amine labeling, the vector needed first to be linearized and then amplified with the correct primers.

Before using the vector combined with the specific aptamer, it was digested using the enzyme EcoRI (New England Biolabs) (Figure 2.3). The linear DNA has free ends, because both strands have been cut. Closed (circular) DNA templates are amplified slightly less efficiently than linear ones.

After a successful linearization, an amplification using the primers #7 and #8 listed in Table 2.1 was performed, using the PCR conditions in Table 2.2. This amplification is needed to link a primary amine to the sense strand and biotin to the antisense strand to allows strands separation. Successful labeling was confirmed by running an agarose gel with conditions described in section 2.1.3.

As after PCR amplification, the product was in double strand and the product required to link silica particle should be in ssDNA, columns of streptavidin (GE Healthcare) were used. These columns enable the strong binding between the immobilized streptavidin to biotinylated substances. The protocol provided by the manufacturer was for proteins purification so some modifications were implemented where the principle basis was the same but the elution was performed using NaOH to denature the strands (Sefah *et al.*, 2010b).

The interaction between biotin-streptavidin is very strong. To the column reusable, this interaction needs to be broken. It could be dissociated using sterile water together with gentle heating to 70°C for few seconds (Holmberg *et al.*, 2005). In this paper they referred that no detectable contamination was found from the previous biotinylated product of each round, or any decrease in binding capacity in the subsequent rounds of use after 4 regenerations of the same bead was observable.

The streptavidin columns were reused 4 times using this methodology.

2.2.3. Bioconjugation

The carbodiimide methodology is one possible approach of aptamer conjugation to silica particles surface and guarantees therefore good immobilization reproducibility. It is based on EDC/NHS activation of the –COOH groups on particle surfaces followed by reaction with amino groups of the aptamer (Figure 2.4).

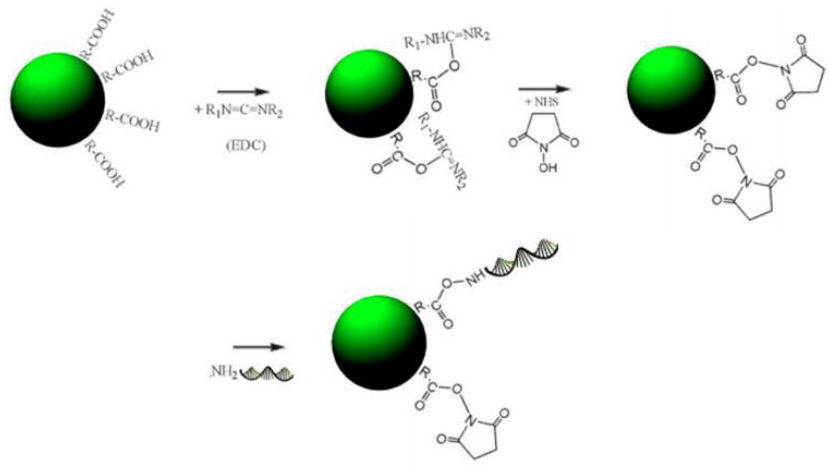

Figure 2.4 – Schematization of silica functionalization with NH_2-aptamer.

The conjugation reaction was carried out in different ratios of aptamer:silica and were dependent in the quantities of DNA obtained after the purification using the columns. When higher quantities of DNA were obtained higher ratios could be tested.

About 40 µL of silica NPs (1 mg) was washed with 0.5 M MES buffer and centrifuged at 11000 x g. Particles were then resuspended in 500 µL of same buffer. To activate the particle surface 1 mg of EDC and 2.5 mg of Sulfo-NHS. These mixtures were incubated 1 h at room temperature under gentle shaking.

The activated particles were washed with PBS (pH=7.4), centrifuged at 11000 x g and the NH_2-aptamer was added. Several concentrations of aptamer and the appropriate controls to validate the method were tested. The mixture was then incubated for 4 h at room temperature under gentle shaking.

Afterwards, particles were washed twice with PBS and resuspended in the same buffer with 30 mM of glycine for 60 min to block free carboxylates.

Aptamer-conjugated nanoparticles were purified performing two washes with PBS, then resuspended in PBS with 0.01% (w/v) of sodium azide (Sigma Aldrich) and finally stored at 4°C for further analysis

2.2.4. Ligation Characterization

Spectrophotometry

For nucleic acid detection, one of the most common methods is the measurement of solution absorbance at 260 nm, using the absorption maximum of nucleic acids at this UV wavelength. In a spectrophotometer, a sample is exposed to ultraviolet light at 260 nm, and the light that passes through the sample is measured. The more light absorbed by the sample, the higher the nucleic acid concentration (Sambrook *et al.*, 1989).

After coupling, the presence of DNA linked to the silica was evaluated by measuring the Optical Density (OD) at 260 nm in a spectrophotometer (Jasco V-560).

Dynamic Light Scattering and zeta potential measurements

The aptamer-silica were collected and diluted to 1 mL. The particle size distribution was measured by dynamic light scattering (DLS) at 25°C in PBS pH=7.4. The intensity-weighted mean value was recorded as the average of three independent measurements. The surface charge (zeta potential in mV) of the aptamer silica nanoprobe in PBS was measured at 25°C. All DLS and zeta potential measurements were carried out using Zetasizer equipment (Nano-ZS, Malvern Instruments). Statistical analysis was performed using GraphPad Prism 6. One-way ANOVA was used for statistical comparisons.

Colorimetric Method

A fluorescent method based on propidium iodide (PI) (Molecular Probes) was used to detect the aptamer bound to the silica NPs' surface. PI binds to DNA by intercalating between the nucleotide bases with little or no sequence preference, and with a stoichiometry of one dye per 4–5 base pairs of DNA. It is important to notice that PI also binds to RNA, and therefore an RNase treatment is required to avoid misreadings. When bound to nucleic acids, the fluorescence excitation maximum for PI is 535 nm, while the emission maximum is 617 nm (Figure 2.5).

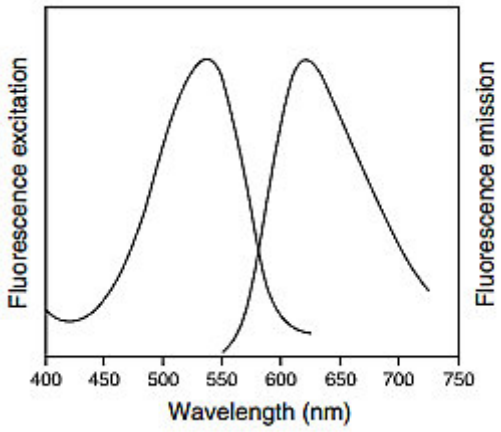

Figure 2.5 - Fluorescence excitation and emission profiles of propidium iodide bound to dsDNA.

Briefly, several concentrations of dsDNA were incubated with 1.5 mM of PI and RNase with a final concentration in solution of 1 μg/mL and 10 μg/mL respectively.

After 30 min of incubation, the relationship between fluorescence intensity of each sample and the aptamer concentration was recorded using a fluorometer (JASCO FP6200).

Quantitative aptamer detection on the silica particles was performed using the abovementioned procedure, except that the aptamer was changed to aptamer-NPs. Therefore, the detection of aptamers on the NPs was performed by monitoring fluorescence intensity at 617nm with the excitation at 535 nm. The number of immobilized aptamer molecules on the NPs was quantitatively determined from the regression equation.

2.3. Binding assays

2.3.1. Cell lines

Two cancer cell lines were used for the recognition and 3T3 cells were used as the control.

2.3.2. Chemicals and Buffers

The solution of 4% (w/v) paraformaldehyde was freshly prepared. To 1 L, 800 mL of 1X PBS was added and heated while stirring at approximately 60°C. Afterwards, 40 g of paraformaldehyde powder (Panreac) was added to the heated PBS solution. NaOH (1 M) was added until the paraformaldehyde powder dissolved.

Once the paraformaldehyde was dissolved the solution was cooled, filtered and the volume of the solution was adjusted to 1 L. The pH was verified using pH strips and adjusted to pH=7.4, using 1 M HCl (Fisher Scientific) when necessary. The solution was aliquoted and frozen.

2.3.3. *In Vitro* Studies

Before performing the studies *in vitro* with the selected cell lines, the resulting dsDNA were boiled at 95°C for 5 min and flash cooled in ice for 5 min. For tests at 37°C, it was cooled to this temperature. The resulting ssDNA aptamers were used for downstream assays.

For the binding methodology, the higher aptamer concentration, conjugated with silica (as described in section 2.2.3) and free aptamer labeled with the fluorophore FAM, were tested. To label the aptamer with FAM, PCR amplification was done using primer #3 and # 6, as shown in Table 2.1, following the conditions described in Table 2.2. Successful labeling was confirmed by running an agarose gel as described in section 2.1.3. Free silica particles, non-labeled aptamer and untreated cells were used as controls.

For the cell recognition experiments, an amount of about 40 000 cells/cm2 was cultured one day prior to the experiments until they were in the logarithmic phase. The number of cells was calculated following the procedure described in section 2.1.4 (Chen *et al.*, 2008; Farokhzad *et al.*, 2004).

Fluorescence Microscopy

The cell lines were cultured until the cover rate on the 24-well plate reached 70-90% confluence. The cells were cultured on glass slides in each well.

On the day of the experiment, the medium was removed and cells were washed two times with pre-warmed 100 µL of 1X PBS, followed by incubation with pre-warmed DMEM supplemented with 10% (v/v) of FBS and 1% (v/v) of antibiotic for 30 min, before the addition of the aptamer. Afterwards, 60 pmol of aptamer was added in 200 µL of supplemented DMEM and the mixture was

incubated. Two temperatures were tested, 4°C and 37°C, at two different incubation times, 1 h and 4 h.

The cells were washed three times with PBS to remove superfluous probes (the ones that did not bind). Finally, cells were fixed with 4% paraformaldehyde for 20 min, followed by a washing step with 100 µL of PBS (Figure 2.6) (Chen *et al.*, 2008; Farokhzad *et al.*, 2004; Shangguan *et al.*, 2006).

Each coverslip was inverted onto a slide. After these procedures, the cells were ready for fluorescence microscopic observation (OLYMPUS BX51). Only the results for the selection conditions are presented, 1 hour at 4°C and all the experiments were repeated twice.

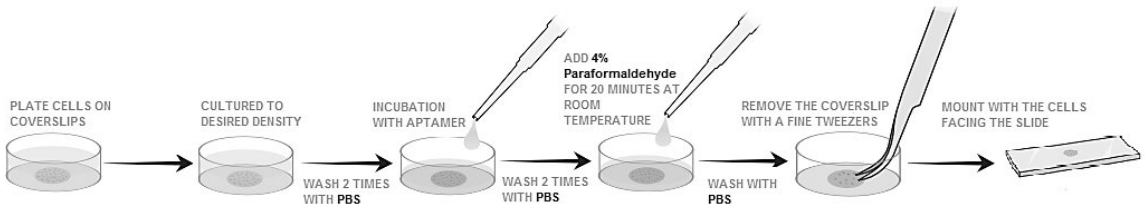

Figure 2.6 - Schematization of the binding methodology.

Flow Cytometry

To determine aptamers selectivity and specificity, flow cytometry was used for binding assays.

The cancer cell lineages were cultured until the cover rate on the 24-well plate reached 70-90% confluence.

On the day of the experiment, the medium was removed and cells were washed twice with pre-warmed 100 µL of 1X PBS, followed by incubation with pre-warmed DMEM supplemented with 10% (v/v) of FBS and 1% (v/v) of antibiotic for 30 min, before the addition of the aptamer.

About 60 pmol of FAM labeled aptamer and silica functionalized with aptamer was incubated with cell lines in 200 µL of supplemented DMEM and placed on ice for 1h (only the conditions of aptamer selection were tested). Unbound aptamers were removed by washing three times with 200 µL PBS. The pellets with the bound sequences were resuspended in 500 µL of PBS. The fluorescence was determined with a flow cytometer (Beckman Coulter Inc.) by counting at least 30,000 single cells per sample. The data were analyzed with FlowJo Analysis Software (Tree Star, Inc.).

CHAPTER 3

RESULTS AND DISCUSSION

3.1. Cell-SELEX

Cell-SELEX was used for the selection using MDA-MB-435 as positive breast cancer cell lines and 3T3 as negative cell lines. A 62 nt ssDNA library with 25 random bases flanked by a 20 nt and a 17 nt primer site sequence was subjected to the Cell-SELEX procedure (Figure 3.1). The library was first incubated with the MDA-MB-435 cell line to allow the binding of the DNA sequences to target cells. Sequences that either did not bind, or only bound weakly to the target cell surface after harsh washing conditions, were discarded. Cycle by cycle the stringency was increased in order to get aptamers with the highest affinity and selectivity. Sequences that bound strongest to the cells were retained and then eluted by heating.

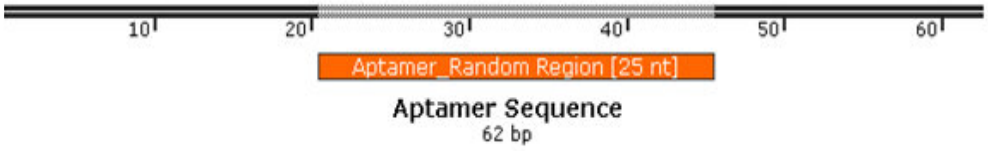

Figure 3.1 – Aptamer Random Region of 25 nt flanked by the primer sites.

The eluted DNA pool was next allowed to incubate with 3T3 cells for counter-selection. The introduction of counter selection provides the opportunity to remove aptamers recognizing common surface markers, while at the same time it allows the enrichment of aptamers recognizing target cell-specific markers. The DNA pool collected after each round (Figure 3.1) of selection was amplified by PCR for the next-round selection and the correct size was confirmed by an agarose gel.

It was established by several papers that after around 10 rounds of selection, the enriched pool should have a considerable increase in affinity for the target cells compared to the initial DNA library (Blank *et al.*, 2001; Guo *et al.*, 2008; Mayer *et al.*, 2010; Meyer *et al.*, 2013). Therefore, in the current work we decided to conduct 10 selection cycles.

Following completion of the selection process, the DNA pool was inserted into the plasmid vector pCR™4-TOPO (Figure 3.2).

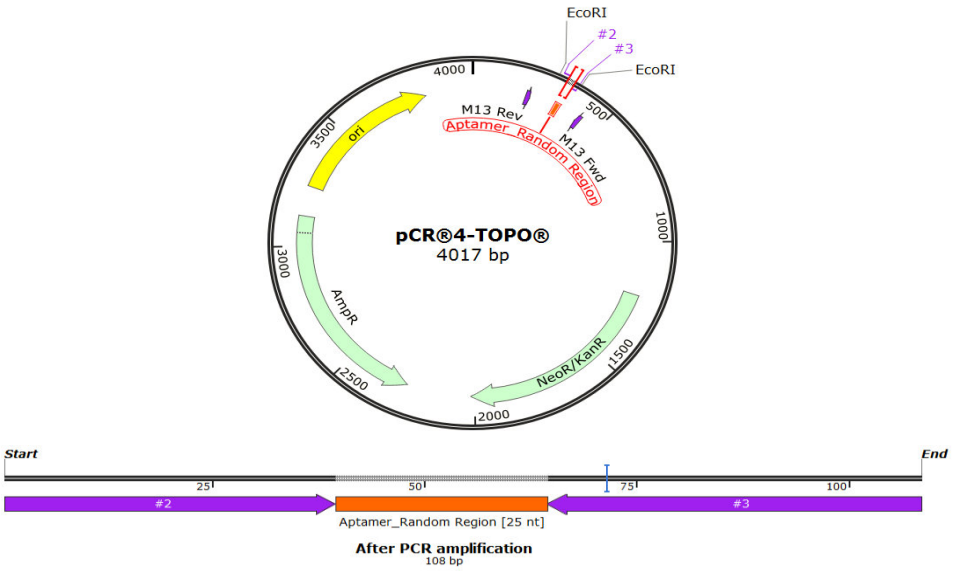

Figure 3.2 - Map of pCR™4-TOPO and the sequence of aptamer inserted in the Cloning Site. Colony PCR with the primers #2 and #3.

To confirm aptamer insertion in pCR™4-TOPO vector, a colony PCR with the primers #2 and #3 listed in Table 2.1 was done and the positive clones were sequenced. Figure 3.3-A represents the vector and Figure 3.3-B the fragment after colony PCR.

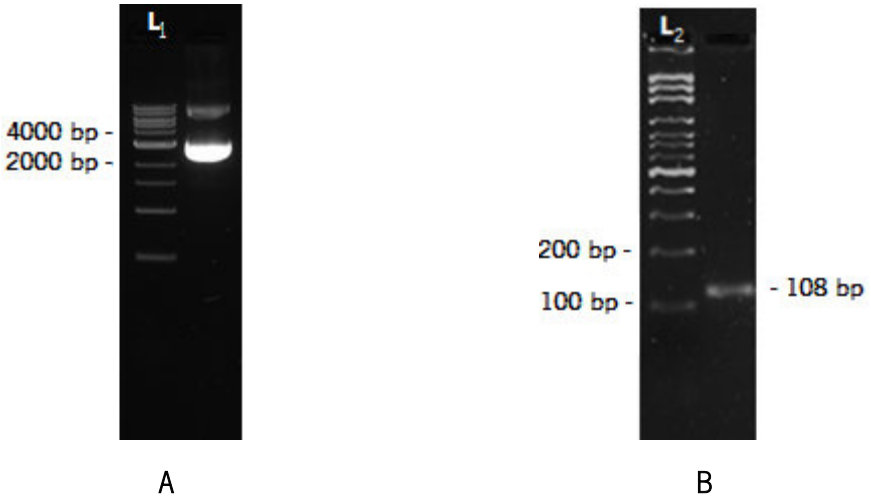

Figure 3.3 – Analysis of PCR-amplified aptamer insertion into pCR™4-TOPO by colony PCR. (A) The pCR™4-TOPO vector and (B) Colony PCR result to confirm the 108 bp. Agarose gel of 1% and 3% respectively. Legend: L1- Ladder de DNA 1kb (New England Biolabs); L2 – Ladder 100 bp DNA (SOLIS BIODYNE).

Sixteen random positive clones were sequenced. The sequences are presented in Table 3.1.

Table 3.1 – Selected aptamer sequences after 10 selection cycles. Only the random region is depicted.

Potential Aptamer ID	Sequences (random region) 5´- end start
#1	**GTCGTGGAGTCAACAAACAAGACAC (25-mer)**
#2	**TGTCGGTTGTGCGCCTACCGCCTGG (25-mer)**
#3	**CGCCTTGTCTTGTACCGTGGAGCAG (25-mer)**
#4	**TTGGCTTTTCTTGGATGATGGACGT (25-mer)**
#5	**TTGAGACGTTAGGCGTCATAAGGGT (25-mer)**
#6	**CCTTTAGGAGCGTCTTTAAGAGCAG (25-mer)**
#7	CGGT (4-mer)
#8	GAGC (4-mer)
#9	CTG (3-mer)
#10	GTTATGC (7-mer)
#11	**ATGGTAGGGTGTTTACGCGAGGGGG (25-mer)**
#12	**ATTTCACTTTAGCTTTTGTCCGTTC (25-mer)**
#13	TTTGAACCCCATCCTTGTTACTGT (24-mer)
#14	TTCCTGCACTGTAGTGACTTGCGT (24-mer)
#15	**AGTGACGGGTCAGTATCGTGGGGTG (25-mer)**
#16	CC (2-mer)

This Cell-SELEX began with a library containing a randomized part of 25 nts, so it is expected that all aptamers have a random region this length. Normally, the random region defines the length of the selected aptamer (Jiménez *et al.*, 2012; Kunii *et al.*, 2011; Sefah *et al.*, 2009; Shangguan *et al.*, 2008). In a first analysis of the obtained sequences, only nine aptamers (bold) have the same length as the random region of initial library of 25 nts. The fact that a desalted library was used, and not a HPLC or SDS-PAGE-purified one, could be one explanation for the sequences #13 and #14 have a 24 instead 25 nts. Another explication could be an unspecific ligation of the primers in a different site, thus leading to shorter sequences. Nucleotide deletions introduced during PCR could be another reason and as many PCR amplifications were done, the probability is greater.

The sequences #7, #8, #9, #10 and #26 are not considered aptamers. The TOPO cloning probably use incorrect fragments instead the aptamer sequence. These artifacts could be achieved because of mispriming or contaminating template.

After that, sequence alignments were performed, in order to assess the complexity of the selected aptamer pool and to group together aptamer clones with homologous sequences

(Table 3.2) (Bing *et al.*, 2010). These alignments were performed only for sequences that have 25 nts. These results were obtained using a Fortran code. There is a great amount of sequence alignment software that can be used for pairwise sequence alignment, but most of them perform global alignments. A global alignment aligns two or more sequences from the beginning to the end, and "forces" the alignment to span the entire length of all query sequences. A global alignment should only be used on sequences that share significant similarity over most of their extents, which is not the case of the aptamers selected (http://blast.ncbi.nlm.nih.gov/Blast.cgi).

Table 3.2 – Sequence alignment for 2 aptamers.

Aptamer 1	vs	Aptamer 2	Bases Homology	%Homology
#11	vs	#15	A--G--GGGT---TA-----GGG-G	48%
#3	vs	#6	C---T-G----GT------GAGCAG	44%
#1	vs	#11	-T-GT-G-GT----A--C-AG----	40%
#4	vs	#5	TTG-----T---G--T-AT----GT	40%
#5	vs	#12	-T---AC-TTAG---T--T--G---	40%
#3	vs	#11	----T-G--T--T--CG-G--G--G	36%
#5	vs	#11	-TG--A-G-T---------A-GGG-	36%
#12	vs	#15	A-T------T---T-T-GT--G-T-	36%
#1	vs	#15	---G--G-GTCA--A-----G----	32%
#2	vs	#15	-GT-----GT--G--T---G----G	32%
#4	vs	#11	-TGG-------T--A-G---G--G-	32%
#5	vs	#6	-----A-G---G-C-T-A--AG---	32%
#5	vs	#15	-------G-T--G--TC-T--GG--	32%
#6	vs	#12	--TT-A-----G--TTT----G---	32%
#6	vs	#15	--T---GG--C----T---G-G--G	32%
#1	vs	#6	----T-G---C--C----A---CA-	28%
#2	vs	#3	-G-C---T-T----C----G----G	28%
#2	vs	#4	T-----TT----G--T---G---G-	28%
#2	vs	#5	T---G----T--GC-T-------G-	28%
#4	vs	#15	---G--------G-AT--TGG----	28%
#6	vs	#11	----TAGG----T--------G--G	28%
#1	vs	#2	-----G--GT---C--AC-------	24%
#1	vs	#3	--C-T-G--T-----------CA-	24%
#1	vs	#4	-T-G----------A-----GAC--	24%
#2	vs	#11	--------GTG------C-----GG	24%
#2	vs	#12	--T----T-T-----T----C-T--	24%
#3	vs	#4	-----T-T--T-----G--G--C--	24%
#3	vs	#15	-G----G--T---------G-G--G	24%
#4	vs	#12	-T--C--TT------T--T------	24%
#11	vs	#12	AT---A---T---T-------G---	24%

Aptamer 1	vs	Aptamer 2	Bases Homology	%Homology
#2	vs	#6	--T----------C-T---G----G	20%
#1	vs	#5	-T-------T---C-----A-----	16%
#3	vs	#5	---------T-G--------AG---	16%
#3	vs	#12	-------T-T-G---------G---	16%
#4	vs	#6	----------T-A-G--C--	16%
#1	vs	#12	-T-------T----------C	12%

At the end of Cell-SELEX process, normally the sequences are aligned into families according sequence homology when the members in each family differ in few numbers of bases (Sefah *et al.*, 2010a; Van Simaeys *et al.*, 2010). It was assumed that sequences in the same family should bind to the same target with same secondary structure. Aptamers in three different families bind to three different targets (Shangguan *et al.*, 2007).

The objective of this work was practically the same; find identical sequences and identify those more repeated in the selected pool. This software enables the find of identical sequences. If many consensuses were obtained, they were then grouped into families. The aptamer that appears more times in each family was used for further tests.

As relatively few aptamers were sequenced it is difficult to group them in families. Nevertheless, for the 16 sequenced aptamers the best result is a sequence homology of 48% between aptamer #11 and #15 corresponding in less than half of the sequence (Figure 3.2). When the rest of the aptamers is analyzed, homology becomes increasingly lower, until 12% between aptamer #1 and #12, which only have 3 equal bases in common at the same position.

The program gives the possibility to perform a comparison between more than two sequences at the same time. Comparing results between 3 sequences (Table A.1) the best result obtained is a sequence consensus of 6 bases corresponding to 24% between aptamer #1, #11 and #15. For 4 sequences in comparison (Table A.2), the best is 3 bases in common for aptamer #1, #11, #4 and #15, which corresponds to 12% of homology. The great majority do not even have a single base consensus.

The choice of the cell lines to be used largely depends on the purpose of the selection. The purpose of this work was to select aptamers that can differentiate between cancer cells and normal cells. It is very likely that the great distance between the positive and negative cell line (one is human and another is mouse cell line) affects the aptamer selection. Maybe the common surface markers are so distant that it was difficult to eliminate them. This could be one important

explanation for the different aptamers recovered and the low amount of sequence homology that could be found among them. The use of another negative lineage more related as MCF10-A which is a mammary epithelial cell may probably increase the similarity between the recovered aptamers.

The DNA pool collected after each round of selection was amplified by PCR. Symmetrical PCR generates dsDNA that was used for the next round of selection. However, the strands of PCR product should be separated in order to obtain the wanted ssDNA for the next round. In order to separate the strands, a PCR must be performed with forward primer and the reverse biotinylated primer to amplify dsDNA. The presence of biotin enables binding to streptavidin-coated beads (Sefah *et al.*, 2010b). Then, the sense ssDNA are separated from the biotin and are recovered to continue the selection process. This could be another explication for the problems observed with the different sequences of aptamers. In the protocol used, after PCR amplification the desired strand was not separated from the undesired (antisense) one and the Cell-SELEX continued in the presence of undesired sequences which may had caused problems in the process of aptamer selection.

In the current work, 10 cycles of selection were done. The enrichment of the selection pools was not monitored. The limit of 10 cycles was established without knowing if this cycle is considered the optimal cycle to select the best aptamers with the highest affinity and selectivity for the cancer cell line. Binding assays should have been carried out after each cycle and under the same conditions, allowing us to compare results. This could be also important to explain the unsuccessful aptamers consensus found.

The nine aptamer sequences (in bold in Table 3.1) plus the sequences with 24 nucleotides (#13 and #14) were further analyzed, in order to obtain relevant structures for binding, such as stems, loops, hairpins or bulges (Table 3.3 and Table A.3). In Table 3.3 are presented only the secondary structures of aptamers with the highest homology that were used for further assays.

The aptamers were selected at 4°C but it is interesting to predict their secondary structure at 37°C to ascertain their potential for *in vivo* applications to further verify their binding ability under such conditions.

Table 3.3 - Predicted aptamer secondary structures by *in silico* analysis with the software mfold. Only the structure(s) with the lowest free energy (dG) are presented. The fixed sequences of PCR primers are indicated in lowercase letters. The random region is represented in uppercase letters and is marked in black rectangular area.

4ºC	37ºC
Aptamer #11 (3 potential structures)	Aptamer #11 (3 potential structures)
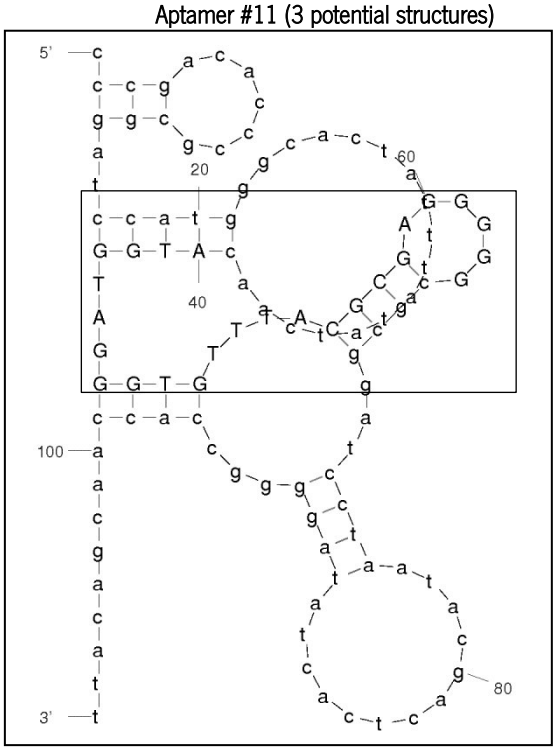	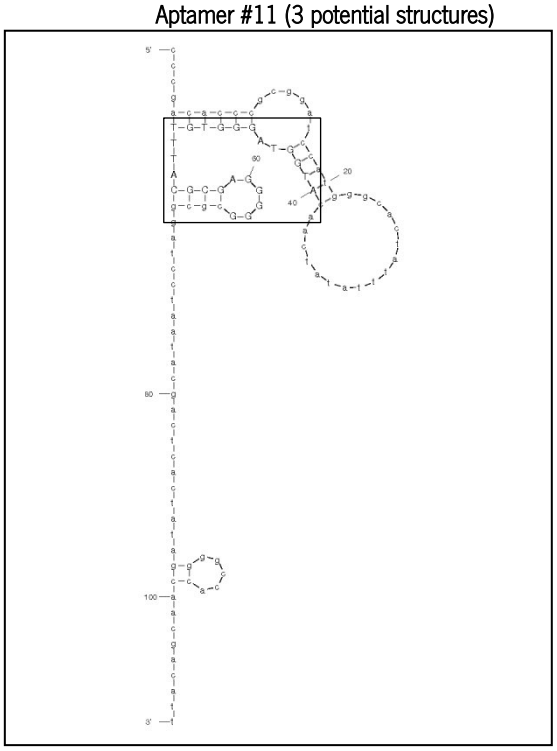
dG= - 26.82 kcal/mol	dG= - 8.96 kcal/mol
Aptamer #15 (1 potential structure)	Aptamer #15 (3 potential structures)
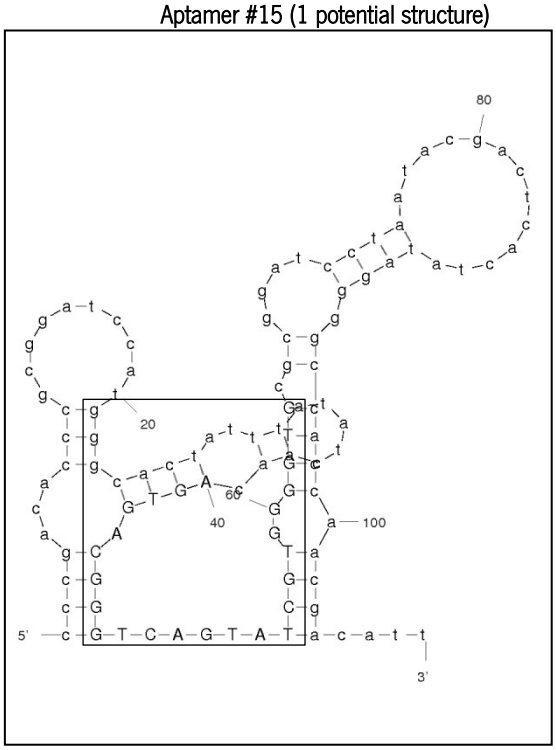	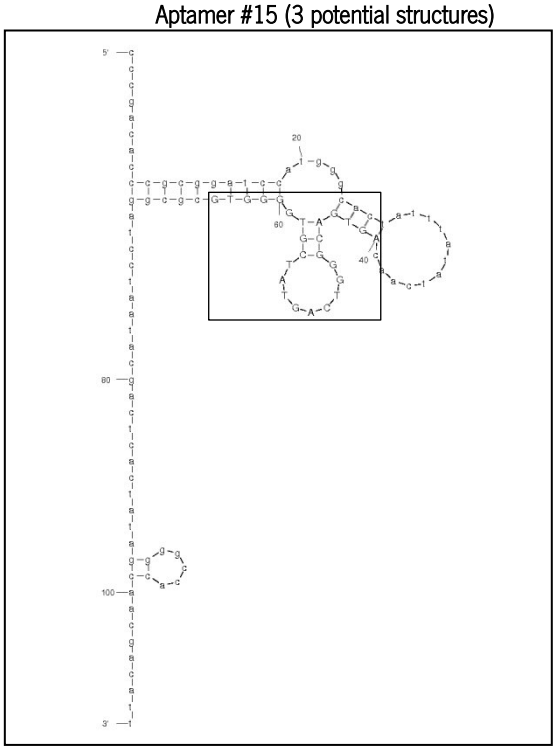
dG= - 25.79 kcal/mol	dG= - 6.16 kcal/mol

The secondary structure of small nucleic acid molecules is largely determined by strong, local interactions such as hydrogen bonds and base stacking. Summing the free energy (thermodynamic state function that we can use as an indicator of whether or not a process in a system will occur spontaneously) for such interactions provides an approximation for the stability of a given structure. Often for any given sequence several alternative secondary structures are predicted within a relative small range of free energies. The knowledge of functional secondary structures can have a significant impact on optimizing desired properties.

It is well known that the secondary structure of DNA aptamers can change under varying temperatures, explaining why some aptamers lose their binding ability at 37°C (Zhang *et al.*, 2012a). As temperature rises, the free energy will decrease and the reaction will become more spontaneous. With higher temperature, the entropy increases (increasing disorder) making the system more negative, then the energy necessary is lower when compared with low temperatures. This can be observed for the free energies of all aptamers selected at 4°C and 37°C (Table 3.3 and Table A.3). They are significantly lower at higher temperatures, so less stable. The lower the Gibbs energy, the more stable the structure.

In relation to the secondary structure, the majority of loops were lost when the temperature was raised. If the bonds were broken, this means that the hydrogen bridges are no longer there. When the temperature was increased, the link was broken and with the breaking of the stems, the loops also disappear. The loops themselves are not formed alone; they are formed because the stems are formed.

When examined at 4°C, which is the temperature used for the selection steps, the aptamer free energies are quite similar. Aptamer #2 and #11 are the ones that have the lowest free energy.

For 4°C, aptamer #1 has two loops at the bottom that completely disappear in the secondary structure at 37°C. The same happens with aptamer #3, #4, #5, #11 and so on.

Aptamer binding properties are a function of both sequence and structure.

In these secondary structure patterns, only the aptamer #1 and #5 contain a loop (the first with 11 nts and the last with 7 nts) that are linked by a stem (forming a hairpin) with 2 to 4 bps length, respectively. Then this structure is maintained by another loop and the rest of the aptamer sequences fold into different structures. The primary sequences of the hairpin structure of these secondary structure segments were very different as possible to observe in the sequence alignments in Table 3.2 and in the secondary structures in Table 3.3 and A.3. The structures formed by these

aptamers could be responsible for binding to the target molecule, however further investigation and more sequenced aptamers were still needed.

Bing and coworkers (Bing *et al.*, 2010) compared the secondary structures of all sequenced aptamers against streptavidin and a conservative bulge-hairpin structure section was found. Nevertheless, the primary sequences of this bulge-hairpin were very different as presented for the aptamers #1 and #5.

The remaining aptamers normally are folded into several different structures. Usually appears between 2 or 3 loops and have single strand regions.

The conserved sequence motif 'AGCAG' locates at loop sections in aptamer #3 and #6, which appears to be significant for binding to the target. The conserved 'TCTTG' sequence shows up in loop sections in aptamer #3 and #4 showing also importance for the binding. When shortening this conserved sequence to 'TCTT', it appears in a loop section of two additional aptamers, #6 and #14, indicating its potential relevance in recognizing breast cancer cells MDA-MB-435.

The sequence 'TTT' and 'CTT' appears again in loop sections in aptamers #4, #11, #12, and #13 and #3, #4, #6 and #12 respectively. Further studies were important to ascertain the importance of all of these conserved domains.

These characterizations based on primary sequences and secondary structures are important, but the aptamers should have been characterized taking into consideration their binding capabilities and dissociation constants (Kd). The Kd is an important parameter for characterizing aptamer binding to the target.

3.2. Bioconjugation Methodology

One possible method of conjugation of aptamers to silica surface is based in EDC/NHS activation of the carboxylic acid groups on particle surfaces followed by reaction with amino groups of the aptamer (section 2.2.3). For this purpose, aptamers need to be labeled with amino groups to guarantee that the linkage is achieved.

The aptamers consensus were expected to be higher, but assuming that the sequences that present higher homology (Table 3.2) are binding to a receptor marker in the MDA-MB-435 cells surface, they will be further used to test their ability to identify the target cells.

Two other sequences, selected using a different breast cancer cell line, and presenting a homology near 100%, were also used in this work for comparison purposes.

From this point on, MDA-MB-435 cells will be referred to as cancer cell line 1. The other breast cancer cell line used will be named cancer cell line 2. Aptamer 1A and 1B will be the designations of the aptamers selected against cancer cell line 1 and aptamer 2A and 2B to those selected against cancer cell line 2.

For a successful amine labeling of the aptamer, the vector was linearized and then amplified by PCR using the correct primers. This amplification is needed to link a primary amine enabling silica coupling. Figure 3.4-A represents the plasmid with the desired aptamer sequence in a linear form. Figure 3.4-B represents the dsDNA labeled with an amine group after PCR amplification with 62 nts.

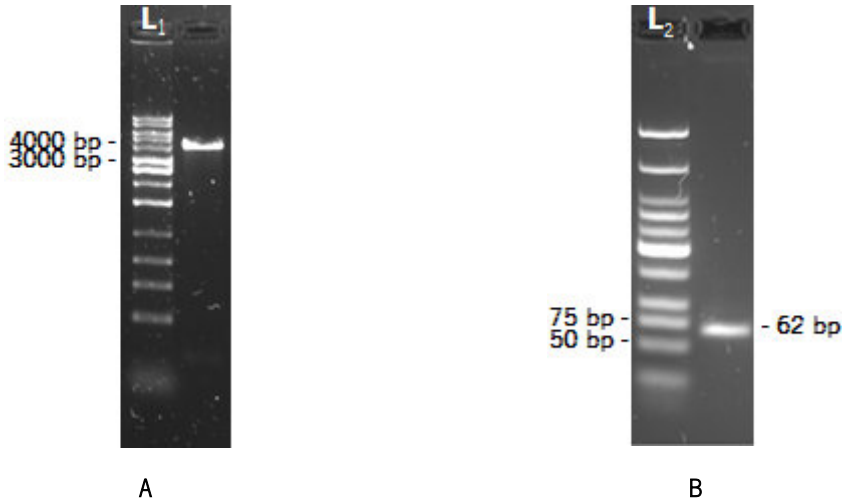

Figure 3.4 - (A) Plasmid Linearized using the enzyme EcoRI and (B) the amine label after PCR amplification. Legend: L1- Ladder de DNA 1kb (SOLIS BIODYNE); L2 – Ladder Low Molecular Weight (New England Biolabs).

After the PCR amplification to obtain labeled DNA, the sense strand of the double stranded product was separated from the antisense strand by using the streptavidin columns. These columns allow binding the biotin/biotinylated substances, thus enabling the separation of sense labeled with NH_2 from biotinylated antisense ssDNA by denaturation and affinity purification with streptavidin-coated Sepharose beads.

During the purification procedure with these columns, a large percentage of DNA was lost. After using the columns, the obtained yield of ssDNA was generally around 30 ng/µL. Despite the low yields of ssDNA recovered, it was further used to functionalize the silica particles.

After the DNA labeling and further purification, the ssDNA could be coupled to the silica particles. The protocol used to for coupling is described in section 2.2.3, with the small alteration that the silica activation pH was changed to obtain a good silica functionalization with aptamer. The activation reaction with EDC and Sulfo-NHS is most efficient at pH=4.5-7; however, the reaction of

Sulfo-NHS activated aptamer with primary amines is most efficient at pH=7-8 (Grabarek and Gergely, 1990). For best results, the first reaction was performed in MES buffer for a wider range of pH=5-9, then exchanged for PBS at pH=7.4 immediately before performing the reaction to the amine aptamer.

For the first ligation, the result was evaluated measuring the absorbance at 260 nm (section 2.2.4). All the supernatant was collected for absorbance measurement. The immobilization was determined based on the absorbance difference at 260 nm between the DNA solution before and after immobilization (Li *et al.*, 2012).

Based on this principle, the aptamer attached to the particle and the recovered aptamer (after incubation) in supernatant were quantified. Figure 3.5-A represents the amount of aptamer 2A attached to a silica particle and Figure 3.5-B illustrates the quantity of aptamer 2A collected in the supernatant.

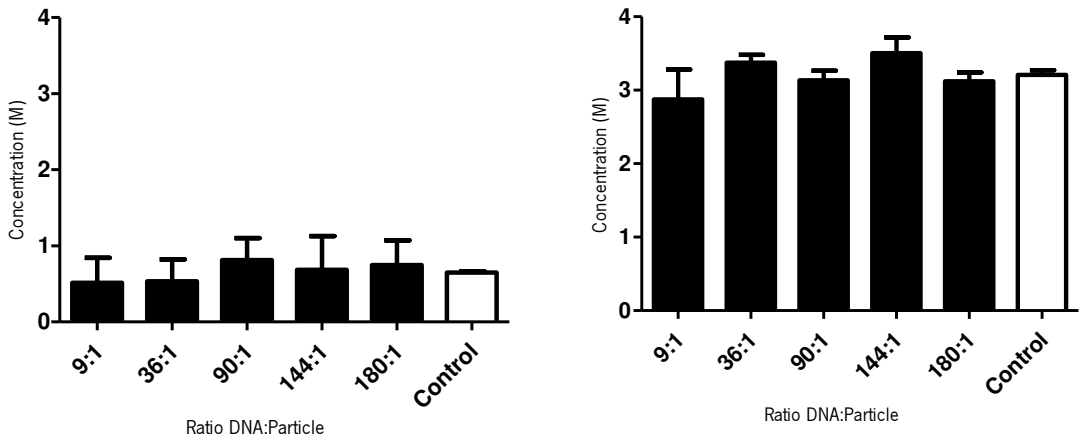

Figure 3.5 – Concentration of the aptamer recovered from the reaction conducted with aptamer 2A testing several ratios of DNA:Particle at pH=9. (A) Concentration of aptamer that was linked to the particle and (B) Concentration of aptamer recovered after the ligation. The control represents a sequence not labeled with amine that was incubated in the same way. Results are presented as Mean ± SD and represent 3 independent experiments.

The control used in this experiment (Figure 3.5) is the aptamer functionalized with silica but not labeled with the amine group. In this case, the covalent ligation was not expected to occur. Therefore, the aptamer amount quantified in this sample should be much lower in the silica functionalized with DNA and much higher in the supernatant. The results show that in this condition, the amount of DNA used was practically the same as the condition 180:1, i.e. the higher amount of DNA per particle.

Changing the ratio DNA:Particle seems to did not improve binding. The ratio 9:1 and 36:1 present an equal amount of aptamer detected but the latter has four times more DNA added to the solution of particles. The same happens for the ratio 90:1 and 180:1; i.e. doubling the amount of DNA added did not represent more ligated. This could mean that there is a coupling limit to the silica particle independent of the amount of aptamer provided, the availability of the particles was always the same. Another possible explanation could be that the methodology used to quantify the aptamer was not very accurate. Despite being a relatively simple methodology, it suffers from low sensitivity and interference from nucleotides and single-stranded nucleic acids. Furthermore, compounds commonly used in the preparation of nucleic acids absorb at 260 nm can lead to abnormally high quantitation levels. Furthermore, the availability of the particles may also be independent of the aptamer amount, since we do not know the amount of reactive groups we have per particle.

As Figure 3.5-B shows, the amount of DNA recovered in the supernatant was practically the same for all the conditions. Comparing the amount of DNA recovered in the supernatant to all ratios DNA:Particle, it represents around 3-, 4-fold the DNA effectively linked to silica particle, indicating that the coupling yield is very low.

Some reasons may be pointed out to explain the obtained results. Limiting/hindering the conjugation the pH of reaction could not be the best and the method for the detection of aptamer conjugation may not be very accurate.

Based on these results, it was decided to abandon the above mentioned methodology and to alternatively use zeta potential. For the following assays, zeta potential measurements were performed to determine if DNA was attached to the particles or not. This methodology doesn't allow us to determine how much DNA is linked to the silica particle. This assay enables only the qualitative determination of the DNA-particle conjugation, if DNA was linked or not.

Zeta potential depends not only on the particle surface, but also on its environment. It can be influenced by ionic strength of the medium or small changes in the pH (Prow *et al.*, 2005).

In these measurements it was expected to obtain a negative zeta potential for the silica particles (before DNA conjugation), that would become increasingly more negatively charged as DNA was conjugated on the particle surface (Chen *et al.*, 2008; Li *et al.*, 2012). Figure 3.6-A illustrates the zeta potential values obtained for aptamer 2A, and Figure 3.6-B the potential zeta for aptamer 2B.

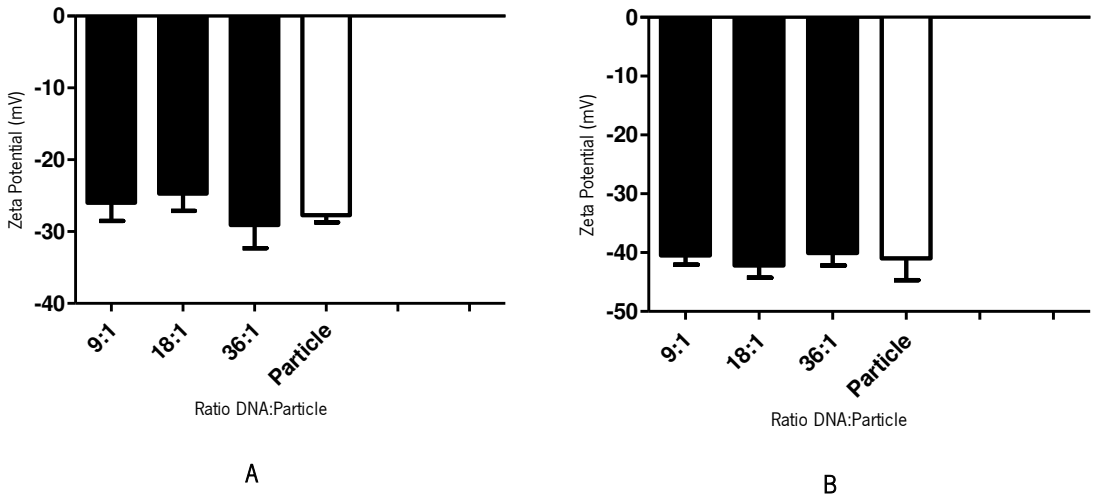

Figure 3.6 – Zeta Potential of the aptamer recovered from the reaction testing several ratio DNA:Particle at pH=7.8 for (A) aptamer 2A and (B) aptamer 2B. The last column represents the zeta potential of the particle not functionalized (control). Results are presented as Mean ± SD and represent 3 independent experiments.

Analyzing Figure 3.6, for each studied aptamer no significant differences could be found between the particle apparently coupled to DNA aptamer and the particle without functionalization. For aptamer 2A, at a DNA:Particle ratio of 36:1, there is a residual difference but is the only ratio that seems to have higher zeta potential than the control. For the remaining ratios evaluated, the zeta potential is lower than the particle itself, for which a higher zeta potential was expected if effectively the particle was functionalized with aptamer.

For the aptamer 2B, the zeta potential seems to be lower when compared with the zeta potential of ligation with a ratio of 18:1. Nevertheless, for the other conditions tested the zeta potential of the non-functionalized silica particle was higher.

In this case, a straightforward comparison is not possible since these results only demonstrate in a qualitative way the attachment (conjugation). If the aptamer bound maximally to the particle, the zeta potential should be approximately the same, regardless of the amount of initial DNA added.

Cai and co-workers (Cai *et al.*, 2012) describe very similar particles to those in study and recorded a zeta potential of -20.3 mV. Compared to our results obtained for aptamer 2A, it can be seen that they are very similar. However, when compared to the results for aptamer 2B, the zeta potential is practically twice as high. These values could be explained by the pH influence on the zeta potential measurements. A zeta potential value on its own without an associated pH is a virtually meaningless number. If the pH of a particle in suspension with a negative zeta potential is increased, then the particles will tend to acquire a more negative charge. If acid is then added to

this suspension a point will be reached where the negative charge is neutralized (Ragbhu Babu and Ragaranjan, 2012). As the pH of the reaction is 7.8, it is possible that the particles acquire more negative charge, thus explaining the increased zeta potential comparing with the values reported by Cai and co-workers.

Again, with zeta potential measurements different results were obtained from what we expected, namely a significant decrease in the zeta potential of the silica functionalized with aptamers compared to silica itself. A possible explanation could be the absence of ligation between aptamer and particle. On the other hand, perhaps the methodology was not the most appropriate to evaluate conjugation explained by noted above, the changes of the surface caused for the pH. Possibly, the columns were not providing an adequate separation of the strands. The columns were several times reutilized so probability the columns were degraded and were not effective to the strands separation.

The zeta potential methodology was decided to change. To evaluate the effective ligation DLS technique was used to determine the size distribution profile of the silica particles (Figure 3.7-A, 3.7-B) (Zhang *et al.*, 2010a, 2012b). The advantage of this technique is that the material can be measured in any buffer of choice. With this benefit, it is not necessary to take in consideration the constraints of pH and ionic strength.

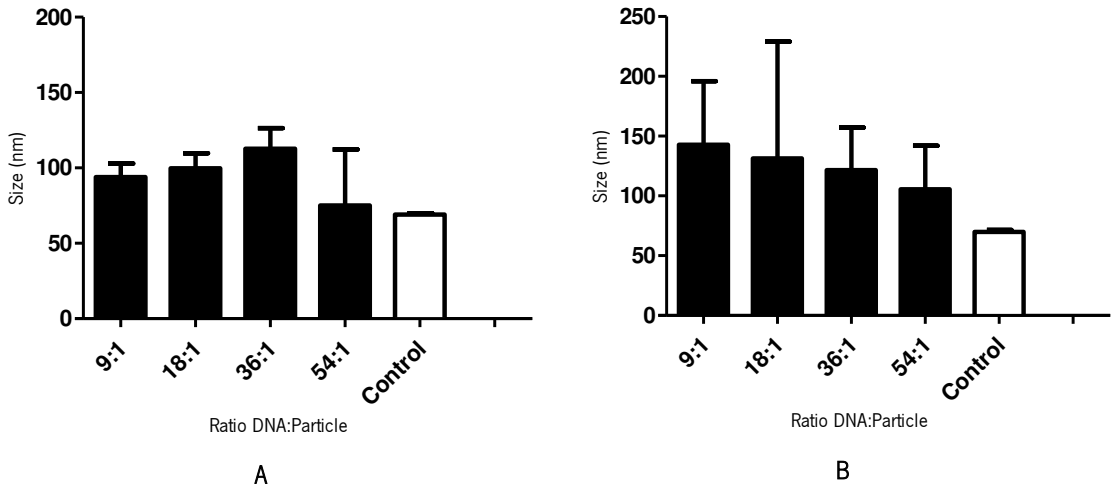

Figure 3.7 – Size measurement of the aptamer recovered from the reaction testing several ratios of DNA:Particle at pH=5 for (A) aptamer 2A and (B) aptamer 2B. The last column represents the size of the particle not functionalized (control). Results are presented as Mean ± SD and represent 3 independent experiments.

It was expected that the silica functionalized with DNA had a larger size than the control. This can be confirmed in Figure 3.7 for all the conditions tested. However, this increase in the functionalized particle size would imply that there should not exist a difference between ratios

DNA:Particle because, as in the previous methodology, the analysis of the attachment was made just to check if DNA was linked or not. Regardless of the number of DNA molecules linked to the silica particle, the size should be the same.

These differences between the conditions tested could be explained by the distinct conformations that DNA molecules can adopt when linked to silica (Figure 3.8).

Figure 3.8 - Possible conformations of DNA molecules hybridized to the surface of silica NPs (A) to (C). (Taken from (Gagnon *et al.*, 2008)).

Another possible explanation could be that the small particles in use (60 nm) may easily aggregate. The size often obtained could be caused by the existence of agglomerated particles and not by the DNA linked to particles. This method to qualitatively confirm DNA linkage to the particle was therefore also discarded.

To definitively eliminate all the problems that may hamper the binding of DNA aptamers to the particles it was decided not to use the streptavidin columns. Besides the low yield of ssDNA recovered and the great losses of DNA during the column separations, they do not give a 100% certainty that the process of denaturation is effective and if we are dealing only with ssDNA.

Therefore, it was decided to use a colorimetric method that allowed the detection of dsDNA. The particles in use have natural fluorescence. The colorimetric method was chosen in order to not affect in any way the measurement of DNA attached to the particle.

As referred to in (section 2.2.4) several concentrations of dsDNA were incubated with PI. A relationship between fluorescence and amount of aptamer (picomol) defines the calibration curve necessary to find out how DNA is linked to the particle. Figure 3.9 represents the calibration curves for aptamer 1A, 1B, 2A and 2B.

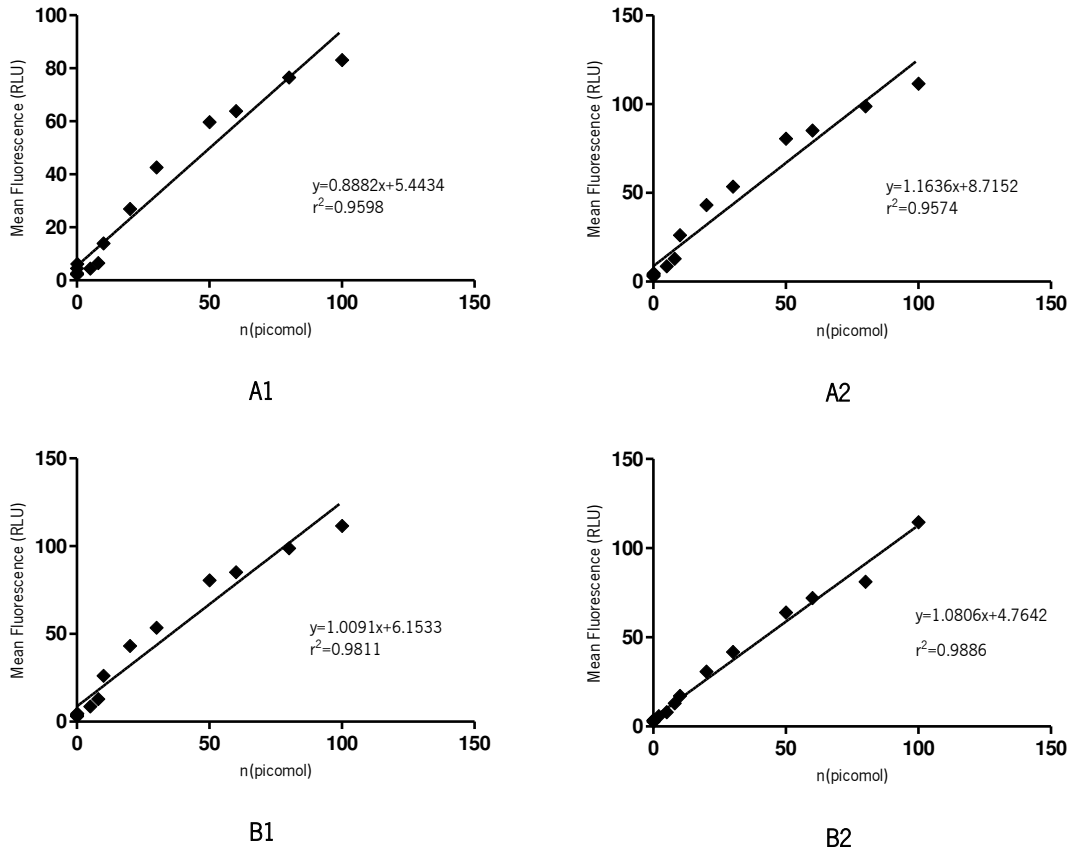

Figure 3.9 – Calibration curves for fluorescence versus aptamer amounts for (A1) aptamer 1A , (A2) aptamer 1B, (B1) aptamer 2A and (B2) aptamer 2B.

Initially, several concentrations of aptamer were tested. After detecting the fluorescence, it was not possible to obtain a calibration curve that had a linear trend. Thus, it was found that fluorescence is, typically, directly proportional (linear) to the concentration; however, there are some factors that affect this linear relationship. For example, when the concentration is too high, light cannot pass through the sample to cause excitation; thus very high concentrations can have very low fluorescence (Kubista *et al.*, 1994; Tohda *et al.*, 2001).

With this information it was decided to lower the concentrations thus achieving the calibration curves with linear trends.

The calibration curves (Figure 3.9) show a good linear relationship between mean fluorescence and DNA number of moles. The proportions of variability of the data sets are all similar and above 0.95, which is considered a good value.

The number of immobilized aptamer molecules on the silica particles can be quantitatively determined from the regression equation of the aptamer.

Figure 3.10-A1 and 3.10-A2 illustrate the results for DNA attachment to particle for aptamer 1A and 1B, and Figure 3.10-B1 and 3.10-B2 the DNA ligation to particle results for aptamer 2A and 2B.

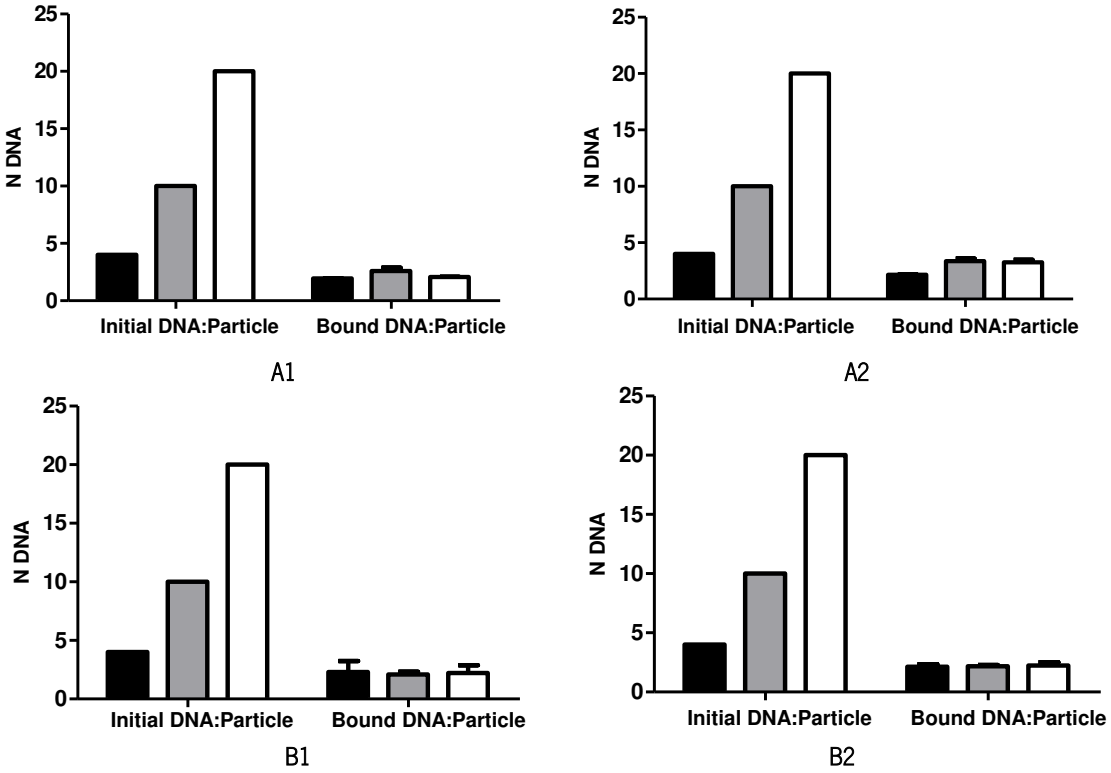

Figure 3.10 – Comparison of available initial DNA and DNA linked to silica at pH=5 for (A1) aptamer 1A, (A2) aptamer 1B, (B1) aptamer 2A and (B2) aptamer 2B. Results are presented as Mean ± SD and represent 2 independent experiments.

Figure 3.10 illustrates the comparison between the initial number of DNA molecules available per particle and the molecules of DNA per particle after the functionalization.

In the first view, these results seem to corroborate what was previously discussed. After an analysis of the spectrophotometry results in Figure 3.5, it was concluded that the silica particles probably had a coupling limit. Regardless of the quantity of aptamer added the silica, the total amount of DNA bound was practically the same for all conditions tested. Observing these last results the conclusion was the same.

These ratios correspond to an average, which means that possibly in the same sample some particles have a lot of DNA molecules while others may only have a few. Probably, when more DNA was added, some particles attached to the majority of the DNA molecules, where other particles did

not bind to DNA, whereas when less DNA was added, the particles could have an equal distribution of DNA for all the particles. In both situations the average could perfectly be the same.

It seems that some DNA was effectively linked to silica. The appropriate controls were performed to validate this methodology. The particles without NH_2-label present lower fluorescence when compared with the results shown in Figure 3.10.

Some experiments were important to confirm that there is no fluorescence competition between the particle and dye. These assays were performed after silica particle functionalization with aptamers using the same conditions as those tested before (Figure 3.10).

It is important to know whether only DNA coupled to particle was measured and to exclude any kind of interference.

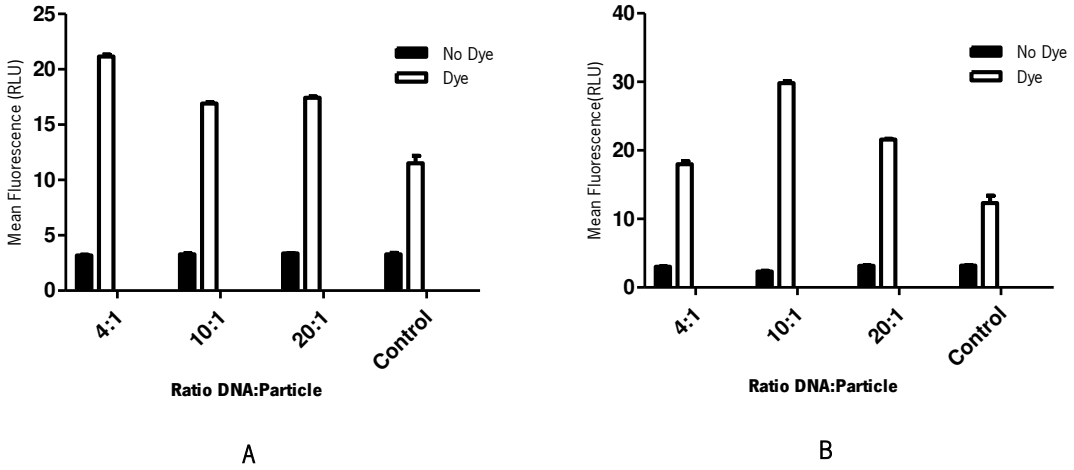

Figure 3.11 – Interaction between particle and dye for the same wavelength (excitation: 535 nm and emission: 617 nm) for (A) aptamer 1A and (B) aptamer 2A. Results are presented as Mean ± SD and represent 2 independent experiments.

As can be observed in Figure 3.11, the control fluorescence (particle functionalized with DNA without amine group labeled) is lower than the DNA labeled attached to particle proving the successful coupling.

To conclude, it is important to say that the fluctuations in the results could be explained by the protocol used, namely the steps regarding the particle washing. After centrifugation, the supernatant was pipetted out. Some functionalized particles with aptamer that are in suspension and not in the 'pellet' may be discarded as well. However, the nanoparticles can be separated from unbound biomolecules using other, more suitable methodologies, such dialysis or filtration.

3.3. Binding Assays

To assess the selectivity and affinity of the selected aptamers, binding assays were performed using the cancer cell lines under study. For these assays, the aptamers were used either labeled with FAM or conjugated with the silica particles.

In order to label DNA with FAM, PCR amplification was used. After PCR, both formulations were in dsDNA form, so a denaturation process was performed to obtain ssDNA as required for the binding assays.

To evaluate the possible losses of fluorescence for DNA labeled with FAM, a comparative graphic between unlabeled aptamer, FAM aptamer and FAM aptamer after denaturation was performed (Figure 3.12).

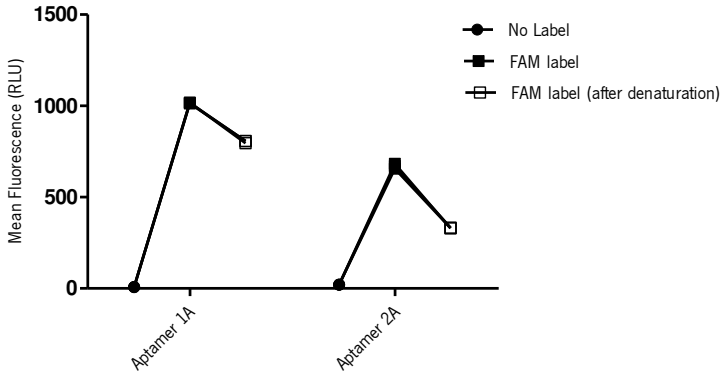

Figure 3.12 –Evaluation of fluorescence loss for different conditions for aptamer 1A and aptamer 2A.

Effectively a fluorescence decrease is notorious. Despite the obvious decrease, the aptamers 1A and 2A were used for the following assays. Since the selection of these two aptamers took place at 4°C, the binding assays with the target cell lines were performed at this temperature but also at 37°C. The binding assays at 37°C were performed to verify the stability of aptamer binding to its target.

Unfortunately, the results for 37°C, both for 1 and 4 h, were not good for any aptamer obtaining low-to-no fluorescence. This may be an indication that the aptamer suffers structural changes with the temperature increasing, removing their ability to bind the cell target. Also, it means that some modifications would be necessary to keep the aptamer stable and able to recognize the target for assays at physiological conditions or *in vivo* studies. However, further testing would be required.

For binding assays at 4°C, for 4 h, the cells start to detach and no microscopic images could be obtained.

For aptamer 1A, two types of probes were tested. For probe 1, corresponding to the silica particles linked to the aptamer, only the major ratio DNA:Particle, 20:1 was tested. Probe 2 corresponds to FAM-aptamer. Two controls were performed: Control 1 represents the silica particles and control 2 represents the unlabeled aptamer. Only the results obtained for the selection conditions are presented, 1 h at 4°C.

Figure 3.13 represents the binding of probe 1 and 2 with the 2 controls, against cancer cell line 1.

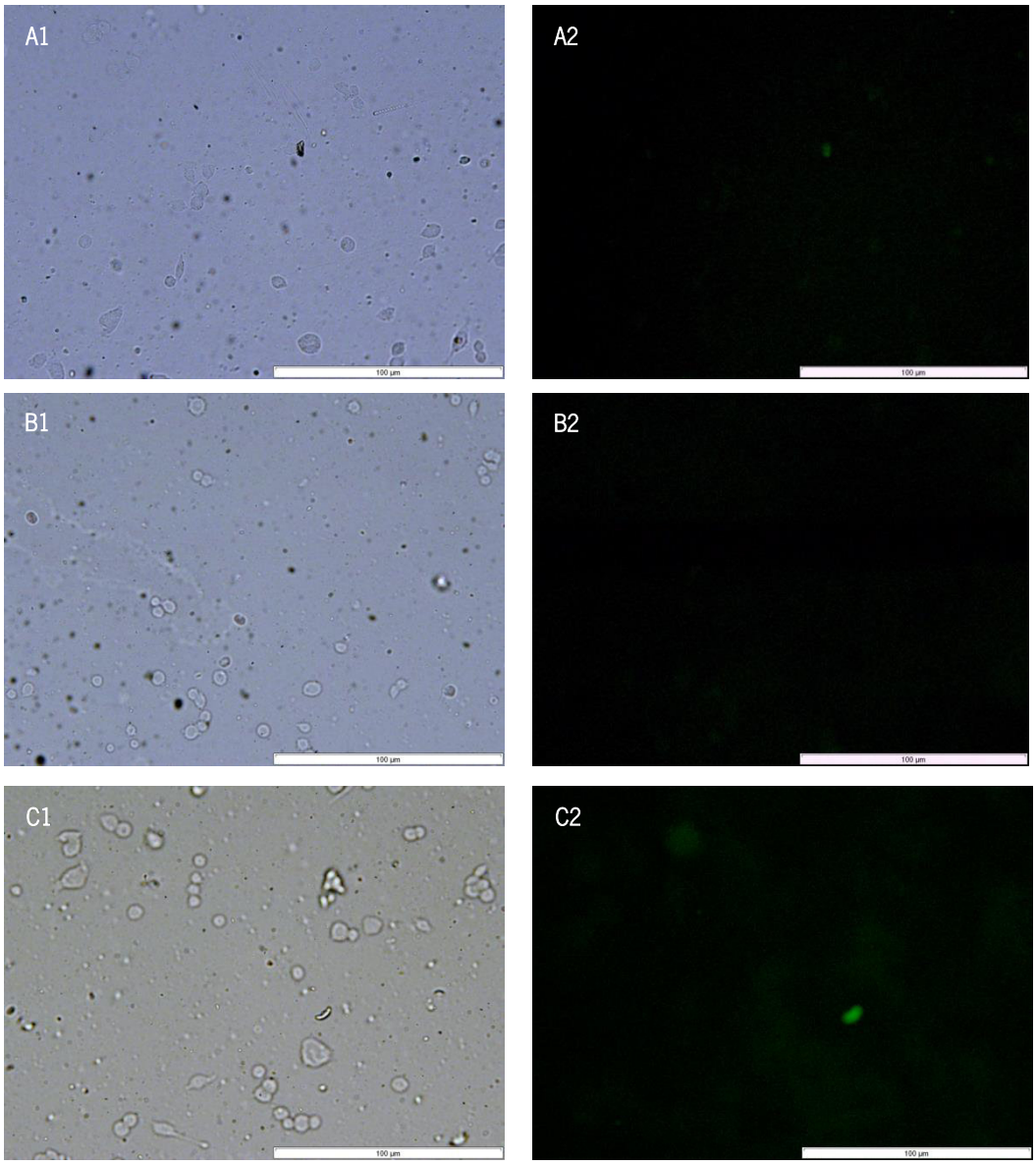

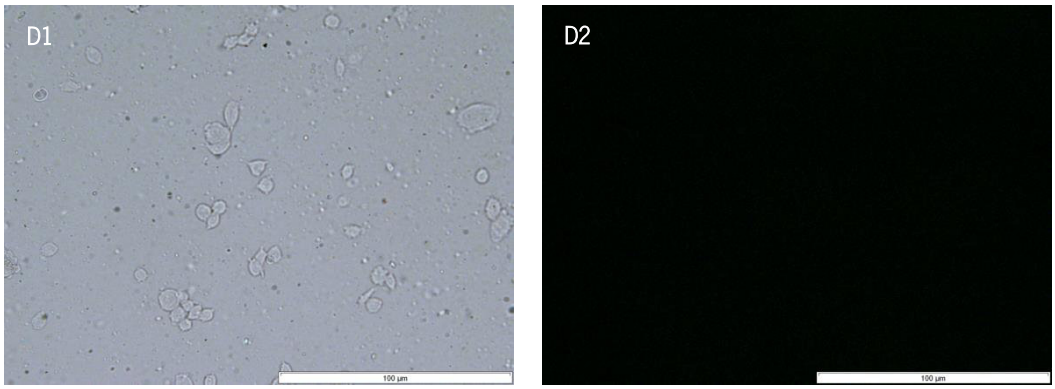

Figure 3.13 – Microscopy images of breast cancer cell line 1 for aptamer 1A. (A) probe 1; (B) probe 2; (C) control group 1; (D) control group 2. Images 1) represent bright field and Images 2) represent fluorescence image (scale bar represents 100 µm).

Analyzing the images, the probe 1 (Figure 3.13-A1, 3.13-A2) seems to slightly hybridize with breast cancer cells mainly located at the bottom. This could be a good result because the aptamer could be recognizing specific markers on the cells surface, indicating that Cell-SELEX was successfully carried out.

Considering the results for control 1 (Figure 3.13-C1 and 3.13-C2), the silica functionalized with aptamer seems to appear in the entire microscope image less bound to the cells. Effectively, it is only necessary to confirm whether or not the aptamer recognizes the 3T3 cells, to be able to say that the aptamer is selective and has affinity only for breast cancer cell line 1.

As can be observed in Figure 3.13-B1 and 3.13-B2 the FAM aptamer appears to bind weakly to cells located mainly on the bottom of image. As expected, in Figure 3.13-D1 and 3.13-D2 any fluorescence occurs.

In order to verify whether the selected aptamers are specifically binding to breast cancer cell lines, the same assay was performed against the counter selection cell line used during Cell-SELEX. Figure 3.14 shows the binding assays for probe 1 and 2 for 3T3 cells.

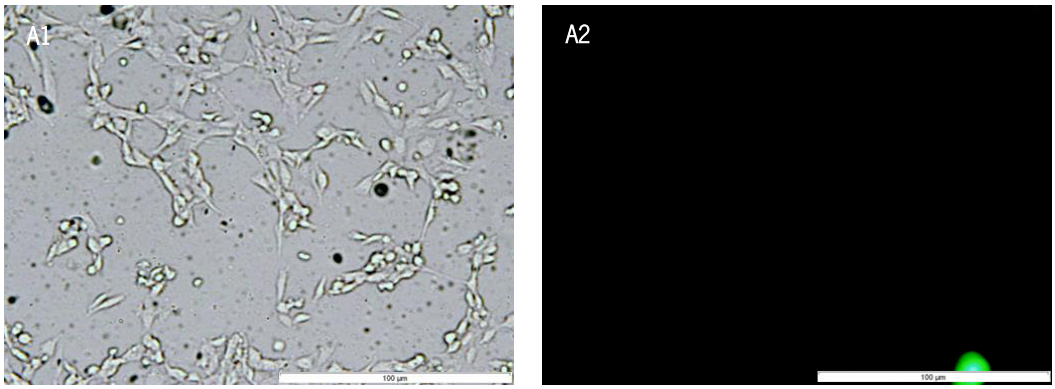

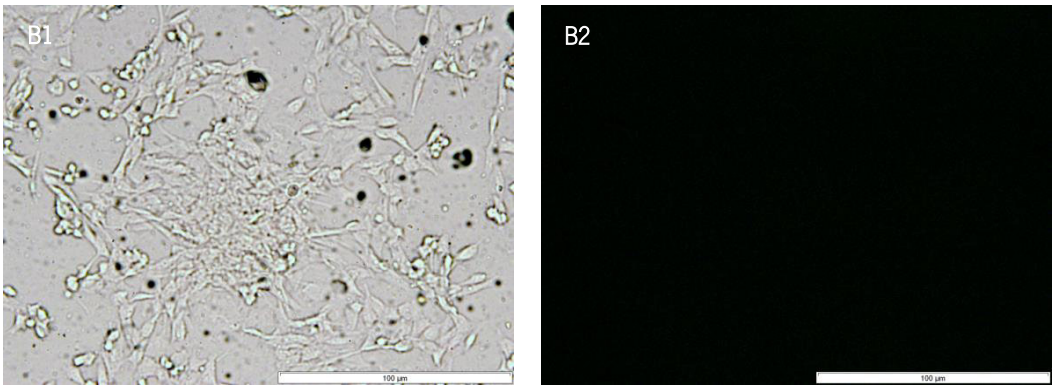

Figure 3.14 - Microscopy images of control cell line 3T3 for aptamer 1A. (A) probe 1; (B) probe 2. Images 1) represent bright field and Images 2) represent fluorescence image (scale bar represents 100 μm).

As can be seen for probe 1 (Figure 3.14-A1, 3.14-A2) and probe 2 (Figure 3.14-B1, 3.14-B2) no hybridization with cells occurred. The fluorescence image for probe 1 (Figure 3.14-A2) shows a little green spot but this does not represent hybridization with any cell. This could be associated to a dirty sample or corresponds to a drop.

According to these results it was possible to identify and independently validate aptamer 1A with affinity for cell surface markers present on the surface of breast cancer cell line 1. These findings indicate that Cell-SELEX was able to evolve aptamers that recognize changes in cell surface macromolecules. Furthermore, it is important to notice that 3T3 cells are considered non-tumorigenic. As we are talking about completely different cell lines, what the aptamer is detecting are differences at the cell surface between breast cancer cell line 1 and 3T3. This not means that the aptamer distinguishes the tumorigenic from non-tumorigenic cells. This distinction was possible with tumorigenic and non-tumorigenic cells at the same lineage.

In summary, from these results it is possible to infer the successful Cell-SELEX, but not to suggest their probable use as diagnostic probes. The affinity of selected aptamers could be a result of the stringent conditions in the later rounds of selection, which removed aptamer candidates that were weakly bound to their targets. In order to clearly demonstrate the potential of aptamer 1A as molecular probes for cancer cell line 1 recognition flow cytometry assays were performed (Figure 3.15).

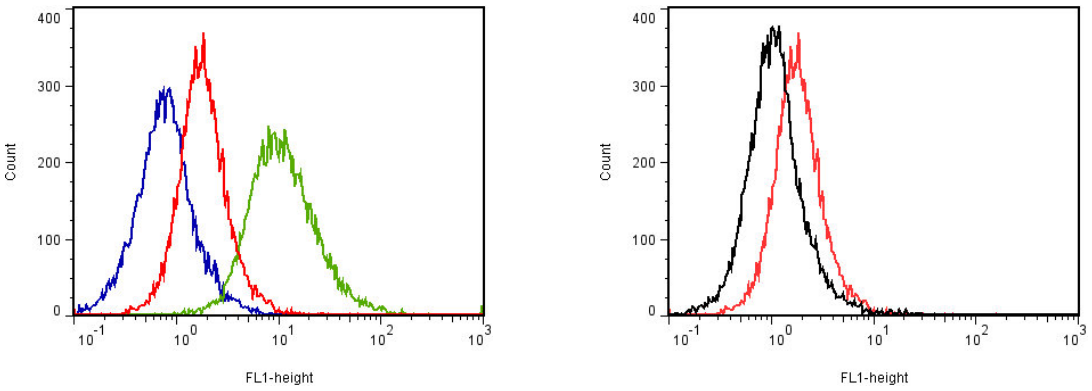

Figure 3.15 – Flow cytometry binding assay histograms for aptamer. (A) Comparison between Target (Blue), Probe 2 (Red) and Probe 1 (Green). (B) Comparison between Control 2 (Black) and Probe 2 (Red).

Comparing the fluorescence of probe 1 and probe 2 with the target, a high fluorescence increase can be observed. This enhancement was notorious for both probes 1 and 2 but mainly for the latter, confirming the microscope pictures presented in Figure 3.13-A2, 3.13-B2. The Figure 3.15-B shows the fluorescence increase for FAM-aptamer when compared with the unlabeled aptamer.

Figure 3.16 represents the fluorescence images of samples used for cytometry assays for probe 1.

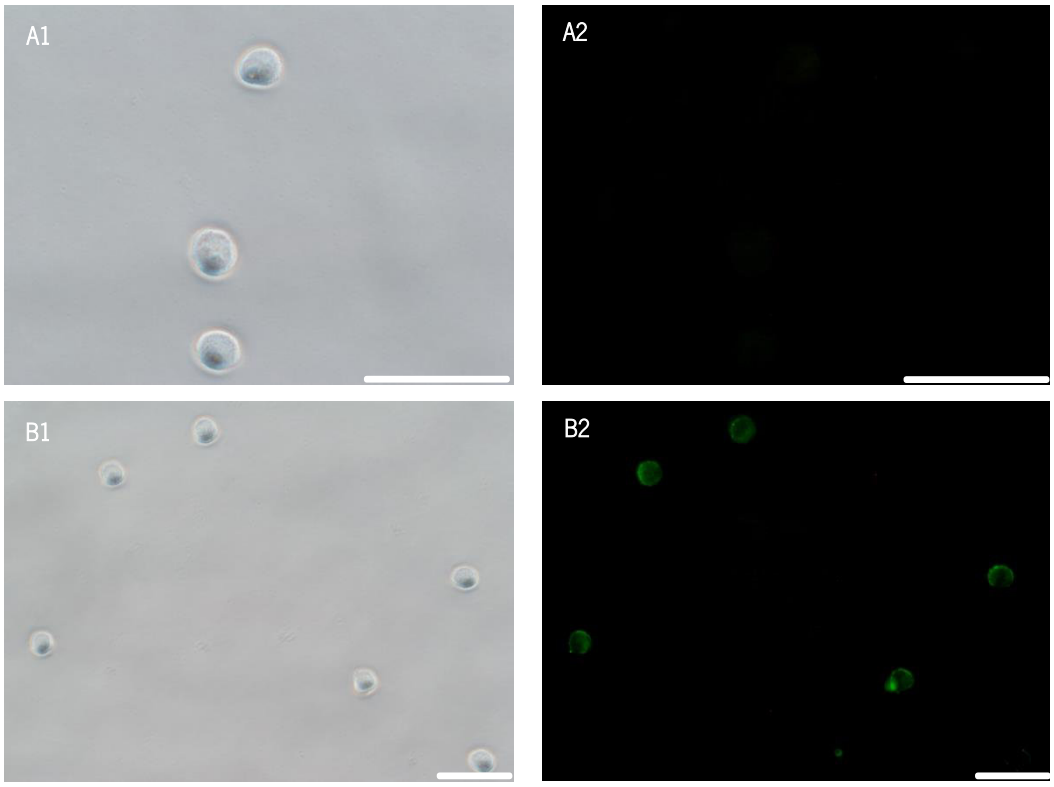

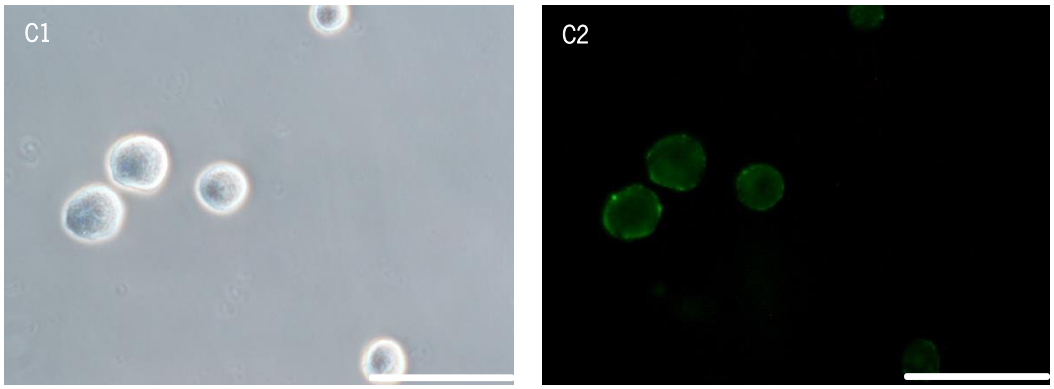

Figure 3.16 - Microscopy images of breast cancer cell line 1 for aptamer 1A. (A) Target: (B) and (C) probe 1. Images 1) represent bright field and Images 2) represent fluorescence image. The scale bar for (A) and (C) represents 200 µm. The scale bar for (B) represents 400 µm.

Microscope images of Figure 3.16-B2 and 3.16-C2 show a significant fluorescence compared to Figure 3.16-A2. The bright spots could represent the aptamer ligation to a specific marker in the cell surface. These results demonstrate the selectivity and affinity of the aptamer 1A for breast cancer cell line 1. Furthermore, probe 1 allowed confirming that silica particles were efficiently functionalized with aptamers.

However, several assays are still needed to confirm these findings, including tests with different tumor cell lines to distinguish cancer types and subtypes; and assays conducted at 37°C to validate the aptamer 1A effectiveness.

For aptamer 2A selected from cancer cell line 2, two types of probes were tested. Probe 3 corresponds to the silica particles functionalized with aptamer 2A. To perform this study, the higher ratio DNA:Particle, 20:1, was tested. Probe 4 represents the FAM-labeled aptamer 2A. A control was used to prove effectiveness. Control 3 represents the non-labeled aptamer. The control where silica particles alone are used was not performed for this aptamer. Figure 3.17 represents the binding of probes 3, probe 4 and control 3 against cancer cell line 2.

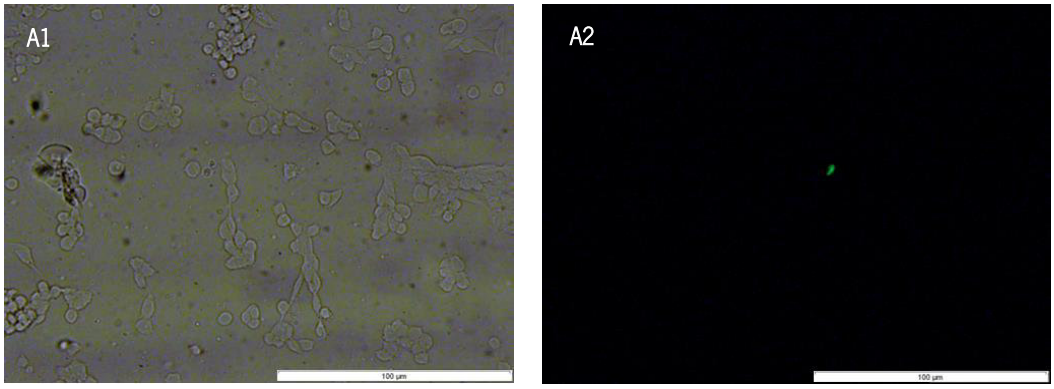

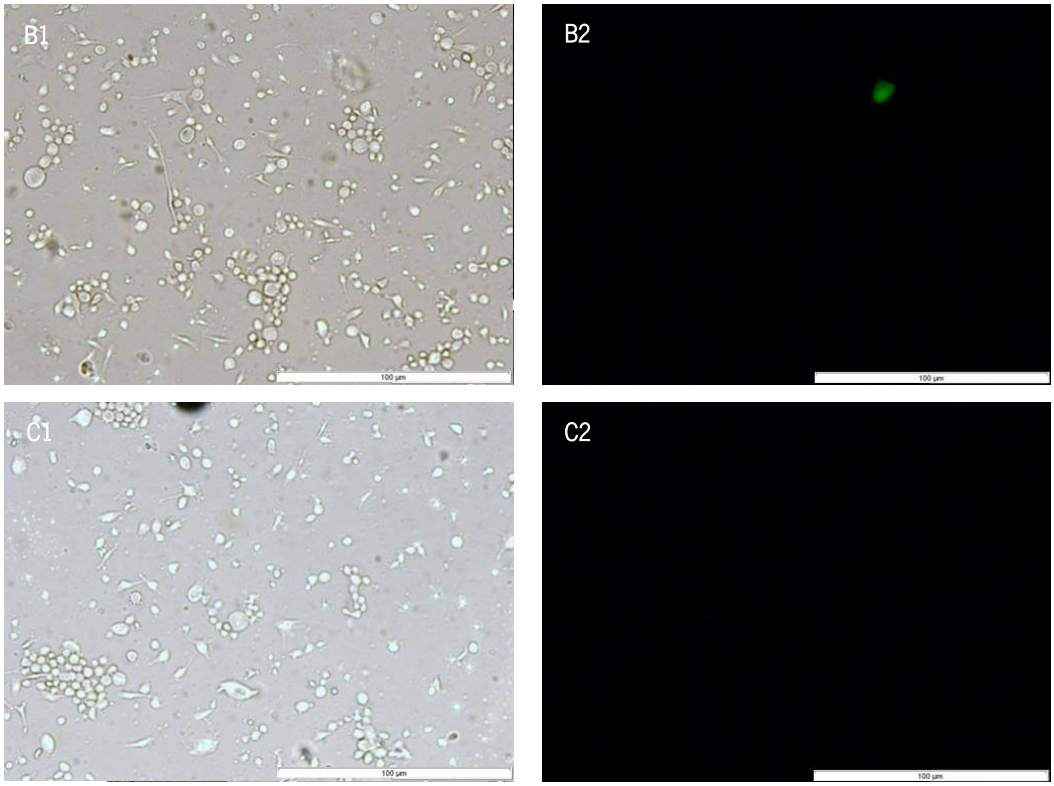

Figure 3.17 -Microscopy images of breast cancer cell line 2 for aptamer 2A. (A) probe 3; (B) probe 4; (C) control group 3. Images 1) represent bright field and Images 2) represent fluorescence image (scale bar represents 100 µm).

The results obtained for aptamer 2A against breast cancer cell line 2 were different from the previous results. For probe 3 (Figure 3.17-A1, 3.17-A2) and probe 4 (Figure 3.17-B1, 3.17-B2) no hybridization with cells was verified. The green spots are probably caused by dirty samples since there are no visible cells (bright field) in the location of fluorescent spots (fluorescent image).

As expected, no fluorescence was detected for control 3 (Figure 3.17-C1, 3.17-C2).

These results seem to indicate that this aptamer 2A is not selective for breast cancer cell lineage 2 since it does not recognize the target cell line.

Despite these results, probe 3 and 4 were still used to perform assays with counter selection cell line (Figure 3.18).

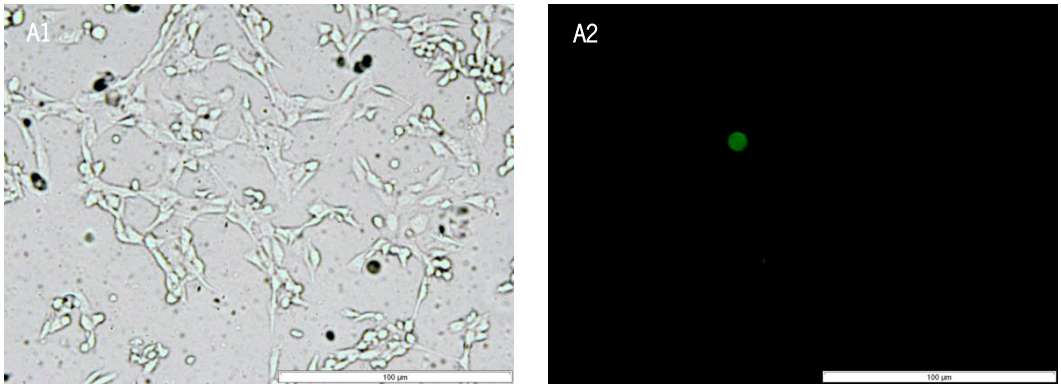

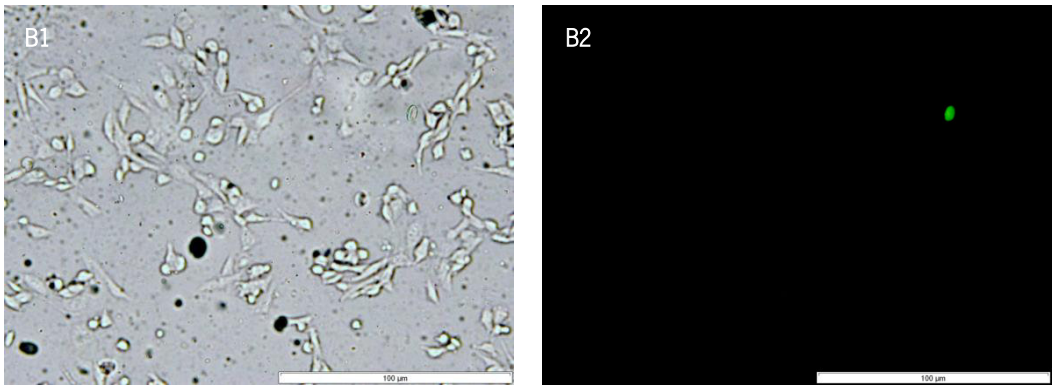

Figure 3.18 - Microscopy images of control cell line 3T3 for aptamer 2A. (A) probe 3; (B) probe 4; 1) represent bright field and Images 2) represent fluorescence image (scale bar represents 100 µm).

As expected, the aptamer 2A does not hybridize with counter selection lineage when using probe 3 (Figure 3.18-A1, 3.18-A2) or probe 4 (Figure 3.18-B1, 3.18-B2).

Results for probe 3 indicate that the probe most likely failed to hybridize since no DNA is bound to silica. However, this is highly unlikely, since the protocol was the same used for the aptamer 1A. Probably, the problem is the affinity of the aptamer 2A.

In order to further confirm the results obtained, a flow cytometry assay was performed (Figure 3.19).

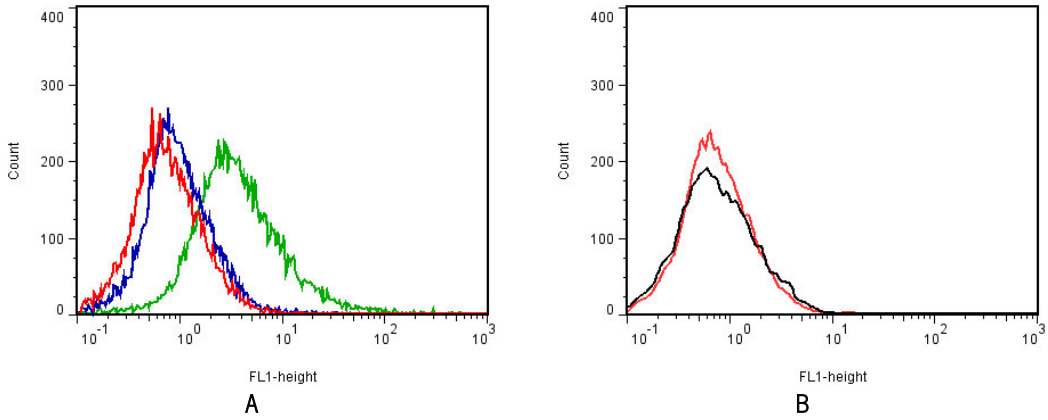

Figure 3.19 - Flow cytometry binding assay histograms for aptamer 2A. (A) Comparison between Target (Blue), Probe 4 (Red) and Probe 3 (Green). (B) Comparison between Control 2 (Black) and Probe 4 (Red).

The cytometry results (Figure 3.19-A) demonstrate that probe 3 has a slightly higher fluorescence than the target sample but was not visible in microscope images. Insufficient cell wash could explain the results. Probe 4 shows no fluorescence in comparison with the target, in agreement with fluorescence pictures

In Figure 3.19-B the fluorescence results for probe 4 and control 3 were the same, confirming the low/inexistent affinity of aptamer 2A for breast cancer cell lineage 2 according to the previous images.

The overall results show that aptamer 1A and aptamer 2A have different behaviors. Aptamer 1A appears to have affinity and selectivity for breast cancer cell line 1 which could mean a successful Cell-SELEX in the enrichment of aptamers that recognize target cell surface markers. Controls 1 and 2 show the effectiveness of this aptamer, validated with the appropriated controls and proved by the microscope images and cytometry for breast cancer cell line 1. To assess the possible affinity of this aptamer to discriminate between several breast cancer cell lines and other types of cells, competition assays for multiple targets could also be performed.

Aptamer 2A had very different results. It does not recognize the cells of breast cancer lineage 2 when using probe 3 or probe 4 meaning a Cell-SELEX inefficient for the recognition markers in the surface of breast cancer cell line 2.

The characterization of the results of the Cell-SELEX herein implemented (section 3.1) were not very good. The characterization in terms of sequence homology has the best result near 50%. Because of this, two other aptamers, 2A and 2B were used as comparison since these presented a homology of almost 100%.

It can be stated that aptamer characterization based on sequence homologies *per se* is not enough. Although aptamer 2A and 2B present higher homology it was proved that the first do not specifically recognize cancer line 2. It is important to mention the absence of data on dissociation constants and binding activity as referred in section 3.1. It is also imperative to acknowledge the lack of an important negative control. The FAM labeled unselected ssDNA library should have been used to determine nonspecific binding.

It is generally known that some fluorescent dyes suffer from severe photobleaching when used for biological applications. To investigate whether silica particles can increase resistance to photobleaching, an assay was performed to compare FAM-aptamer (Figure 3.20) and silica aptamer (Figure 3.21).

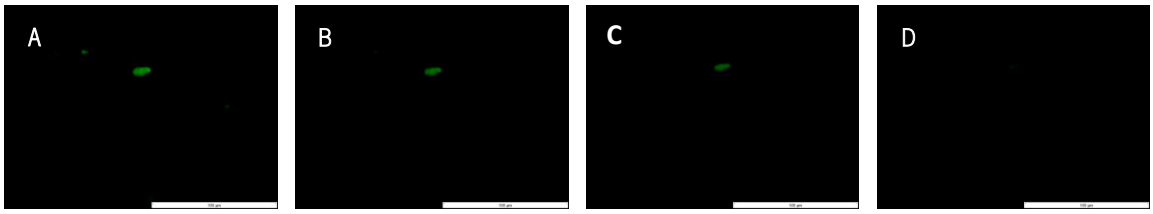

Figure 3.20 - Photostability of labeled FAM aptamer 1A . The fluorescent images were acquired at (A) 0 s, (B) 60 s, (C) 2 min, (D) 10 min (scale bar represents 100 μm).

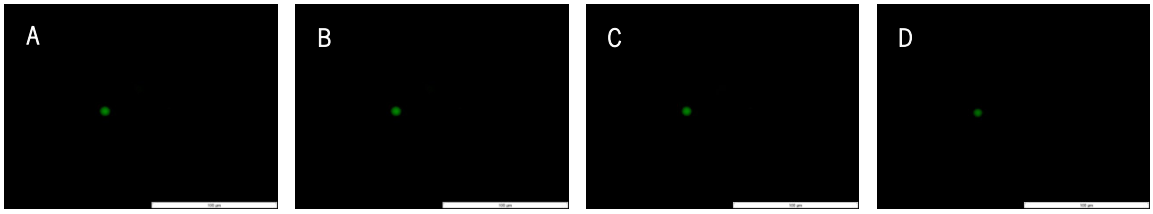

Figure 3.21 - Photostability of aptamer 1A conjugated with silica particles .The fluorescent images were acquired at (A) 0 s, (B) 60 s, (C) 2 min, (D) 10 min (scale bar represents 100 μm).

The fluorescent images were acquired at 0 s, 60 s, 2 min and 10 min. As shown in Figure 3.20 the fluorescence of FAM was bleached quickly. After 60 s of irradiation a notorious reduction in fluorescence was verified. Ten minutes later no fluorescence was observed.

The silica particles, compared with the common organic dye FAM, display a dramatically increased photostability. The green signals were clearly distinguishable to the naked eye, even after intense irradiation for 10 min. The silica particles in study contain a high amount of covalently bound fluorescence dye in the silica matrix. As the fluorescence dye was entrapped in the matrix probably the quenching is lower what increases the photobleaching resistance.

CHAPTER 4

MAIN CONCLUSIONS AND SUGGESTIONS FOR FORTHCOMING WORK

The experimental work was performed under the goal of selecting a panel of new aptamers capable of recognizing breast cancer cells using an iterative method, Cell-SELEX. The selection was targeted against the MDA-MB-435 breast carcinoma cell line and using 3T3 mouse embryonic fibroblast lineage as counter selection.

After 10 rounds of selection, selected aptamers were characterized according to their sequence homology and secondary structure looking for similarities.

The aptamers were then effectively functionalized in silica particles using the carbodiimide methodology. A colorimetric method was used for characterizing the ligation taking into account the intercalating DNA bases.

FAM-labeled aptamers or aptamers conjugated with fluorescent silica nanoparticles were tested in order to assess their binding affinity to target and non-target cells. For aptamer 1A, a faint hybridization of the aptamer seems to occur and the results were validated for the respective controls. For aptamer validation, several assays are still needed, namely tests with different breast cancer cell lines to distinguish cancer types and subtypes; and assays conducted at 37°C to validate it effectiveness. For the aptamer 2A no binding to the cells was verified, contradicting the expected results based on homology. It can be concluded that aptamers characterization based on their homologies *per se* is not enough. The aptamer with higher homology did not show affinity or specificity for the cancer cell line used as target. A deepest characterization for all the aptamer pool may also be performed.

This means that for probe 1A a successful Cell-SELEX was implemented and the silica functionalization with aptamers was well achieved. However, further characterizations and modifications of either Cell-SELEX or ligation are still need.

Several modifications could be made to the cell-SELEX experimental setup including separation of DNA strands in order to use ssDNA in each round of selection; the monitoring of the selection pool enrichment in order to select the aptamers with the highest affinity and selectivity. To study the aptamer binding to the target, a characterization based in binding capabilities and dissociation constants is also important. A closer cell line should also be chosen for the counter-selection, to obtain more selective aptamers. The greater the distance between target and non-target cells, the higher interference in the aptamer selection is expected. The use of another negative cell line such as MCF10-A, could be more indicated.

A better characterization of silica-aptamer ligation is also important to elucidate the mechanism of functionalization with respect to their photostability, size, surface charge, surface

functionality, optical and spectral features, and morphology providing a feedback that can then be shaped to improve the ligation experimental setup.

In conclusion, the present study demonstrates the usefulness of Cell-SELEX for selecting aptamers that can specifically recognize cancer cells. If some improvements, as the ones referred above, are implemented in the Cell-SELEX, panels of aptamers evolved against different cancer cell lines to distinguish cancer types could be used to relate diagnosis and prognosis. Since aptamers specific for a variety of molecular markers in the biological systems can be obtained through Cell-SELEX, in conjugation with the silica particles or another type of NP can be potentially applied to many other imaging systems capable of specifically binding to various target cells.

CHAPTER 5

REFERENCES

Adler, A., Forster, N., Homann, M., and Göringer, H.U. (2008). Post-SELEX chemical optimization of a trypanosome-specific RNA aptamer. *Combinatorial Chemistry & High Throughput Screening*. 11: 16–23.

Alivisatos, A.P. (1996). Semiconductor Clusters, Nanocrystals, and Quantum Dots. *Science*. 271: 933–937.

Aravind, A., Veeranarayanan, S., and Poulose, A. (2012a). Aptamer-Functionalized Silica Nanoparticles for Targeted Cancer Therapy. *Bionanoscience*. 2: 1–8.

Aravind, A., Jeyamohan, P., Nair, R., and Veeranarayanan, S. (2012b). AS1411 Aptamer Tagged PLGA-Lecithin-PEG Nanoparticles for Tumor Cell Targeting and Drug Delivery. *Biotechnology and Bioengineering*. 109: 2920–2931.

Avci-Adali, M., Paul, A., Ziemer, G., and Wendel, H.P. (2008). New strategies for in vivo tissue engineering by mimicry of homing factors for self-endothelialisation of blood contacting materials. *Biomaterials*. 29: 3936–3945.

Bae, S.W., Tan, W., and Hong, J. (2012). Fluorescent dye-doped silica nanoparticles: new tools for bioapplications. *Chemical Communications*. 48: 2270–2282.

Bagalkot, V., Zhang, L., and Levy-Nissenbaum, E. (2007). Quantum dot-aptamer conjugates for synchronous cancer imaging, therapy, and sensing of drug delivery based on bi-fluorescence resonance energy transfer. *Nano Letters*. 7: 3065–3070

Balamurugan, S., Obubuafo, A., Soper, S. a, and Spivak, D. a (2008). Surface immobilization methods for aptamer diagnostic applications. *Analytical and Bioanalytical Chemistry*. 390: 1009–1021.

Bates, P. J., Laber, D. A., Miller, D. M., Thomas, S. D., and Trent, J. O. (2009). Discovery and development of the G-rich oligonucleotide AS1411 as a novel treatment for cancer. *Experimental and molecular pathology*. 86: 151–64.

Becker, K.C.D., and Becker, R.C. (2006). Nucleic acid aptamers as adjuncts to vaccine development. *Current Opinion in Molecular Therapeutics*. 8: 122–129.

Becker, R. C., and Chan, M. Y. (2009). REG-1, a regimen comprising RB-006, a Factor IXa antagonist, and its oligonucleotide active control agent RB-007 for the potential treatment of arterial thrombosis. *Current opinion in molecular therapeutics*. 11: 707–15.

Bing, T., Yang, X., Mei, H., Cao, Z., and Shangguan, D. (2010). Conservative secondary structure motif of streptavidin-binding aptamers generated by different laboratories. *Bioorganic & Medicinal Chemistry*. 18: 1798–1805.

Blank, M., and Blind, M. (2005). Aptamers as tools for target validation. *Current Opinion in Chemical Biology*. 9: 336–342.

Blank, M., Weinschenk, T., Priemer, M., and Schluesener, H. (2001). Systematic evolution of a DNA aptamer binding to rat brain tumor microvessels. selective targeting of endothelial regulatory protein pigpen. *Journal of Biological Chemistry*. 276: 16464–16468.

Bunka, D.H.J., and Stockley, P.G. (2006). Aptamers come of age – at last. *Nature Reviews Microbiology*. 4: 588–596.

Cai, L., Chen, Z., Chen, M., Tang, H., and Pang, D. (2012). MUC-1 aptamer-conjugated dye-doped silica nanoparticles for MCF-7 cells detection. *Biomaterials*. 34: 371–381.

Cao, Z., Tong, R., Mishra, A., Xu, W., Wong, G.C.L., Cheng, J., and Lu, Y. (2009). Reversible cell-specific drug delivery with aptamer-functionalized liposomes. *Angewandte Chemie International Edition*. 48: 6494–6498.

Cerchia, L., Hamm, J., Libri, D., Tavitian, B., and de Franciscis, V. (2002). Nucleic acid aptamers in cancer medicine. *FEBS Letters*. 528: 12–16.

Chakravarthy, U., Adamis, A. P., Cunningham, E. T., Goldbaum, M., Guyer, D. R., Katz, B., and Patel, M. (2006). Year 2 efficacy results of 2 randomized controlled clinical trials of pegaptanib for neovascular age-related macular degeneration. *Ophthalmology*. 113: 1508-1525.

Chan, M. Y., Cohen, M. G., Dyke, C. K., Myles, S. K., Aberle, L. G., Lin, M., and Rusconi, C. P. (2008). Phase 1b randomized study of antidote-controlled modulation of factor IXa activity in patients with stable coronary artery disease. *Circulation*. 117: 2865–74.

Chan, W.C. (1998). Quantum Dot Bioconjugates for Ultrasensitive Nonisotopic Detection. *Science*. 281: 2016–2018.

Chen, X.-C., Deng, Y.-L., Lin, Y., Pang, D.-W., Qing, H., Qu, F., and Xie, H.-Y. (2008). Quantum dot-labeled aptamer nanoprobes specifically targeting glioma cells. *Nanotechnology*. 19: 1-6.

Chiu, T.-C., and Huang, C.-C. (2009). Aptamer-functionalized nano-biosensors.*Sensors*. 9: 10356-10388

Chu, T.C., Marks, J.W., Lavery, L.A., Faulkner, S., Rosenblum, M.G., Ellington, A.D., and Levy, M. (2006a). Aptamer:toxin conjugates that specifically target prostate tumor cells. *Cancer Research*. 66: 5989–5992.

Chu, T.C., Shieh, F., Lavery, L. a, Levy, M., Richards-Kortum, R., Korgel, B. a, and Ellington, A.D. (2006b). Labeling tumor cells with fluorescent nanocrystal-aptamer bioconjugates. *Biosensors and Bioelectronics*. 21: 1859–1866.

Cui, Z.-Q., Ren, Q., Wei, H.-P., Chen, Z., Deng, J.-Y., Zhang, Z.-P., and Zhang, X.-E. (2011). Quantum dot-aptamer nanoprobes for recognizing and labeling influenza A virus particles. *Nanoscale*. 3: 2454–2457.

DeNardo, S.J., DeNardo, G.L., Miers, L.A., Natarajan, A., Foreman, A.R., Gruettner, C., Adamson, G.N., and Ivkov, R. (2005). Development of tumor targeting bioprobes ((111)In-chimeric L6

monoclonal antibody nanoparticles) for alternating magnetic field cancer therapy. *Clinical Cancer Research*. 11: 7087s–7092s.

Descalzo, A.B., Martínez-Máñez, R., Sancenón, F., Hoffmann, K., and Rurack, K. (2006). The supramolecular chemistry of organic-inorganic hybrid materials. *Angewandte Chemie International Edition*. 45: 5924–5948.

Dey, A.K., Griffiths, C., Lea, S.M., and James, W. (2005). Structural characterization of an anti-gp120 RNA aptamer that neutralizes R5 strains of HIV-1. *RNA.* 11: 873–884.

Diener, J. L., Daniel Lagassé, H. A., Duerschmied, D., Merhi, Y., Tanguay, J.-F., Hutabarat, R., and Schaub, R. (2009). Inhibition of von Willebrand factor-mediated platelet activation and thrombosis by the anti-von Willebrand factor A1-domain aptamer ARC1779. *Journal of thrombosis and haemostasis.* 7: 1155–1162.

Dobson, J. (2006). Magnetic nanoparticles for drug delivery. *Drug Development Research*. 67: 55–60.

Dua, P., Kim, S., and Lee, D.-K. (2011). Nucleic acid aptamers targeting cell-surface proteins. *Methods*. 54: 215–225.

Ellington, A.D., and Szostak, J.W. (1990). In vitro selection of RNA molecules that bind specific ligands. *Nature*. 346: 818–822.

Famulok, M., and Mayer, G. (2011). Aptamer modules as sensors and detectors. *Accounts of Chemical Research*. 44: 1349–1358.

Fang, X., and Tan, W. (2010). Aptamers generated from cell-SELEX for molecular medicine: a chemical biology approach. *Accounts of Chemical Research*. 43: 48–57.

Farokhzad, O.C., Jon, S., Khademhosseini, A., Tran, T.-N.T., Lavan, D. a, and Langer, R. (2004). Nanoparticle-aptamer bioconjugates: a new approach for targeting prostate cancer cells. *Cancer Research*. 64: 7668–7672.

Ferreira, C.S.M., Missailidis, S., Hall, W., and Keynes, M. (2007). Aptamer-based therapeutics and their potential in radiopharmaceutical design. *Brazilian Archives of Biology and Technology*. 50: 63–76.

Fishburn, C.S. (2008). The pharmacology of PEGylation: balancing PD with PK to generate novel therapeutics. *Journal of Pharmaceutical Sciences*. 97: 4167–4183.

Forbes, N. (2010). Engineering the perfect (bacterial) cancer therapy. *Nature Reviews Cancer*. 10: 785–794.

Forouzanfar, M.H., Foreman, K.J., Delossantos, A.M., Lozano, R., Lopez, A.D., Murray, C.J.L., and Naghavi, M. (2011). Breast and cervical cancer in 187 countries between 1980 and 2010: a systematic analysis. *Lancet*. 378: 1461–1484.

Gagnon, Z., Senapati, S., Gordon, J., and Chang, H.-C. (2008). Dielectrophoretic detection and quantification of hybridized DNA molecules on nano-genetic particles. *Electrophoresis.* 29: 4808–4812.

Gilbert, J. C., DeFeo-Fraulini, T., Hutabarat, R. M., Horvath, C. J., Merlino, P. G., Marsh, H. N., ... Schaub, R. G. (2007). First-in-human evaluation of anti von Willebrand factor therapeutic aptamer ARC1779 in healthy volunteers. *Circulation*. 116: 2678–86.

Goebl, N., Berridge, B., Wroblewski, V. J., and Brown-Augsburger, P. L. (2007). Development of a sensitive and specific in situ hybridization technique for the cellular localization of antisense oligodeoxynucleotide drugs in tissue sections. *Toxicologic pathology*. 35: 541–548.

Grabarek, Z., and Gergely, J. (1990). Zero-length crosslinking procedure with the use of active esters. *Analytical Biochemistry*. 185: 131–135.

Gragoudas, E. S., Adamis, A. P., Cunningham, E. T., Feinsod, M., and Guyer, D. R. (2004). Pegaptanib for neovascular age-related macular degeneration. *The New England journal of medicine*. 351: 2805–2816.

Green, N.M. (1975). Avidin. *Advances in Protein Chemitry*. 29: 85–133.

Grüttner, C., Müller, K., Teller, J., Westphal, F., Foreman, A., and Ivkov, R. (2007). Synthesis and antibody conjugation of magnetic nanoparticles with improved specific power absorption rates for alternating magnetic field cancer therapy. *Journal of Magnetism and Magnetic Materials*. 311: 181–186.

Guo, K.-T., Ziemer, G., Paul, A., and Wendel, H.P. (2008). CELL-SELEX: Novel perspectives of aptamer-based therapeutics. *International Journal of Molecular Sciences*. 9: 668–678.

Han, K., Liang, Z., and Zhou, N. (2010). Design strategies for aptamer-based biosensors. *Sensors*. 10: 4541–4557.

Hergt, R., Dutz, S., Müller, R., and Zeisberger, M. (2006). Magnetic particle hyperthermia: nanoparticle magnetism and materials development for cancer therapy. *Journal of Physics: Condensed Matter*. 18: S2919–S2934.

Hermanson, G.T. (2008). Bioconjugate Techniques. Second Edition. *Academic Press*, San Diego

Herr, J.K., Smith, J.E., Medley, C.D., Shangguan, D., and Tan, W. (2006). Aptamer-conjugated nanoparticles for selective collection and detection of cancer cells. *Analytical Chemistry*. 78: 2918–2924.

Hilliard, L.R., Zhao, X., and Tan, W. (2002). Immobilization of oligonucleotides onto silica nanoparticles for DNA hybridization studies. *Analytical Chimistry Acta*. 470: 51–56.

Holmberg, A., Blomstergren, A., Nord, O., Lukacs, M., Lundeberg, J., and Uhlén, M. (2005). The biotin-streptavidin interaction can be reversibly broken using water at elevated temperatures. *Electrophoresis*. 26: 501–510.

Hu, Y., Duan, J., Zhan, Q., Wang, F., Lu, X., and Yang, X.-D. (2012). Novel MUC1 aptamer selectively delivers cytotoxic agent to cancer cells in vitro. *PLoS One*. 7: 1-10.

Huang, C.-C., Huang, Y.-F., Cao, Z., Tan, W., and Chang, H.-T. (2005). Aptamer-modified gold nanoparticles for colorimetric determination of platelet-derived growth factors and their receptors. *Analytical Chemistry*. 77: 5735–5741.

Huang, Y., Lin, Y., Lin, Z., and Chang, H. (2009). Aptamer-modified gold nanoparticles for targeting breast cancer cells through light scattering. *Journal of Nanoparticle Research*. 11: 775–783.

Jayasena, S.D. (1999). Aptamers: an emerging class of molecules that rival antibodies in diagnostics. *Clinical Chemistry*. 45: 1628–1650.

Jiang, Y., Zhu, C., Ling, L., Wan, L., Fang, X., and Bai, C. (2003). Specific aptamer-protein interaction studied by atomic force microscopy. *Analytical Chemistry*. 75: 2112–2116.

Jiménez, E., Sefah, K., López-Colón, D., Van Simaeys, D., Chen, H.W., Tockman, M.S., and Tan, W. (2012). Generation of lung adenocarcinoma DNA aptamers for cancer studies. *PLoS One*. 7: 1-7.

Kang, H., O'Donoghue, M.B., Liu, H., and Tan, W. (2010). A liposome-based nanostructure for aptamer directed delivery. *Chemical Communications*. 46: 249–251.

Kang, W.J., Chae, J.R., Cho, Y.L., Lee, J.D., and Kim, S. (2009). Multiplex imaging of single tumor cells using quantum-dot-conjugated aptamers. *Small* . 5: 2519–2522.

Kanoatov, M., Javaherian, S., and Krylov, S. (2011). Aptamer-facilitated Protein Isolation from Cells. *Protocol Exchange*.

Kanwar, J.R., Roy, K., and Kanwar, R.K. (2011). Chimeric aptamers in cancer cell-targeted drug delivery. *Critical Reviews in Biochemistry and Molecular Biology*. 46: 459–477.

Klajn, R., Stoddart, J.F., and Grzybowski, B.A. (2010). Nanoparticles functionalised with reversible molecular and supramolecular switches. *Chemical Society Reviews*. 39: 2203–2237.

Kolb, H.C., Finn, M.G., and Sharpless, K.B. (2001). Click Chemistry: Diverse Chemical Function from a Few Good Reactions. *Angewandte Chemie International Edition*. 40: 2004–2021.

Kubista, M., Sjöback, R., Eriksson, S., and Albinsson, B. (1994). Experimental correction for the inner-filter effect in fluorescence spectra. *Analyst*. 119: 417-419.

Kulbachinskiy, a. V. (2007). Methods for selection of aptamers to protein targets. *Biochemistry*. 72: 1505–1518.

Kulkarni, O., Eulberg, D., Selve, N., Zöllner, S., Allam, R., Pawar, R. D., and Anders, H.-J. (2009). Anti-Ccl2 Spiegelmer permits 75% dose reduction of cyclophosphamide to control diffuse proliferative lupus nephritis and pneumonitis in MRL-Fas(lpr) mice. *The Journal of pharmacology and experimental therapeutics*. 328: 371–377.

Kunii, T., Ogura, S., Mie, M., and Kobatake, E. (2011). Selection of DNA aptamers recognizing small cell lung cancer using living cell-SELEX. *Analyst*. 136: 1310–1312.

Lee, J.F., Stovall, G.M., and Ellington, A.D. (2006). Aptamer therapeutics advance. *Current Opinion in Chemical Biology*. 10: 282–289.

Lee, J.H., Yigit, M. V, Mazumdar, D., and Lu, Y. (2010). Molecular diagnostic and drug delivery agents based on aptamer-nanomaterial conjugates. *Advanced Drug Delivery Reviews*. 62: 592–605.

Li, L., Yin, Q., Cheng, J., and Lu, Y. (2012). Polyvalent Mesoporous Silica Nanoparticle-Aptamer Bioconjugates Target Breast Cancer Cells. *Advanced Healthcare Materials*. 1: 567-572.

Liu, W.-T. (2006). Nanoparticles and their biological and environmental applications. *Journal of Bioscence and Bioengineering*. 102: 1–7.

Maasch, C., Buchner, K., Eulberg, D., Vonhoff, S., and Klussmann, S. (2008). Physicochemical stability of NOX-E36, a 40mer L-RNA (Spiegelmer) for therapeutic applications. *Nucleic acids symposium series*. 52: 61–62.

Maeda, H., Wu, J., Sawa, T., Matsumura, Y., and Hori, K. (2000). Tumor vascular permeability and the EPR effect in macromolecular therapeutics: a review. *Journal of Controled Release*. 65: 271–284.

Mann, A., and Bhavane, R. (2011). Thioaptamer conjugated liposomes for tumor vasculature targeting. *Oncotarget*. 2: 298–304.

Mascini, M. (2008). Aptamers and their applications. *Analytical and Bioanalytical Chemistry*. 390: 987–988.

Mayer, G., Ahmed, M.-S.L., Dolf, A., Endl, E., Knolle, P.A., and Famulok, M. (2010). Fluorescence-activated cell sorting for aptamer SELEX with cell mixtures. *Nature Protocols*. 5: 1993–2004.

McNeil, S.E. (2005). Nanotechnology for the biologist. *Journal of Leukocyte Biolology*. 78: 585–594.

Medintz, I.L., Uyeda, H.T., Goldman, E.R., and Mattoussi, H. (2005). Quantum dot bioconjugates for imaging, labelling and sensing. *Nature Materials*. 4: 435–446.

Medley, C.D., Bamrungsap, S., Tan, W., and Smith, J.E. (2011). Aptamer-conjugated nanoparticles for cancer cell detection. *Analytical Chemistry*. 83: 727–734.

Meyer, S., Maufort, J.P., Nie, J., Stewart, R., McIntosh, B.E., Conti, L.R., Ahmad, K.M., Soh, H.T., and Thomson, J. a (2013). Development of an Efficient Targeted Cell-SELEX Procedure for DNA Aptamer Reagents. *PLoS One*. 8: 1-7.

Misono, T.S., and Kumar, P.K.R. (2005). Selection of RNA aptamers against human influenza virus hemagglutinin using surface plasmon resonance. *Analytical Biochemistry*. 342: 312–317.

Missailidis, S., and Hardy, A. (2009). Aptamers as inhibitors of target proteins. *Expert Opinion on Therapeutic Patents*. 19: 1073–1082.

Missailidis, S., and Perkins, A. (2007). Update: aptamers as novel radiopharmaceuticals: their applications and future prospects in diagnosis and therapy. *Cancer Biotherapy and Radiopharmaceuticals*. 22: 453–468.

Mongelard, F., and Bouvet, P. (2010). AS-1411, a guanosine-rich oligonucleotide aptamer targeting nucleolin for the potential treatment of cancer, including acute myeloid leukemia. *Current opinion in molecular therapeutics*. 12: 107–14.

Nakajima, N., and Ikada, Y. (1995). Mechanism of amide formation by carbodiimide for bioconjugation in aqueous media. *Bioconjugate Chemistry*. 6: 123–130.

Natarajan, A., Xiong, C.-Y., Gruettner, C., DeNardo, G.L., and DeNardo, S.J. (2008). Development of multivalent radioimmunonanoparticles for cancer imaging and therapy. *Cancer Biotherapy and Radiopharmaceuticals*. 23: 82–91.

Ng, E.W.M., Shima, D.T., Calias, P., Cunningham, E.T., Guyer, D.R., and Adamis, A.P. (2006). Pegaptanib, a targeted anti-VEGF aptamer for ocular vascular disease. *Nature Reviews Drug Discovery*. 5: 123–132.

Ni, X., and Castanares, M. (2011). Nucleic acid aptamers: clinical applications and promising new horizons. *Current Medicinal Chemistry*. 18: 4206–4214.

Ohuchi, S. (2012). Cell-SELEX Technology. *BioResearch. Open Access*. 1: 265–272.

Pestourie, C., Tavitian, B., and Duconge, F. (2005). Aptamers against extracellular targets for in vivo applications. *Biochimie*. 87: 921–930.

Phillips, J. a, Lopez-Colon, D., Zhu, Z., Xu, Y., and Tan, W. (2008). Applications of aptamers in cancer cell biology. *Analytica Chimica Acta*. 621: 101–108.

Proske, D., Blank, M., Buhmann, R., and Resch, A. (2005). Aptamers–basic research, drug development, and clinical applications. *Applied Microbiology and Biotechnology*. 69: 367–374.

Prow, T.W., Rose, W.A., Wang, N., Reece, L.M., Lvov, Y., and Leary, J.F. (2005). Biosensor-Controlled Gene Therapy/Drug Delivery with Nanoparticles for Nanomedicine. T. Vo-Dinh, W.S. Grundfest, D.A. Benaron, and G.E. Cohn, eds. 199–208.

Ragbhu Babu, K., and Ragaranjan, D.K. (2012). Electro Kinetic Potential Technique for Ore Beneficiation of CaCO3. *Journal of Environmental Science, Computer Science and Engineering & Technology*. 2: 187–191.

Rodrigues, L., and Kluskens, L. (2011). Synthetic Biology & Bioinformatics Prospects in the Cancer Arena. *Computational Biology and Applied Bioinformatic*s. 8: 159-186.

Rostovtsev, V. V, Green, L.G., Fokin, V. V, and Sharpless, K.B. (2002). A stepwise huisgen cycloaddition process: copper(I)-catalyzed regioselective "ligation" of azides and terminal alkynes. *Angewandte Chemie International Edition*. 41: 2596–2599.

Sambrook, J., Fritsch, E.F., and Maniatis, T. (1989). Molecular Cloning: A Laboratory Manual (Cold Spring Harbor, N.Y. Cold Spring Harbor Laboratory Press).

Sandberg, J.A., Parker, V.P., Blanchard, K.S., Sweedler, D., Powell, J.A., Kachensky, A., Bellon, L., Usman, N., Rossing, T., and Borden, E., (2000). Pharmacokinetics and tolerability of an antiangiogenic ribozyme (ANGIOZYME) in healthy volunteers. *Journal of Clinical Pharmacology*. 40: 1462–1469.

Santra, S., Wang, K., Tapec, R., and Tan, W. (2001). Development of novel dye-doped silica nanoparticles for biomarker application. *Journal of Biomedical Optics*. 6: 160–166.

Sayyed, S. G., Hägele, H., Kulkarni, O. P., Endlich, K., Segerer, S., Eulberg, D., and Anders, H.-J. (2009). Podocytes produce homeostatic chemokine stromal cell-derived factor-1/CXCL12, which contributes to glomerulosclerosis, podocyte loss and albuminuria in a mouse model of type 2 diabetes. *Diabetologia*. 52: 2445–2454.

Sefah, K., Tang, Z.W., Shangguan, D.H., Chen, H., Lopez-Colon, D., Li, Y., Parekh, P., Martin, J., Meng, L., and Phillips, J.A., (2009). Molecular recognition of acute myeloid leukemia using aptamers. *Leukemia*. 23: 235–244.

Sefah, K., Meng, L., Lopez-Colon, D., Jimenez, E., Liu, C., and Tan, W. (2010a). DNA aptamers as molecular probes for colorectal cancer study. *PLoS One*. 5: 1-14.

Sefah, K., Shangguan, D., Xiong, X., O'Donoghue, M.B., and Tan, W. (2010b). Development of DNA aptamers using Cell-SELEX. *Nature Protocols*. 5: 1169–1185.

Shangguan, D., Li, Y., Tang, Z., Cao, Z.C., Chen, H.W., Mallikaratchy, P., Sefah, K., Yang, C.J., and Tan, W. (2006). Aptamers evolved from live cells as effective molecular probes for cancer study. *Proceedings of National Academy of Sciences*. 103: 11838–11843.

Shangguan, D., Tang, Z., Mallikaratchy, P., Xiao, Z., and Tan, W. (2007). Optimization and modifications of aptamers selected from live cancer cell lines. *Chembiochem.* 8: 603–606.

Shangguan, D., Meng, L., Cao, Z.C., Xiao, Z., Fang, X., Li, Y., Cardona, D., Witek, R.P., Liu, C., and Tan, W. (2008). Identification of liver cancer-specific aptamers using whole live cells. *Analytical Chemistry*. 80: 721–728.

Shankar, S., and Pillai, M. (2011). Translating cancer research by synthetic biology. *Molecular BioSystems*. 7: 1802–1810.

Shibata, S., Taniguchi, T., Yano, T., and Yamane, M. (1997). Formation of Water-Soluble Dye-Doped Silica Particles. *Journal of Sol-Gel Science and Technology*. 10: 263–268.

Van Simaeys, D., López-Colón, D., Sefah, K., Sutphen, R., Jimenez, E., and Tan, W. (2010). Study of the Molecular Recognition of Aptamers Selected through Ovarian Cancer Cell-SELEX. *PLoS One.* 5: 1-7.

Song, K.-M., Lee, S., and Ban, C. (2012). Aptamers and their biological applications. *Sensors*. 12: 612–631.

Spange, S. (2000). Silica surface modification by cationic polymerization and carbenium intermediates. *Progress in Polymer Science*. 25: 781–849.

Sperling, R. a, and Parak, W.J. (2010). Surface modification, functionalization and bioconjugation of colloidal inorganic nanoparticles. *Philosophical Transactions of the Royal Society A Mathematical, Physical & Engineering Sciences*. 368: 1333–1383.

Sperling, R.A., Rivera Gil, P., Zhang, F., Zanella, M., and Parak, W.J. (2008). Biological applications of gold nanoparticles. *Chemical Society Reviews*. 37: 1896–1908.

Stalin, C., and Dineshkumar, P. (2012). Aptamers Role in Basic Drug Research and Development - An Overview. *International Journal o Pharmacy Sciences*. 4: 35–42.

Staros, J., Wright, R., and Swingle, D. (1986). Enhancement by N-hydroxysulfosuccinimide of water-soluble carbodiimide-mediated coupling reactions. *Analytical Biochemistry*. 156: 220–222.

Stöber, W., Fink, A., and Bohn, E. (1968). Controlled growth of monodisperse silica spheres in the micron size range. *Journal of Colloid and Interface Science*. 26: 62–69.

Stoltenburg, R., Reinemann, C., and Strehlitz, B. (2007). SELEX–a (r)evolutionary method to generate high-affinity nucleic acid ligands. *Biomolecular Engineering*. 24: 381–403.

Strehlitz, B., Reinemann, C., Linkorn, S., and Stoltenburg, R. (2012). Aptamers for pharmaceuticals and their application in environmental analytics. *Bioanalytical Reviews*. 4: 1–30.

Strober, W. (2001). Trypan blue exclusion test of cell viability. *Current Protocols in Immunology*. Appendix 3, Appendix 3B.

Tan, L., Neoh, K.G., Kang, E.-T., Choe, W.S., and Su, X. (2011). PEGylated anti-MUC1 aptamer-doxorubicin complex for targeted drug delivery to MCF7 breast cancer cells. *Macromolecular Bioscience*. 11: 1331–1335.

Tan, W., Wang, K., He, X., Zhao, X.J., Drake, T., Wang, L., and Bagwe, R.P. (2004). Bionanotechnology based on silica nanoparticles. *Medical Research Reviews*. 24: 621–638.

Taylor-Pashow, K.M.L., Della Rocca, J., Huxford, R.C., and Lin, W. (2010). Hybrid nanomaterials for biomedical applications. *Chemical Communications*. 46: 5832–5849.

Teng, Y., Girvan, A. C., Casson, L. K., Pierce, W. M., Qian, M., Thomas, S. D., and Bates, P. J. (2007). AS1411 alters the localization of a complex containing protein arginine methyltransferase 5 and nucleolin. *Cancer research*. 67: 10491–10500.

Tohda, K., Lu, H., Umezawa, Y., and Gratzl, M. (2001). Optical detection in microscopic domains. 2. Inner filter effects for monitoring nonfluorescent molecules with fluorescence. *Analytical Chemistry*. 73: 2070–2077.

Tombelli, S., Minunni, M., and Mascini, M. (2005). Analytical applications of aptamers. *Biosensores and Bioelectronics*. 20: 2424–2434.

Tu, D., Blaha, G., Moore, P.B., and Steitz, T.A. (2005). Structures of MLSBK antibiotics bound to mutated large ribosomal subunits provide a structural explanation for resistance. *Cell*. 121: 257–270.

Tuerk, C., and Gold, L. (1990). Systematic evolution of ligands by exponential enrichment: RNA ligands to bacteriophage T4 DNA polymerase. *Science*. 249: 505–510.

Ulrich, H., and Wrenger, C. (2009). Disease-specific biomarker discovery by aptamers. *Cytometry*. 75: 727–733.

Varghese, J.N., Epa, V.C., and Colman, P.M. (1995). Three-dimensional structure of the complex of 4-guanidino-Neu5Ac2en and influenza virus neuraminidase. *Protein Science*. 4: 1081–1087.

Wang, L., Wang, K., Santra, S., Zhao, X., Hilliard, L.R., Smith, J.E., Wu, Y., and Tan, W. (2006). Watching Silica Nanoparticles Glow in the Biological World. *Analytical Chemistry*. 78: 646–654.

Waters, E. K., Richardson, J., Schaub, R. G. and Kurz, J. C. (2009). Effect of NU172 and bivalirudin on ecarin clotting time in human plasma and whole blood. *Journal of Thrombosis and Haemostasis*. 7: 683.

Wilchek, M., and Bayer, E.A. (1988). The avidin-biotin complex in bioanalytical applications. *Analytical Biochemistry*. 171: 1–32.

Willis, M.C., Collins, B.D., Zhang, T., Green, L.S., Sebesta, D.P., Bell, C., Kellogg, E., Gill, S.C., Magallanez, A., Knauer, S., *et al.* (1998). Liposome-anchored vascular endothelial growth factor aptamers. *Bioconjugate Chemistry*. 9: 573–582.

Yang, Y.-W. (2011). Towards biocompatible nanovalves based on mesoporous silica nanoparticles. *Medchemcomm*. 2: 1033-1049.

Yang, L., Zhang, X., Ye, M., Jiang, J., Yang, R., Fu, T., Chen, Y., Wang, K., Liu, C., and Tan, W. (2011). Aptamer-conjugated nanomaterials and their applications. *Advanced Drug Delivery Reviews*. 63: 1361–1370.

Ye, M., Hu, J., Peng, M., Liu, J., Liu, J., Liu, H., Zhao, X., and Tan, W. (2012). Generating Aptamers by Cell-SELEX for Applications in Molecular Medicine. *International Journal of Molecular Sciences*. 13: 3341–3353.

Yigit, M.V., Mazumdar, D., Kim, H.-K., Lee, J.H., Odintsov, B., and Lu, Y. (2007). Smart "turn-on" magnetic resonance contrast agents based on aptamer-functionalized superparamagnetic iron oxide nanoparticles. *Chembiochem*. 8: 1675–1678.

Zhang, J., Jia, X., Lv, X.-J., Deng, Y.-L., and Xie, H.-Y. (2010a). Fluorescent quantum dot-labeled aptamer bioprobes specifically targeting mouse liver cancer cells. *Talanta.* 81: 505–509.

Zhang, K., Sefah, K., Tang, L., Zhao, Z., Zhu, G., Ye, M., Sun, W., Goodison, S., and Tan, W. (2012a). A novel aptamer developed for breast cancer cell internalization. *ChemMedChem*. 7: 79–84.

Zhang, Y., Chen, Y., Han, D., Ocsoy, I., and Tan, W. (2010b). Aptamers selected by cell-SELEX for application in cancer studies. *Bioanalysis*. 2: 907–918.

Zhang, Y., Fei, W.-W., and Jia, N.-Q. (2012b). A facile method for the detection of DNA by using gold nanoparticle probes coupled with dynamic light scattering. *Nanoscale Research Letters*. 7: 564.

Zhao, X., Tapec-Dytioco, R., and Tan, W. (2003). Ultrasensitive DNA detection using highly fluorescent bioconjugated nanoparticles. *Journal of the American Chemical Society*. 125: 11474–11475.

Zhou, J., and Rossi, J.J. (2009). The therapeutic potential of cell-internalizing aptamers. *Current Topics in Medical Chemistry*. 9: 1144–1157.

Zrazhevskiy, P., Sena, M., and Gao, X. (2010). Designing multifunctional quantum dots for bioimaging, detection, and drug delivery. *Chemical Societys Reviews*. 39: 4326–4354.

CHAPTER 6

APPENDIXES

Table A.1 - Sequence alignment for 3 aptamers.

Aptamer 1	vs	Aptamer 2	vs	Aptamer 3	Bases Homology	Homology
#1	vs	#11	vs	#15	---G--G-GT----A-----G----	24%
#3	vs	#6	vs	#11	----T-G-----T--------G--G	20%
#1	vs	#3	vs	#6	----T-G----------CA-	16%
#1	vs	#4	vs	#11	-T-G----------A-----G----	16%
#2	vs	#3	vs	#15	-G-------T---------G----G	16%
#2	vs	#4	vs	#5	T----------G--T-------G-	16%
#2	vs	#6	vs	#15	--T----------T---G----G	16%
#3	vs	#6	vs	#15	------G----------G-G--G	16%
#3	vs	#11	vs	#15	------G--T----------G--G	16%
#4	vs	#5	vs	#12	-T------T------T--T------	16%
#5	vs	#6	vs	#12	-----A-----G---T-----G---	16%
#5	vs	#11	vs	#12	-T---A---T----------G---	16%
#5	vs	#11	vs	#15	-------G-T----------GG--	16%
#5	vs	#12	vs	#15	---------T-----T--T--G---	16%
#6	vs	#11	vs	#15	------GG----------G--G	16%
#11	vs	#12	vs	#15	A--------T---T-------G---	16%
#1	vs	#2	vs	#11	--------GT-------C-------	12%
#1	vs	#3	vs	#11	----T-G--T----------	12%
#1	vs	#4	vs	#15	---G----------A-----G----	12%
#1	vs	#5	vs	#11	-T-------T---------A-----	12%
#2	vs	#4	vs	#15	----------G--T---G-----	12%
#2	vs	#5	vs	#15	---------T--G--T---------	12%
#2	vs	#11	vs	#15	--------GT----------G	12%
#2	vs	#12	vs	#15	--T------T-----T---------	12%
#3	vs	#5	vs	#6	----------G--------AG---	12%
#3	vs	#5	vs	#12	---------T-G---------G---	12%
#4	vs	#5	vs	#11	-TG----------G-	12%
#4	vs	#5	vs	#15	----------G--T--T------	12%
#4	vs	#11	vs	#15	---G----------A-----G----	12%
#5	vs	#6	vs	#11	-----A-G----------G---	12%
#5	vs	#6	vs	#15	-------G-------T-----G---	12%
#6	vs	#12	vs	#15	--T----------T-----G---	12%
#1	vs	#2	vs	#5	---------T---C----------	8%
#1	vs	#2	vs	#15	--------GT----------	8%
#1	vs	#3	vs	#15	------G--T----------	8%
#1	vs	#5	vs	#12	-T-------T----------	8%
#1	vs	#6	vs	#11	----T-G----------	8%
#1	vs	#6	vs	#15	------G---C----------	8%
#1	vs	#11	vs	#12	-T-------T----------	8%
#2	vs	#3	vs	#4	-------T----------G-----	8%
#2	vs	#3	vs	#6	----------G----G	8%
#2	vs	#3	vs	#11	---------T----------G	8%

Aptamer 1	vs	Aptamer 2	vs	Aptamer 3	Bases Homology	Homology
#2	vs	#3	vs	#12	-------T-T----------	8%
#2	vs	#4	vs	#6	----------T---G-----	8%
#2	vs	#4	vs	#12	-------T-------T---------	8%
#2	vs	#5	vs	#6	----------C-T---------	8%
#2	vs	#5	vs	#11	---------T----------G-	8%
#2	vs	#5	vs	#12	---------T-----T---------	8%
#2	vs	#6	vs	#12	--T----------T---------	8%
#3	vs	#4	vs	#6	----------G--C--	8%
#3	vs	#5	vs	#11	---------T----------G---	8%
#3	vs	#5	vs	#15	---------T----------G---	8%
#3	vs	#6	vs	#12	----------G---------G---	8%
#3	vs	#11	vs	#12	---------T----------G---	8%
#3	vs	#12	vs	#15	---------T----------G---	8%
#4	vs	#5	vs	#6	----------T-A-------	8%
#4	vs	#6	vs	#15	----------T---G-----	8%
#4	vs	#12	vs	#15	----------T--T------	8%
#6	vs	#11	vs	#12	-----A----------G---	8%
#1	vs	#2	vs	#3	---------T----------	4%
#1	vs	#2	vs	#6	----------C----------	4%
#1	vs	#2	vs	#12	---------T----------	4%
#1	vs	#3	vs	#4	----------C--	4%
#1	vs	#3	vs	#5	---------T----------	4%
#1	vs	#3	vs	#12	---------T----------	4%
#1	vs	#4	vs	#5	-T----------	4%
#1	vs	#4	vs	#6	----------C--	4%
#1	vs	#4	vs	#12	-T----------	4%
#1	vs	#5	vs	#6	----------C----------	4%
#1	vs	#5	vs	#15	---------T----------	4%
#1	vs	#12	vs	#15	---------T----------	4%
#2	vs	#3	vs	#5	---------T----------	4%
#2	vs	#4	vs	#11	----------G-	4%
#2	vs	#6	vs	#11	----------G	4%
#2	vs	#11	vs	#12	---------T----------	4%
#3	vs	#4	vs	#11	----------G--------	4%
#3	vs	#4	vs	#12	-------T----------	4%
#3	vs	#4	vs	#15	----------G-----	4%
#4	vs	#6	vs	#12	----------T---------	4%
#4	vs	#11	vs	#12	-T----------	4%
#1	vs	#2	vs	#4	----------	0%
#1	vs	#6	vs	#12	----------	0%
#3	vs	#4	vs	#5	----------	0%
#4	vs	#6	vs	#11	----------	0%

Table A.2 - Sequence alignment for 4 aptamers.

Aptamer 1 vs Aptamer 2 vs Aptamer 3 vs Aptamer 4							Bases Homology	Homology
#1	vs	#4	vs	#11	vs	#15	---G----------A-----G----	12%
#1	vs	#2	vs	#11	vs	#15	--------GT----------	8%
#1	vs	#3	vs	#6	vs	#11	----T-G----------	8%
#1	vs	#3	vs	#11	vs	#15	------G--T----------	8%
#1	vs	#2	vs	#3	vs	#5	---------T----------	4%
#1	vs	#2	vs	#3	vs	#11	---------T----------	4%
#1	vs	#2	vs	#3	vs	#12	---------T----------	4%
#1	vs	#2	vs	#3	vs	#15	---------T----------	4%
#1	vs	#2	vs	#5	vs	#6	----------C----------	4%
#1	vs	#2	vs	#5	vs	#11	---------T----------	4%
#1	vs	#2	vs	#5	vs	#12	---------T----------	4%
#1	vs	#2	vs	#5	vs	#15	---------T----------	4%
#1	vs	#2	vs	#11	vs	#12	---------T----------	4%
#1	vs	#2	vs	#12	vs	#15	---------T----------	4%
#1	vs	#3	vs	#4	vs	#6	----------C--	4%
#1	vs	#3	vs	#5	vs	#11	---------T----------	4%
#1	vs	#3	vs	#5	vs	#12	---------T----------	4%
#1	vs	#3	vs	#5	vs	#15	---------T----------	4%
#1	vs	#3	vs	#6	vs	#15	------G----------	4%
#1	vs	#3	vs	#11	vs	#12	---------T----------	4%
#1	vs	#3	vs	#12	vs	#15	---------T----------	4%
#1	vs	#4	vs	#5	vs	#11	-T----------	4%
#1	vs	#4	vs	#5	vs	#12	-T----------	4%
#1	vs	#4	vs	#11	vs	#12	-T----------	4%
#1	vs	#2	vs	#3	vs	#4	----------	0%
#1	vs	#2	vs	#3	vs	#6	----------	0%
#1	vs	#2	vs	#4	vs	#5	----------	0%
#1	vs	#2	vs	#4	vs	#6	----------	0%
#1	vs	#2	vs	#4	vs	#11	----------	0%
#1	vs	#2	vs	#4	vs	#12	----------	0%
#1	vs	#2	vs	#4	vs	#15	----------	0%
#1	vs	#2	vs	#6	vs	#11	----------	0%
#1	vs	#2	vs	#6	vs	#12	----------	0%
#1	vs	#2	vs	#6	vs	#15	----------	0%
#1	vs	#3	vs	#4	vs	#5	----------	0%
#1	vs	#3	vs	#4	vs	#11	----------	0%
#1	vs	#3	vs	#4	vs	#12	----------	0%
#1	vs	#3	vs	#4	vs	#15	----------	0%
#1	vs	#3	vs	#5	vs	#6	----------	0%
#1	vs	#3	vs	#6	vs	#12	----------	0%
#1	vs	#4	vs	#5	vs	#6	----------	0%
#1	vs	#4	vs	#5	vs	#15	----------	0%
#1	vs	#4	vs	#6	vs	#11	----------	0%

Aptamer 1 vs Aptamer 2 vs Aptamer 3 vs Aptamer 4							Bases Homology	Homology
#1	vs	#4	vs	#6	vs	#12	----------	0%
#1	vs	#4	vs	#6	vs	#15	----------	0%
#1	vs	#4	vs	#12	vs	#15	----------	0%

Table A.3- Predicted aptamer secondary structures by *in silico* analysis with the software mfold. Only the structure(s) with the lowest free energy (dG) are presented. The fixed sequences of PCR primers are indicated in lowercase letters. The random region is represented in uppercase letters and is marked in black rectangular area.

4°C	37°C
Aptamer #1 (3 potential structures)	Aptamer #1 (3 potential structures)
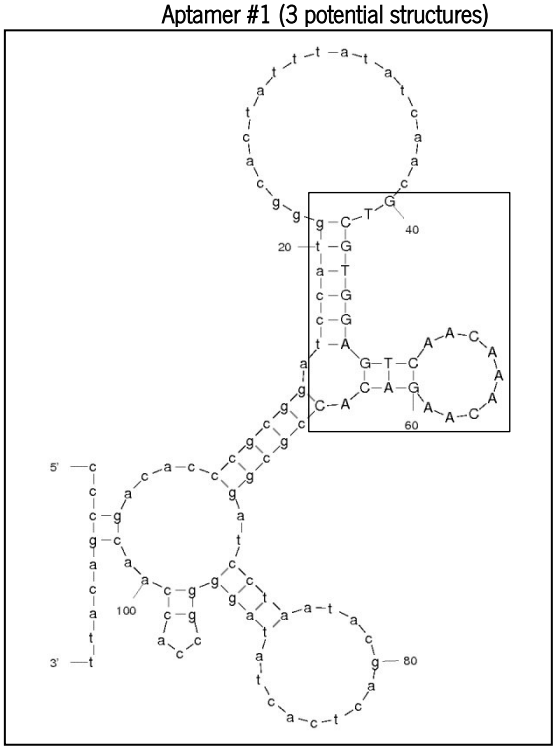	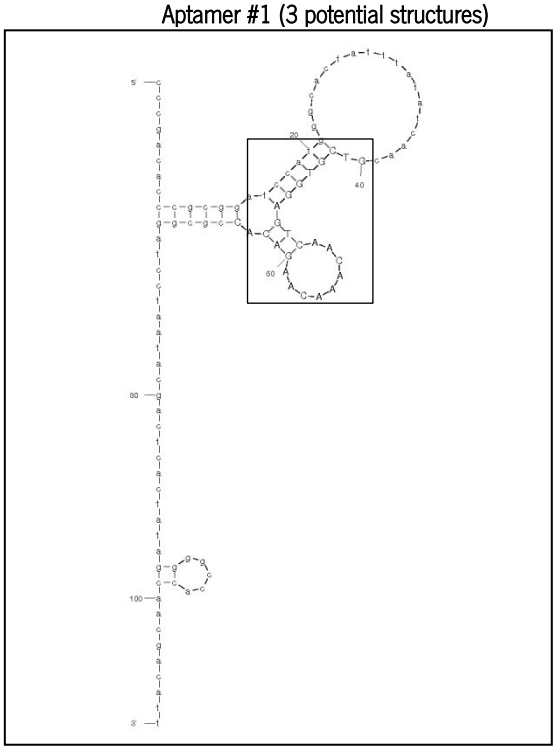
dG= - 22.05 kcal/mol	dG= - 6.57 kcal/mol

4°C	37°C
Aptamer #2 (10 potential structures)	Aptamer #2 (4 potential structures)
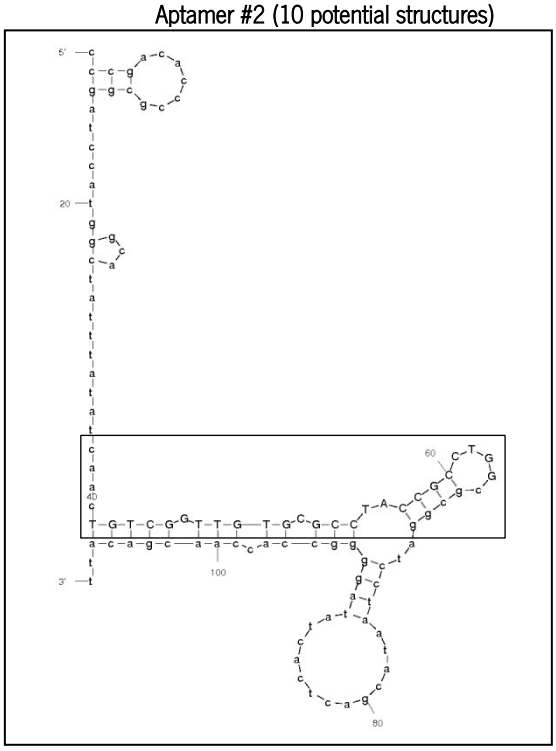	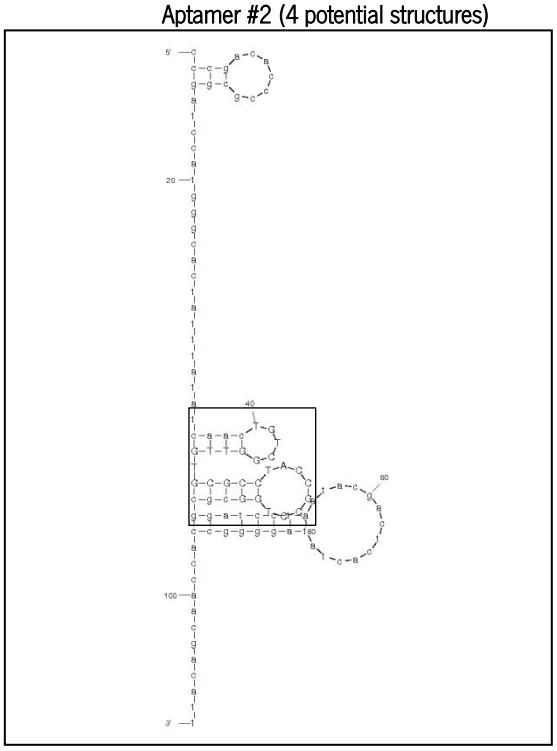
dG= - 27.50 kcal/mol	dG= - 8.95 kcal/mol
Aptamer #3 (3 potential structures)	Aptamer #3 (6 potential structures)
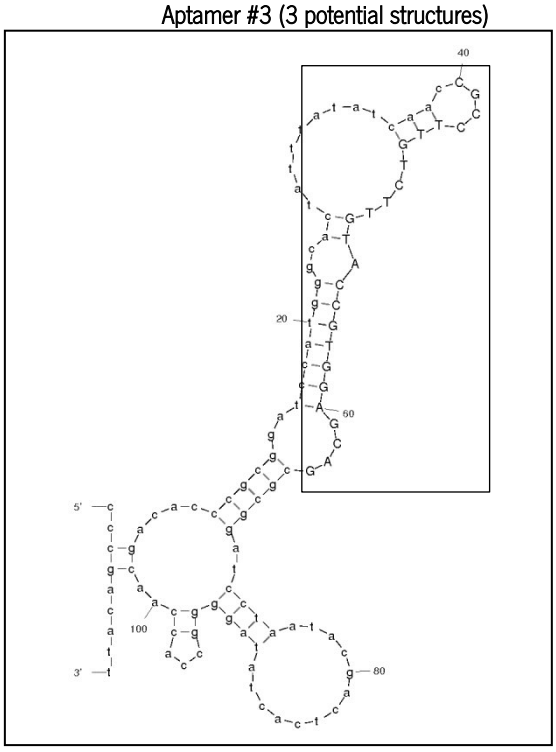	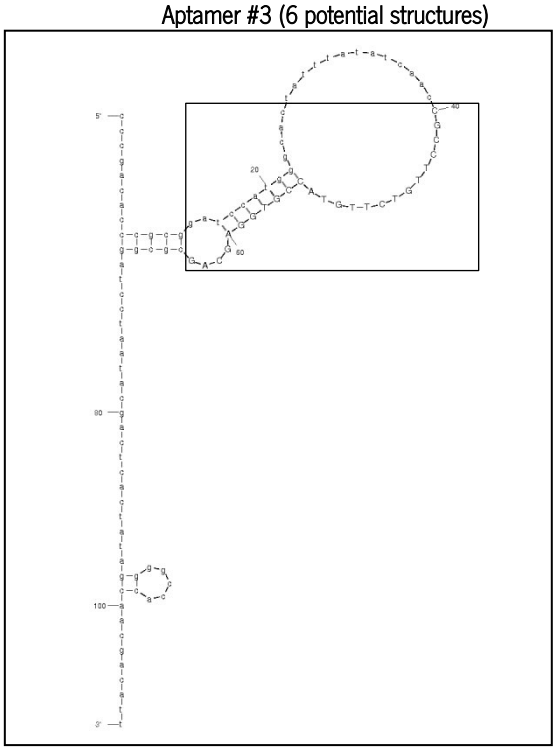
dG= - 23.10 kcal/mol	dG= - 6.38 kcal/mol

4°C	37°C
Aptamer #4 (8 potential structures)	Aptamer #4 (3 potential structures)
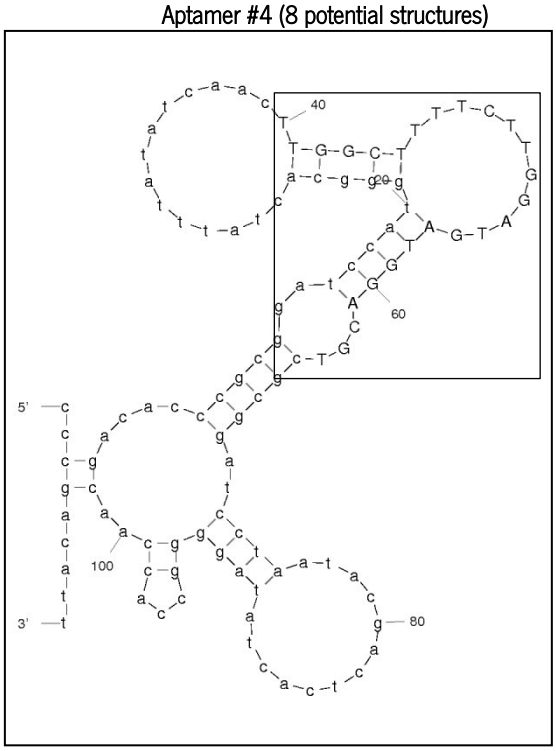	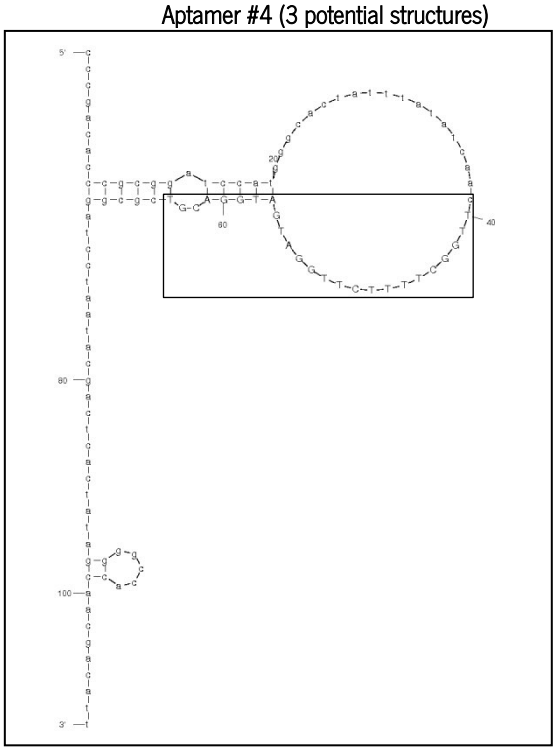
dG= - 19.98 kcal/mol	dG= - 5.80 kcal/mol
Aptamer #5 (10 potential structures)	Aptamer #5 (2 potential structures)
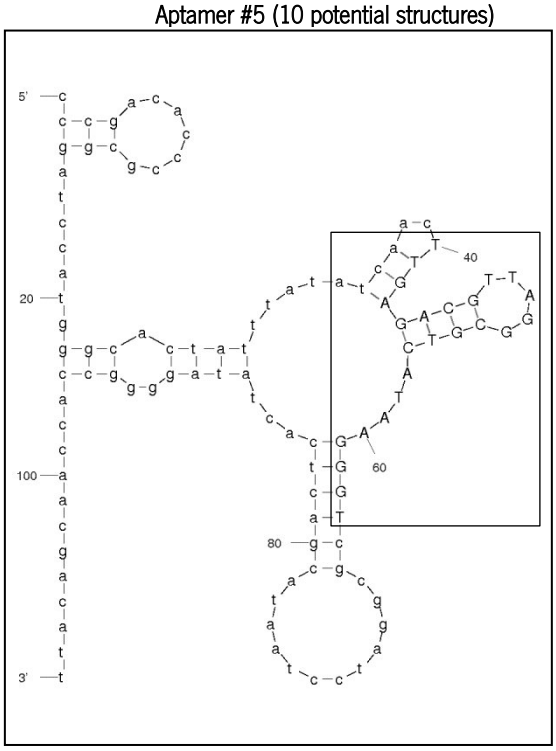	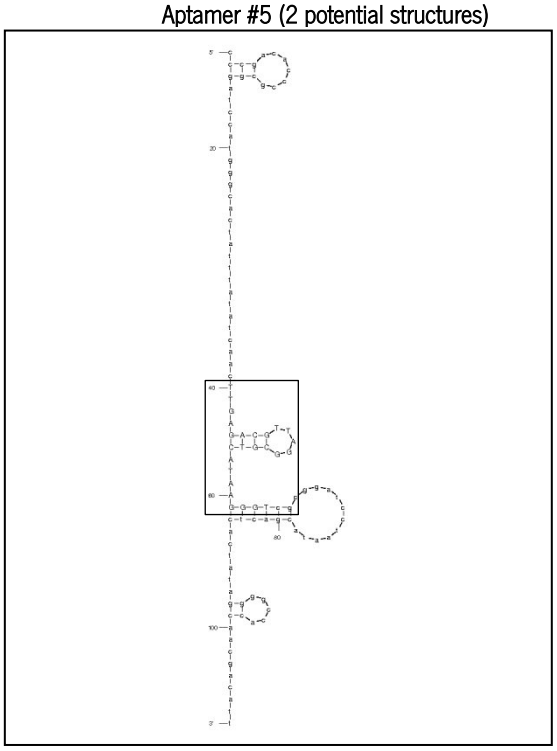
dG= - 23.16 kcal/mol	dG= - 7.48 kcal/mol

4ºC	37ºC
Aptamer #6 (7 potential structures)	Aptamer #6 (7 potential structures)
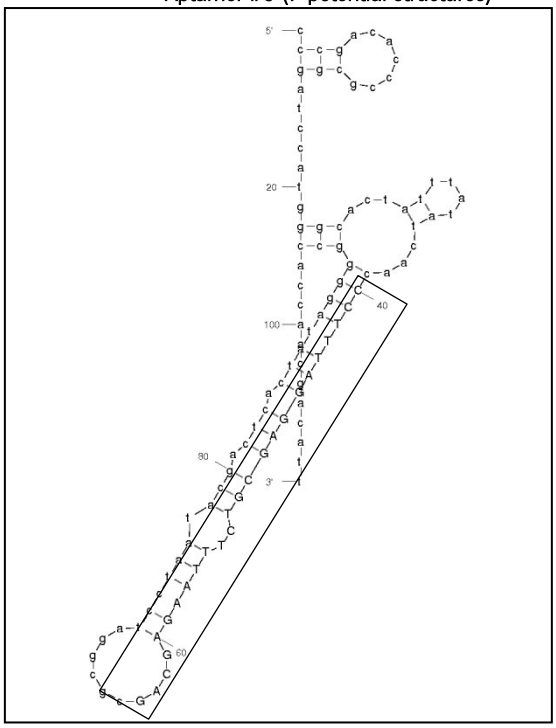	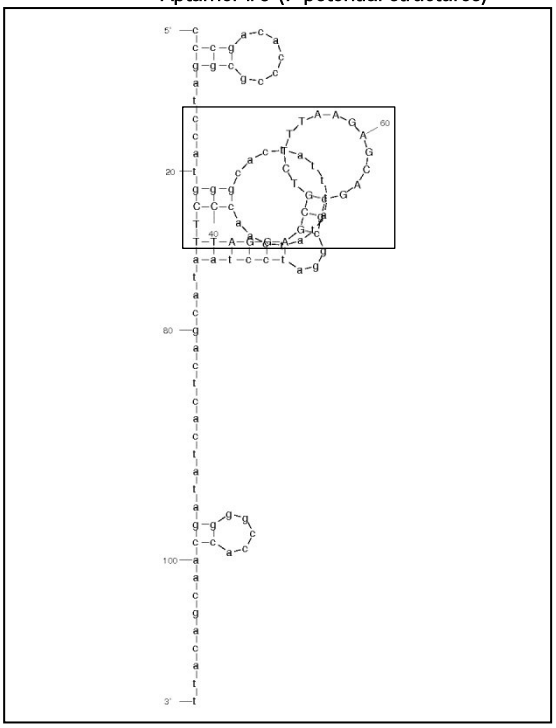
dG= - 21.18 kcal/mol	dG= - 7.82 kcal/mol
Aptamer #12 (2 potential structures)	Aptamer #12 (3 potential structures)
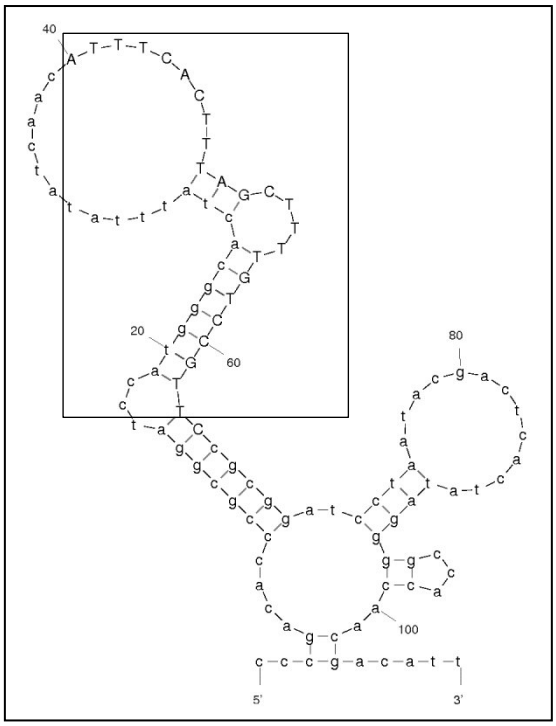	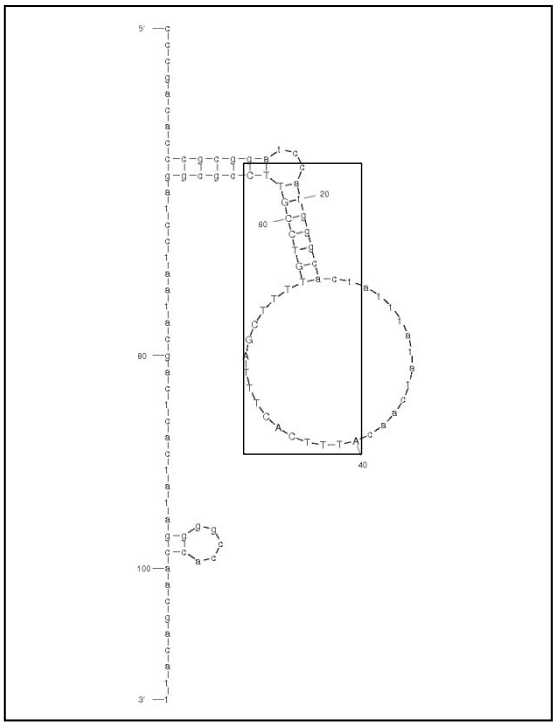
dG= - 19.20 kcal/mol	dG= - 6.35 kcal/mol

4°C	37°C
Aptamer #13 (4 potential structures)	Aptamer #13 (4 potential structures)
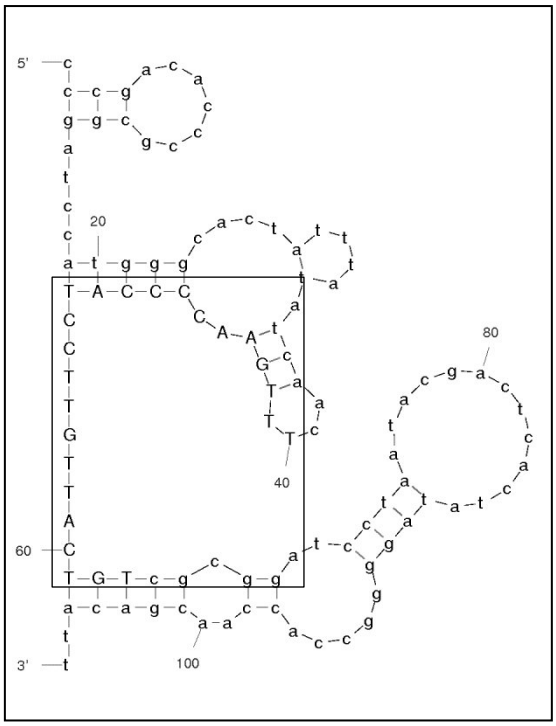	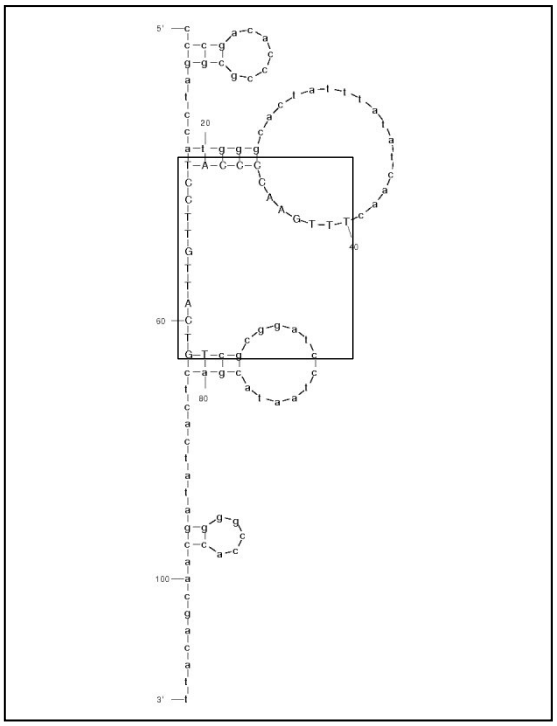
dG= - 19.48 kcal/mol	dG= - 4.98 kcal/mol
Aptamer #14 (9 potential structures)	Aptamer #14 (6 potential structures)
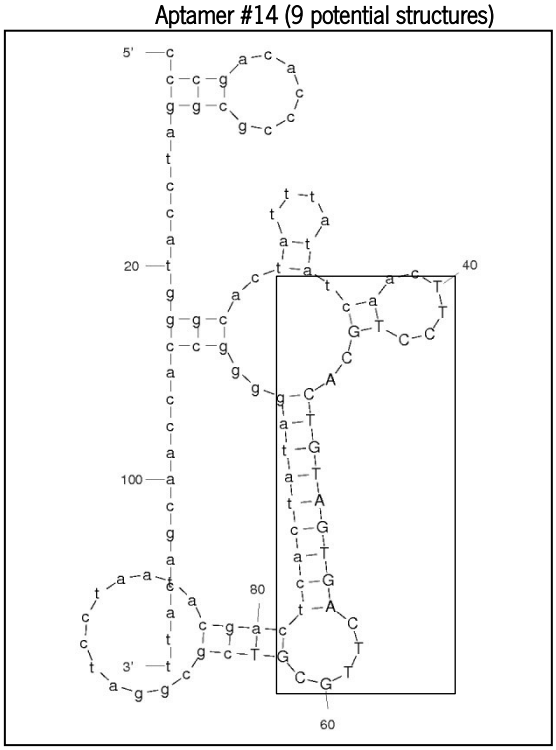	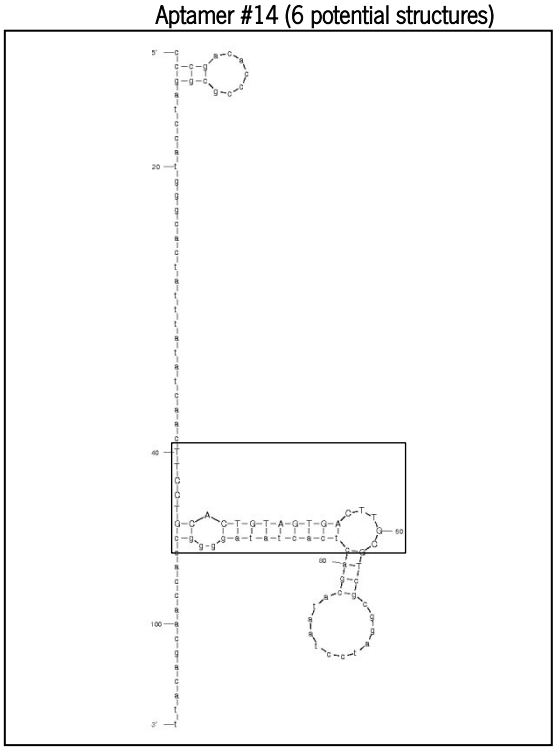
dG= - 20.03 kcal/mol	dG= - 5.40 kcal/mol